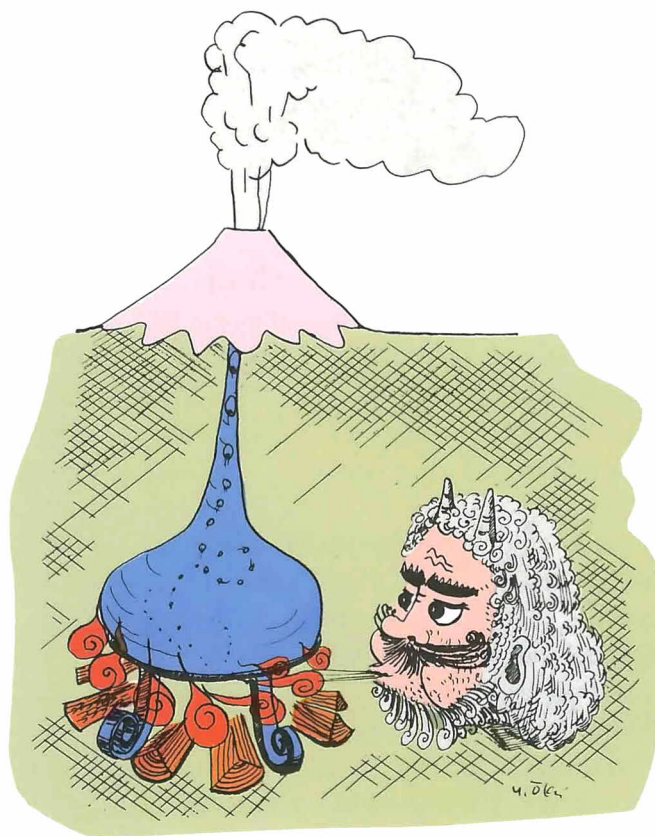


Y. Oki, S. Aramaki, K. Nakamura and K. Hakamata

*Volcanoes of Hakone,
Izu and Oshima*



Contents

	Page
Forward	2
1. Geologic Setting	3
2. The Tertialy Basement Formations (Aramaki)	5
3. Hakone Volcano (Oki and Hakamata)	8
3.1 Introduction	8
3.2 Topography	9
3.3 Geology	11
Foundations of Hakone	11
Geologic history of Hakone	11
Structure of the Hakone caldera	18
4. The Quaternary Volcanoes of the Izu Peninsula (Aramaki)	22
4.1 General statement	22
4.2 Yugawara volcano	23
4.3 Taga volcano	24
4.4 Usami volcano	24
4.5 Amagi volcano	24
4.6 Volcanoes in the western row	25
4.7 Higashi-Izu Monogenetic Volcano Group	25
5. Izu-Oshima Volcano (Nakamura)	34
5.1 Introduction	34
5.2 Topography	34
5.3 Geology	36
Older volcanoes	36
Oshima volcano	39
Stratigraphy of the Younger Oshima group	40
Caldera	50
Common sequence in great eruptions	51
Periodicity of the great eruptions	52
Recent activity	54
Flank volcanoes and tectonic stress	56
6. Petrology (Aramaki)	60
6.1 Chemical and mineralogical characteristics	60
6.2 Zonal variations	62
6.3 Difference in the groundmass pyroxenes	63

7. Hot Springs (Oki)	65
7.1 Hot springs and hydrothermal system of Hakone	65
Historical aspect	65
Thermal structure	66
Hydrology of thermal waters	66
Zonal distribution of thermal waters	66
Compositional trend of thermal waters	70
Genetic model of Hakone hydrothermal system	71
Seismic activity of Hakone	72
Sodium chloride waters	73
Sodium chloride budget	75
Isotope geochemistry	75
7.2 Hot springs of the Izu Peninsula	78
7.3 Hot eye and cold eyelid	82
7.4 Legal aspect of Hot springs	84
References	86



to Professor Hisashi Kuno

Yasue OKI; Hot Spring Research Institute of Kanagawa Pref.,
Hakone, Kanagawa 250 – 03, Japan.

Shigeo ARAMAKI; Earthquake Research Institute, Univ. of Tokyo,
Tokyo 113, Japan.

Kazuaki NAKAMURA; Earthquake Research Institute, Univ. of Tokyo,
Tokyo 113, Japan.

Kazuo HAKAMATA; Owakidani Natural History Museum,
Hakone, Kanagawa 250 – 06, Japan.



Rokudo-jizo carved in 1300 A.D. on a block of augite-hypersthene andesite from the Futago lava dome, a post caldera cone of Hakone volcano. The Jizo has long been worshipped for both safety in travel and happiness in life which is said to be assured by a penny into the red offertory box (before the economic inflation of this century).

Forward

Japan is a chain of volcanic islands forming a part of the Circum Pacific Mobile Belt, sometimes referred to as the Girdle of Fire. There are about 200 Quaternary volcanoes in Japan, of which 60 are known as active or in eruption during the historic time. Japan is one of the ideal places for the study of volcanoes developed in the mobile belt between the Asian continent and the Pacific. Volcanoes of Hakone, Izu, and Oshima belonging to the Fuji volcanic zone, the northern extension of the Izu-Mariana Island Arc, have been studied geologically by many scientists, particularly by Professor H. Kuno who contributed important concepts regarding the origin of volcanoes and volcanic rocks through his extensive study of these areas. It would be stimulating for earth scientists to visit these areas and to have their own experiences with these volcanoes.

This book is prepared as a field guide for these geologically attractive volcanoes. It is hoped that this book will help the reader to understand the whole life of the volcanoes, which now provide us the most spectacular features, natural resources, and sometimes unwelcome hazards to our life.

We all express our sincere gratitude to late professor Hisashi Kuno who conducted us to the fields of volcanology. Our thanks are due to Mr. M. Orui, Mr. H. Sawada, Odakyu Railway Co. Ltd. and Hakone Town office who kindly allowed us to use attractive photographs. Mayor S. Katsumata and vice-Mayor K. Shinano of Hakone Town encouraged us materially to publish this book to whom we are cordially grateful.

Yasue Oki
Shigeo Aramaki
Kazuaki Nakamura
Kazuo Hakamata
— 1978 —

1. Geologic Setting

The distribution of Japanese volcanoes is divided into two major zones, the East and the West Japan volcanic belts (Sugimura, 1960). One is an extension of the Kurile Arc down to Hokkaido, linking with the Honshu Arc and joining with the Izu-Mariana Arc in the central part of Honshu. Volcanoes of these arcs are related to the subduction of the Pacific plate along Kurile-Japan-Izu-Mariana trenches. The other is a volcanic zone extending along the Japan Sea coast of west Honshu and linking with the Ryukyu Arc through the volcanoes in Kyushu (Fig. 1-1).

The Fuji volcanic zone, of the East Japan volcanic belt, runs through the area called the Fossa Magna Region, which can be compared with a wedge driven into the middle of the Honshu island. During the period from early to middle Miocene time, the Honshu had been split into the eastern and the western halves by the development of a huge volcano-tectonic depression called the Fossa Magna. This event was followed by an extensive transgression of sea

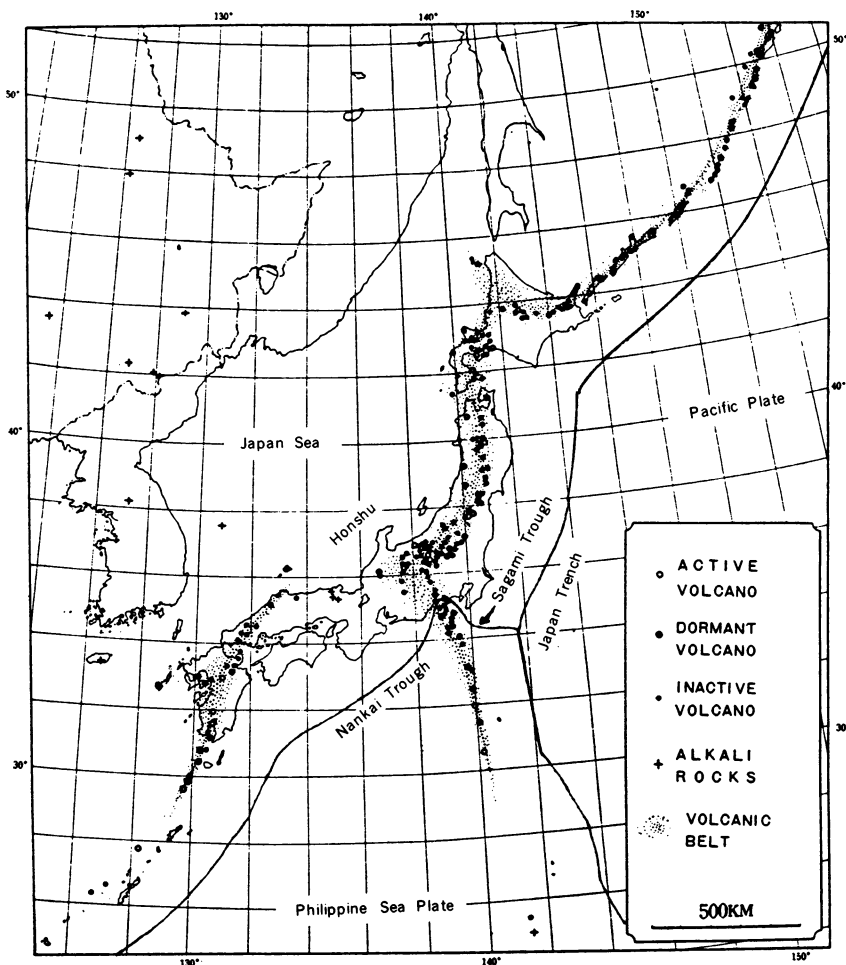


Fig. 1-1 Volcanoes and volcanic belts (Sugimura, 1960).
Plate boundary are after Sugimura (1972) Kagaku, vol. 42, p. 192 — 202

with accumulation of thick sedimentary pile made up mostly of submarine volcanic materials. The early stage of the volcanic activity in the southern Fossa Magna was characterized by tholeiitic basalt and andesite, then followed by a small amount of dacite. The later stage of the volcanism was characterized by the rocks of the calc-alkaline series. The thickness of these volcanogeneous sediments totals over 10,000 m being widely suffered burial metamorphism ranging from the zeolite facies to the pumpellyite-prehnite facies. These hydrothermally altered rocks are green or dark green in color and sometimes called collectively as the green tuff formation. They were intruded by stocks of quartz gabbro, quartz diorite, and granodiorite. The ore deposit of the Kuroko type made up of sulfides of Zn, Cu, Pb, and Cd was also associated with the submarine volcanism.

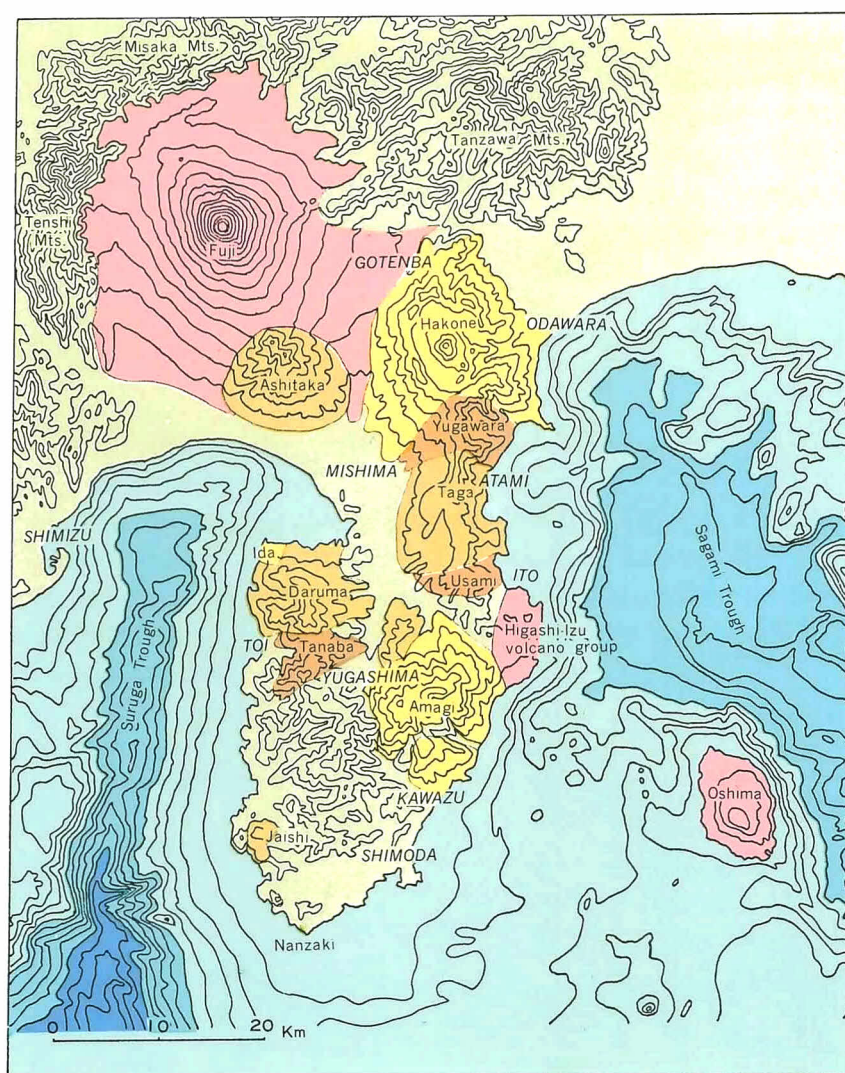


Fig. 1-2. Volcanoes in the Fuji, Hakone, Izu and Oshima areas.

In Quaternary, the area has been uplifted above the sea level, and the volcanic activity has taken place to build up a number of volcanoes of the Fuji volcanic zone.

Tectonic setting of the area is quite interesting or complicated, because of the fact that the Hakone-Izu peninsula-Oshima area occupies the northernmost portion of the Philippine Sea plate (Fig. 1-2). This part of the Philippine Sea plate has collided against central Honshu during the Quaternary. Further west, the plate goes down under southwest Honshu along the Nankai trough. In this context, the Oshima volcano is situated on the ocean side plate, contrary to normal island arc volcanoes which rest on the overlying plate. Toward east along the Sagami trough, which branches off from the Japan trench, the Philippine Sea plate moves almost transcurrently with a component of subduction. The last movement of this portion of the plate boundary caused the great Kanto earthquake in 1923. This plate boundary is believed to be continuous westward somewhere between Fuji and Izu peninsula to the Nankai trough. This means that the actively colliding plate boundary cuts across the active island arc volcanic belt here.

2. The Tertiary Basement Formations

The Hakone, Izu and Oshima areas have been the site of vigorous volcanism both above and below the water since the Miocene time as was the case with southern Fossa Magna region where Hakone and Fuji volcanoes now tower. The thick submarine volcanic formation, the Yugashima group, equivalent to the Misaka group in the Fossa Magna, makes up the immediate basement of the whole region of Izu, indicating that during the most part of Miocene, submarine volcanism added at least a few thousand meters of material to the upper crust of Izu. The nature and structure of the concealed lower part of the crust whose total thickness is between 25 and 30 km is yet to be determined. The xenoliths carried by the younger lavas yield informations about the nature of the underlying crust. Except the relatively frequent occurrence of "granitic" inclusions, no positive evidence indicative of old sialic crust such as gneiss and schist are found. Most of the "granitic" inclusions are quartz dioritic, i.e. with little K-feldspars and can be interpreted as akin to volcanic suites. One possibility is thus the Izu peninsula has no continental foundation contrary to other parts of the Japanese islands, probably including Fossa Magna, where sporadic tectonic inliers suggest the presence of older Paleozoic or still older landmass.

The submarine volcanism in Miocene time was mainly basaltic and andesitic which produced abundant volcanoclastic masses, lava flows and shallow intrusive bodies. There is a tendency of increasing proportion of acidic (dacitic) products towards the end of Miocene. The name Shirahama group is assigned to such younger submarine formations. Shirahama literally means, in Japanese, "white beach" reflecting the abundance of light-colored dacitic material. Figure 2-1 shows a generalized geologic map of the middle and southern part of the Izu peninsula. Rocks of the Yugashima and Shirahama groups make up the sole basement which is broken up by many faults. The displacement of the faults is however generally not large and the structure is the repetition of gentle synclines and anticlines and domes and basins. Probably during the Pliocene, the area was emerged with the volcanism still continuing. It is very difficult to distinguish the Miocene volcanic formations from the Pliocene and also the Pliocene from the Pleistocene, as very few fossils and radioactive age data are available. Also probably by this time the thick pile of volcanic material constituting the Yugashima and Shirahama groups was extensively metamorphosed to the zeolite facies and hydrothermally altered. Shallow intrusive masses of diorite, quartz gabbro, porphyrite, etc. are numerous and the mineralization characterized by Au, Ag, Zn, Pb, Cu, etc. and sometimes extensive silicification was wide-spread through the regions.

During the Pliocene time, the Izu peninsula and the southern Fossa Magna region were gradually uplifted and emerged. By the end of the Pliocene, the coast line of the Izu peninsula had roughly the same outline as the present one.

Therefore most of the late Pliocene and all the Pleistocene volcanoes were emplaced on land. Many of the Pliocene volcanoes undoubtedly formed stratovolcanoes and some probably formed rows of pyroclastic edifices and flat lava fields. The rocks range from mafic basalts to felsic dacites but mafic andesites predominate by volume. The most striking are the basalt piles along the eastern coast of the northern peninsula, such as Tenshozan basalt group, Hata basalt group and Ajiro (Aziro) basalt group. They are made up mostly of basalts and mafic andesites with mineralogy and chemistry characteristic to the so-called Izu-Hakone volcanic area (Kuno, 1950; Tsuya, 1937 etc).

Thick piles of andesitic volcanics, such as Inamura andesite group, Awarada andesite group and the Tanna Tunnel andesites are contemporaneous with these basalts.

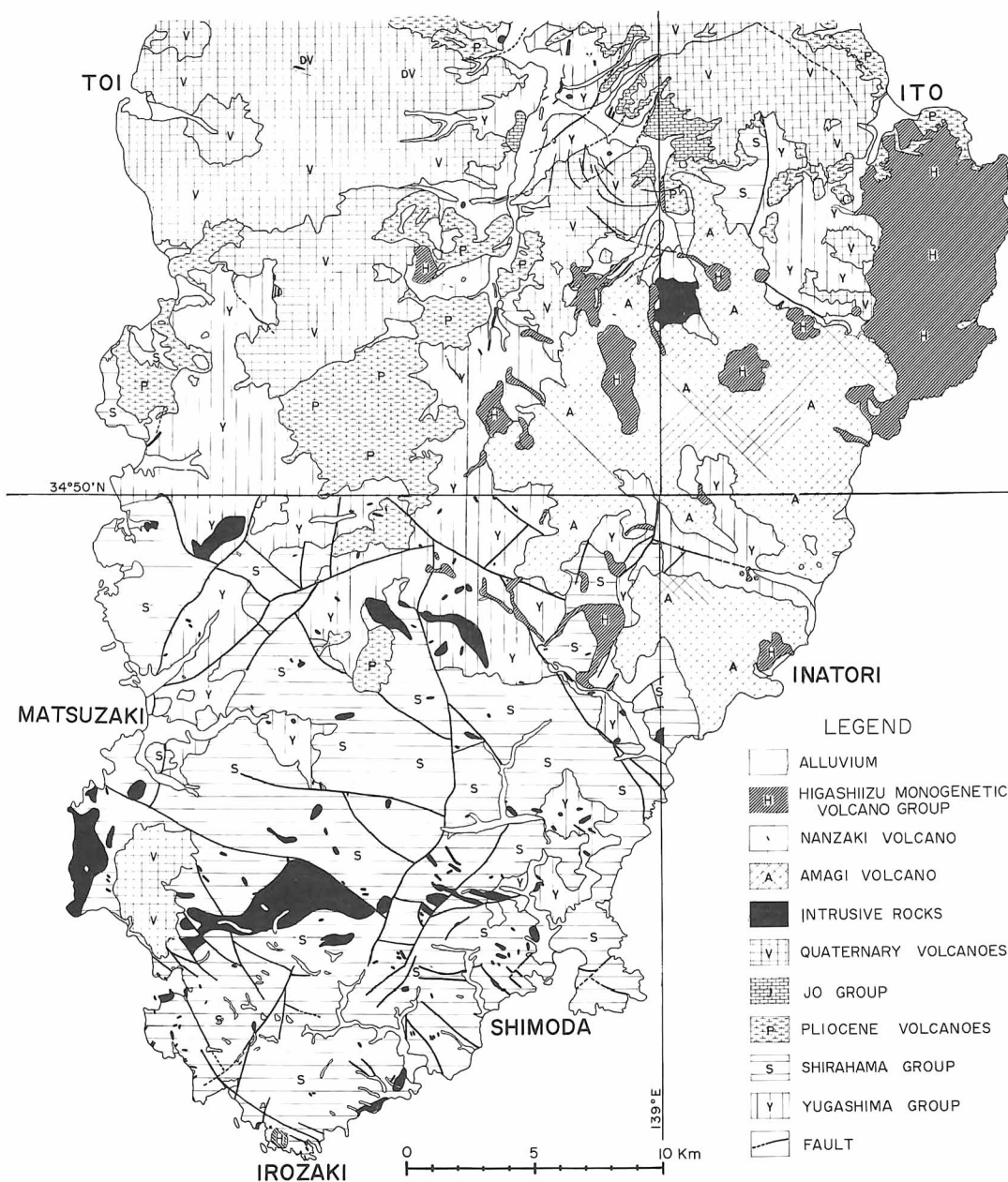


Fig. 2-1. Generalized geologic map of the middle and southern parts of the Izu peninsula. Compiled from the geologic maps (scale 1 : 50,000) published by the Geological Survey of Japan.

3. Hakone Volcano

3.1 Introduction

Hakone has been set apart as National Park since 1933. There are many fascinating sceneries of volcanoes, many historical remains, and hot springs with comfortable hotels, well protected driveways and railways. Before the development of modern transportation system, the Hakone volcano was one of the most serious traffic obstacles in the Old Days of Japan. Visitors now can reach Hakone through any of the three major entrances by car (Fig. 3-1). The East Entrance from Odawara is a twisted road through either the Haya-kawa canyon or the Sukumo-gawa canyon. By combining mountain train with cable-car and ropeway you can also arrive in Hakone easily. The West Entrance Road is on the flat slope of the volcano, starting from Mishima to Hakone Pass, which offers extensive view of Suruga Bay and Pacific Ocean. The Northern Entrance Road parting from the Tomei Expressway at Gotemba gives more perfectly conical view of the Fuji volcano.

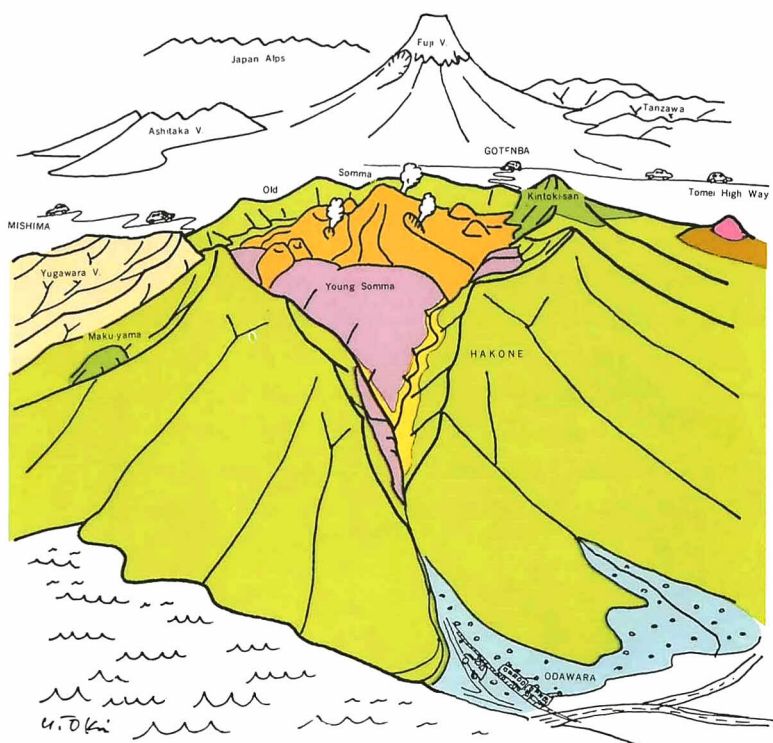


Fig. 3-1 Hakone volcano and three Entrances.

3.2 Topography

Hakone is a triple volcano composed of two overlapping calderas and seven post-caldera cones (Fig. 3-2). The main body of the volcanic edifice about 20 km long and 15 km wide is a large composite cone, which once reached a height of 2,700 m above the sea level. The 800 to 1,200 m high circular ridge 11 km in the N-S diameter and 10 km in the E-W diameter is called the Old Somma. Table mountains about 800 m high in the eastern half of the caldera forming an inner circular ridge are remains of a shield volcano, which once filled up the caldera, and called the Young Somma.

Fig. 3-2. Geologic solid-model of Hakone volcano after Kuno (1950 b)



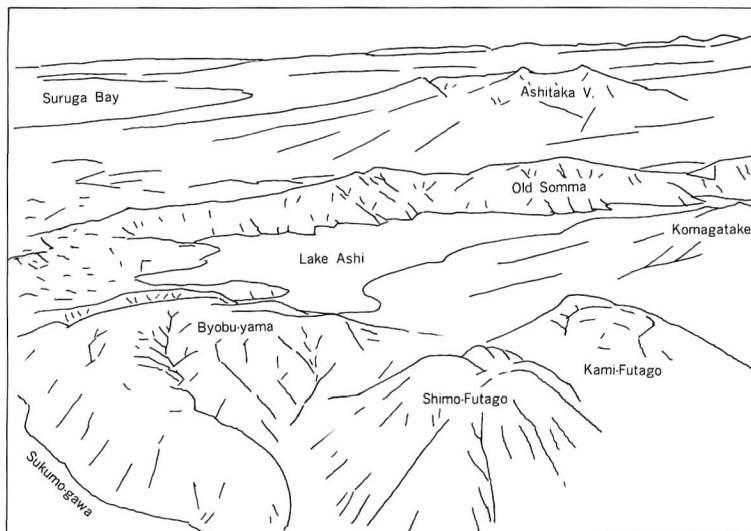


Fig. 3-3. Hakone caldera (photo : Odakyu Railway Co.).

The highest peak Kami-yama 1,438m occupying the central part of the caldera is one of the post-caldera cones and is associated with active solfataras. Ashinoko is a caldera lake dammed up by a dry mudflow (avalanche) derived by the hydroexplosion of Kami-yama. The eastern slope of Hakone has been deeply carved by Haya-kawa and Sukumo-gawa valleys, in which the sequence of volcanic profile can be seen. Many hot springs are found along the valleys.

3.3 Geology

Kuno (1950 b) extensively studied the geology of Hakone and classified the volcano into three major geologic units; Old Somma, Young Somma, and Post-caldera cones (Fig. 3-4). Table 3-1 gives the stratigraphic succession of the major geologic units related with Hakone.

Foundations of Hakone

Hakone stands on flat mountains composed of Miocene and Pliocene sediments called the Yugashima group (lower Miocene), the Ashigara group, the Haya-kawa tuff breccias, and the Sukumo-gawa andesite group (middle Miocene to Pliocene).

The Yugashima group here exposed locally in the bottom of the canyons of Haya-kawa and Sukumo-gawa is dark greenish and compact rocks of basalt and andesite. Larger exposures of the Yugashima group are seen in the bottom of deeply dissected calderas of Quaternary volcanoes of Usami, Taga and Yugawara.

The Ashigara group occurring in the northern part of Hakone consists of clastic sediments derived mostly from the Tanzawa mountains of the lower Miocene eugeosynclinal sediments. The total thickness is more than 5 km.

The Haya-kawa tuff breccias are light brownish rocks of dacite tuff and tuff breccia frequently rich in pumice fragments. They are exposed largely along the valleys of Haya-kawa and Sukumo-gawa. The exposed thickness is several hundred meters.

The Sukumo-gawa andesite group was extruded immediately after the emplacement of the Haya-kawa tuff breccias. The andesite group consists of grayish or brownish tuff breccia, volcanic breccia, and lava of glassy two pyroxene andesite, most of which is scoriaceous and blocky, sometimes intercalated with layers of the Haya-kawa tuff breccias. The thickness of the group is about 200 m.

Geologic history of Hakone

Kuno (1952) proposed a schematic diagram showing the geologic development of Hakone as given in Figure 3-5. The following interpretation is based mostly on Kuno's classic works combined with new evidence obtained recently.

First stage, huge composite cone

The eruptive activity of Hakone began about 400,000 years ago that first built up a huge composite cone of 130 km³ reaching 2,700 m above the sea level. The early stage of the eruption threw out agglomerate and lava of tholeiitic basalt up to 100 to 200 m thick. The later stage was explosive with alternate

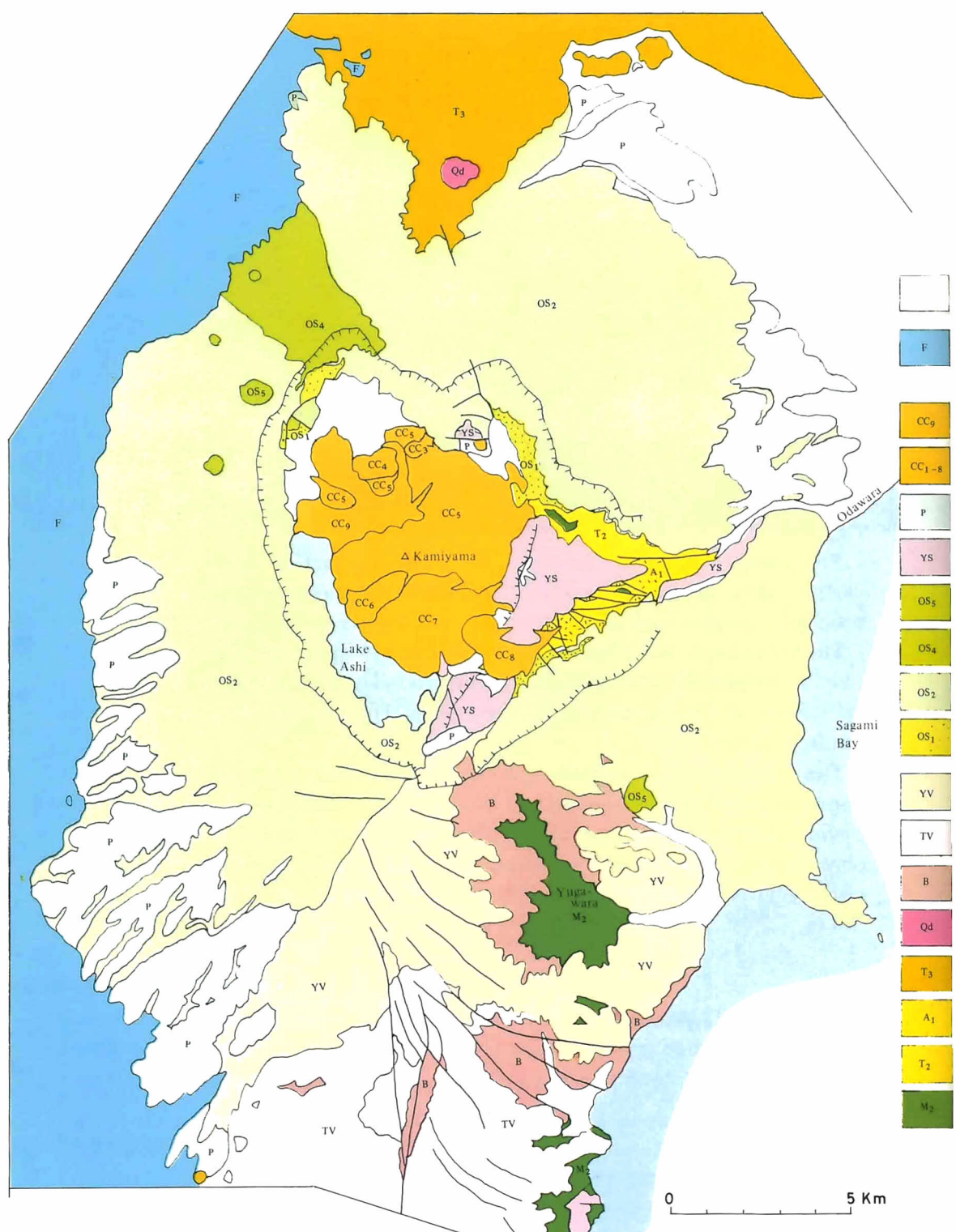


Fig. 3-4. Geologic map of Hakone volcano after Kuno (1950 b), simplified and partly revised.

Table 3-1. Geologic map and stratigraphic succession of Hakone volcano, Kuno (1950 b), partly revised.

	Lake deposits, talus and river gravels		
F	Fuji volcano		
	Hakone volcano		
	Kanmuri-gatake pyroclastic flow and lava spine		2,900 y B. P.
CC ₉	Kami-yama avalanche debris dammed up Ashinoko		3,100 y B.P.
CC _{1 - 8}	Central cone lavas, including nuée ardente and mud-flow deposits		
—	Second caldera collapse and erosion	—	30,000 y B.P.
P	Pumice flows	45,000 ~ 70,000 y B.P.	
YS	Young Somma Lavas		130,000 y B.P.
—	First caldera collapse and erosion	—	200,000 y B.P.
OS ₅	Satellite cones	} Old Somma Lavas	400,000 y B.P.
OS ₄	Kintoki-san lavas		
OS ₂	Andesite lavas		
OS ₁	Basalt lavas and agglomerates		
~~~~	Erosion	~~~~	
YV	<b>Yugawara volcano</b>		
~~~~	Erosion	~~~~	
TV	Taga volcano		
~~~~	Erosion	~~~~	
B	<b>Basalts and andesites of Pliocene</b> (Younger or middle Pliocene)		
Qd	<b>Quartz diorite plug</b> (Pliocene)		
~~~~	Erosion	~~~~	
T ₃	Ashigara group	Older Pliocene	
A ₁	Sukumo-gawa andesite group	to	
T ₂	Haya-kawa tuff breccias	Middle Miocene	
~~~~	Erosion	~~~~	
M ₂	<b>Yugashima group</b>	Older Miocene	

eruption of andesite lavas and pyroclastic materials, whose thickness is 300 to 600 m on the wall of the present caldera. The total thickness at the center of the cone seems to exceed 1,000 m. These rocks forming the main cone are collectively called the Old Somma Lavas.

Volcanic ash, lapilli and pumice produced during this stage are widely spread over areas to the east of Hakone. These layers are called the Tama tephra, which are well preserved in the thickness of 30 to 60 m on the Oiso Hills 20 km east of Hakone, suggesting violent explosion of Plinian to Vulcanian type took place repeatedly. The major part of basalt and andesite in this stage is characterized by the presence of pigeonite pyroxene in the groundmass and is classified as the pigeonitic rock series (see p.63 ).

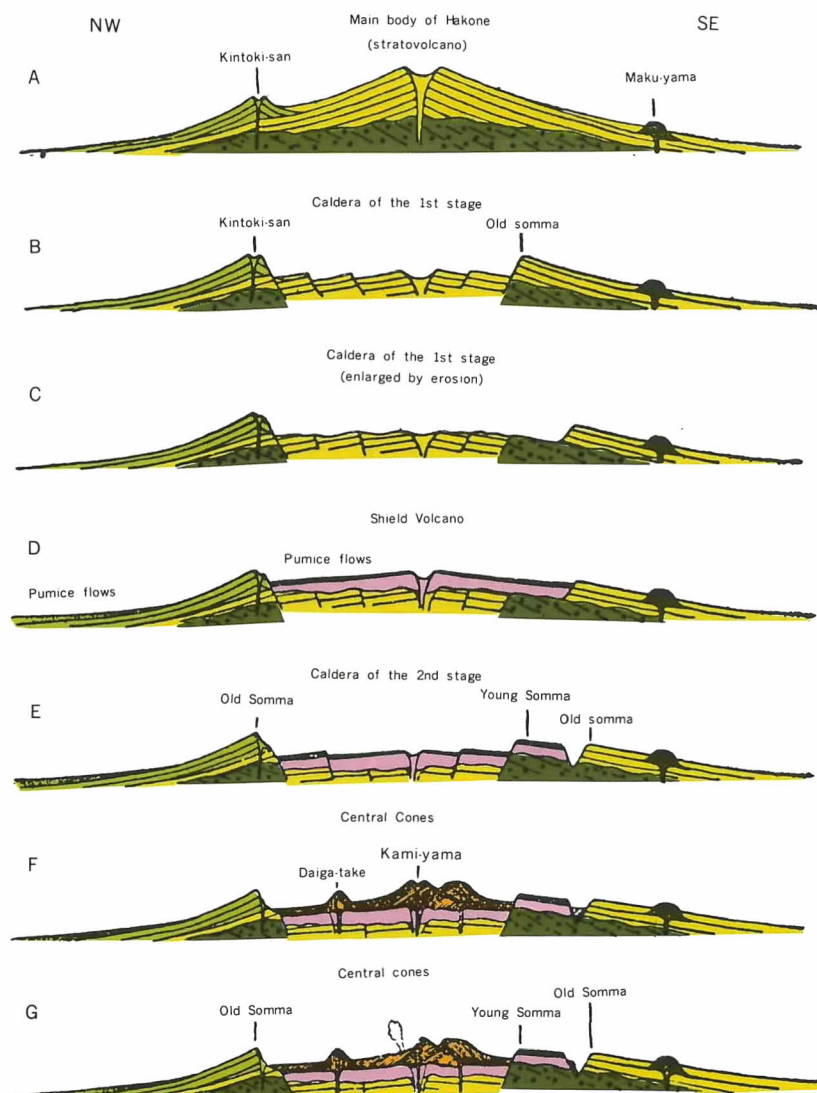
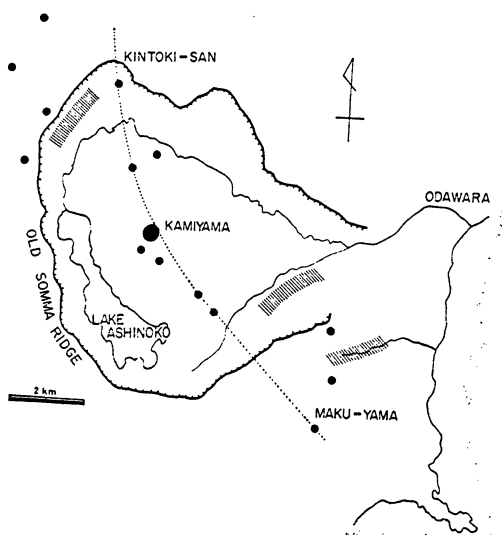


Fig. 3-5. Geologic development of Hakone volcano (Kuno, 1950 b)

### Satellite cones and dikes

Several satellite cones of pyroxene andesite and dacite including Kintoki-san and Maku-yama were formed on the main cone along the northwest-southeast direction called the Kintoki-san–Maku-yama dislocation line. Kuno (1964) observed 96 dikes in a zone 855 m wide over this dislocation line and estimated that about 215 dikes filled the zone of dike swarm. This further implies the edifice was expanded 650 m by the intrusion of dikes, the average thickness of which is 2.85 m.

Nakamura (1969) emphasized that the northwest trending compressional stress prevailed during the first and later stages, resulting the appearance of several satellitic and central cones as well as the penetration of the dike swarm as described above. Hakone is actually a volcano of the central eruption, however, the preferred distribution of satellite cones and dike swarm in a NW trending zone is suggestive of the existence of a rift zone, through which magma had been extracted (cf Fig. 5-12).



**Fig. 3-6.** Distribution of satellite cones, dikes, and post caldera cones (Kuno 1964, Nakamura 1977).

### The first caldera

It was about 200,000 years ago, the central part of the main body collapsed to form the first caldera about 8 km in original diameter. Machida (1971) recognized that three units of the pumice flow of the first stage exist in the upper horizon of the tephra in the Oiso Hill, suggesting that catastrophic explosions took place to form a caldera of the Krakatoa type.

This was followed by a long period of erosion during which the eastern part of the caldera wall was much breached. The debris from this as well as from the other part of the caldera were removed by the rivers which cut out a canyon

through the eastern rim toward Sagami Bay. Thus, the caldera was much enlarged toward the east beyond the original boundary of the collapse. The Tertiary basement rocks of Hakone were finally exposed along the bottom of valleys.

#### **Shield volcano, the second stage**

The second period of eruption started with explosion of more salic materials about 130,000 years ago. After repeated explosions of pumiceous ash and lapilli, fluid lavas of felsic andesite and dacite, all of the pigeonitic rock series, poured out and built a flat cone of shield volcano within the caldera. The fluid lavas flowed down the canyon and filled it up. The aggregate thickness of the lavas is about 300 m at maximum and the materials extracted during the second stage was about  $14 \text{ m}^3$ , which is one tenth of the volume of the main cone. The pyroclastics, mostly pumice falls, of the second stage are well preserved in the Oiso Hills.

#### **The second caldera**

It was about 70,000 to 45,000 years ago, when a great amount of dacite and andesite pumice was erupted from the central crater of the shield. Pumice flows spread over the surface of the shield as well as on the outer slopes of the main cone. Eleven successive flows have been recognized. One of the pumice flows reached a point as far as 50 km from the crater. The total volume of the pyroclastic flows amounts to  $15 \text{ km}^3$ . After the pumice eruptions, the central part of the shield volcano collapsed to form the second caldera, which largely overlapped the collapsed area of the first caldera. The eastern part of the shield was left as table mountains, whose summits form an arcuate ridge indicating the eastern rim of the second caldera, which is called the Young Somma (Fig. 3-7). Two major drainages inside the caldera have developed just along the boundary between the Young Somma Lavas and the Old Somma Lavas.

#### **Post-caldera cones, the third stage**

The third period of eruption was caused by viscous magma of augite-hypersthene andesite of the hypersthenic rock series. In the early stage about 30,000 years ago violent explosions took place and scattered pyroclastic fragments mostly pumice over the extensive areas of the southern Kanto district. Immediately after this event, seven post-caldera cones, one composite cone and six lava domes, were built along the Kintoki-san Maku-yama dislocation line. The order of formation of the post-caldera cones from north to south can be seen in comparing the degree of denudation of dome-slopes. A nuée ardente was discharged from the summit crater of Kami-yama, a post-caldera composite cone and run through the Haya-kawa canyon down to Yumoto, the East Entrance. A  $^{14}\text{C}$  age of a charcoal fragment from the nuée ardente is  $20,000 \pm 690 \text{ B.P.}$  The total volume of the post-caldera cones amounts to  $10 \text{ km}^3$ .





**Fig. 3-7.** Futago-yama, twin domes of post caldera cones and Ashinoko, caldera lake (photo : Odakyu Railway Co.).

#### **Ahsinoko, caldera lake**

The last phase of the activity was a strong phreatic explosion followed by extrusion of lava spine in the explosion crater. The northwestern part of Kami-yama was largely collapsed by the phreatic explosion and the debris flowed down to the west wall of the caldera as dry avalanche, which dammed up a drainage of the caldera floor to form a caldera lake Ashinoko (Fig. 3-8).  $^{14}\text{C}$  age of a cedar from the avalanche deposit is  $3,100 \pm 90$  B.P. Following this explosion, the central part of the explosion crater was updomed by the rising of very stiff magma, and finally a lava spine came out through the roof of the dome. Another thin layer of pyroclastic flow veneered the surface of the avalanche.  $^{14}\text{C}$  age of the charcoal trunk from the pyroclastic flow is  $2,900 \pm 100$  B.P. (Oki and Hakamata 1975). Solfataric activity is still taking place at some places on the flank of Kami-yama such as Owaku-dani, Bozu-jiigoku, Soun-jigoku and Yunohana-zawa on the east flank of Koma-gatake.

## Structure of the Hakone caldera

The main edifice of Hakone collapsed two times which resulted in the formation of Old and Young calderas. Thus, the original surface of the foundation in central part was assumed to be at some depth of a thousand meters or more below the surface. Many deep wells drilled for thermal waters allowed us to make inspection of drill-cores for the study of the caldera structure (Kuno et al. 1970). Twenty deep drillholes selected for detailed examination are plotted in Figure 3-8 together with columnar sections.

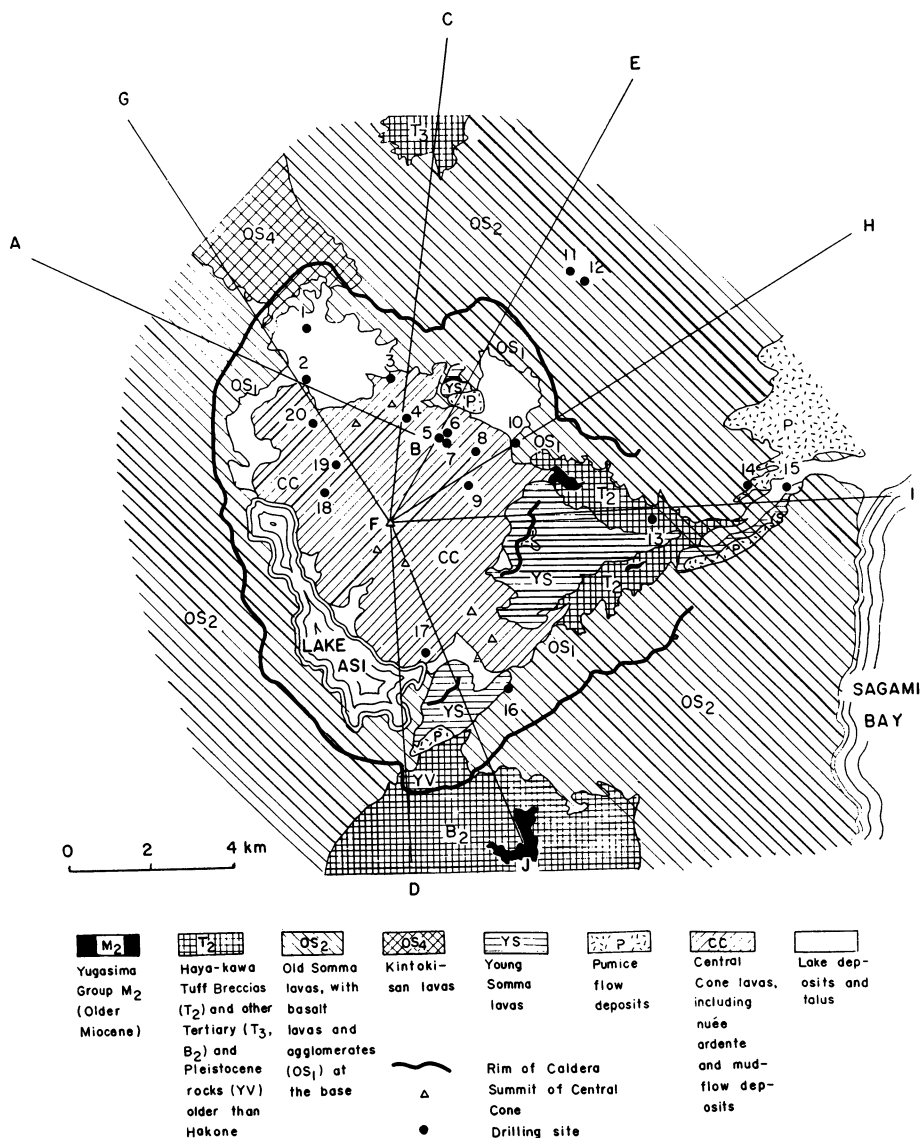
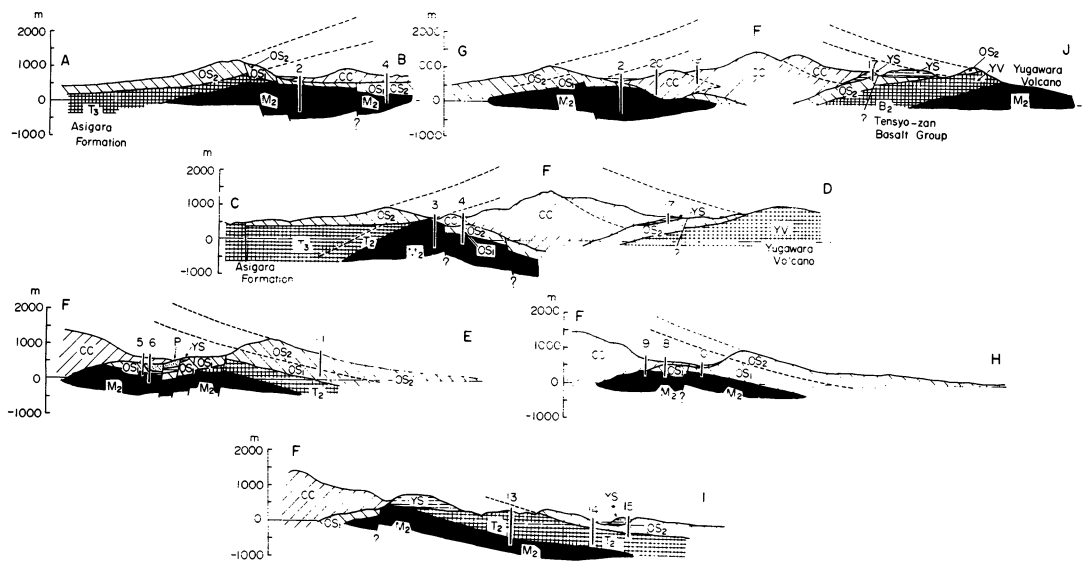


**Fig. 3-8.** Simplified geologic map of Hakone volcano showing the drill sites and the positions of cross sections of Fig. 3-9 (Kuno et al. 1970).

The most striking facts are the surface of the Tertiary Yugashima group lies at fairly shallow depth within the caldera. The Old and the Young Somma Lavas are rather thin and sometimes missing in the bottom of the caldera. This fact implies that the engulfment responsible for the formation of the Hakone caldera was not so large, but that a huge amount of the volcanic edifice was blown away by catastrophic explosions and removed by erosion. The revised section of the structure of the Hakone caldera inferred from drill data are shown in Figure 3-9, 3-10.



Yokoyama (1966) made a gravity study on Hakone and found the presence of low Bouguer anomaly in the middle of the caldera like some other caldera of the Krakatoa type. He explained this gravity low by assuming a flat inverted cone made up of low density material, which he terms the fall back of the ejecta. It may correlate with the loose, shattered material produced by the collapse of the volcanic edifice. A region about 2 km in diameter in the middle of the caldera may be filled with pumice from the vent.

Kuno et al. (1970) estimated the amount of subsidence in the caldera floor based on the difference of the altitudes between the extrapolated boundary of certain geologic horizons and the real one observed in the column of drill core (Fig. 3-11).

It is seen that the subsidence begins at points about 1 km from the caldera wall. This means that the diameter of the original caldera has been enlarged 2 to 3 km by later erosion. The average subsidence is about 600 m at a distance of 2 km from the wall and is 1,200 m at a distance of 3 km. In the center of the caldera it is probably about 1,800 m.

The mode of subsidence in the Hakone caldera was examined with two models. If the magma reservoir has a shape of laccolith whose diameter is much larger than that of the caldera, the subsidence would take place along the ring fracture (Fig. 3-12 A). If the reservoir has a shape of a cupola of small diameter, but with a great vertical extension, small blocks separated by radial and concentric fractures would be engulfed step by step into the reservoir by stoping. The later model seems to be more adequate to Hakone.

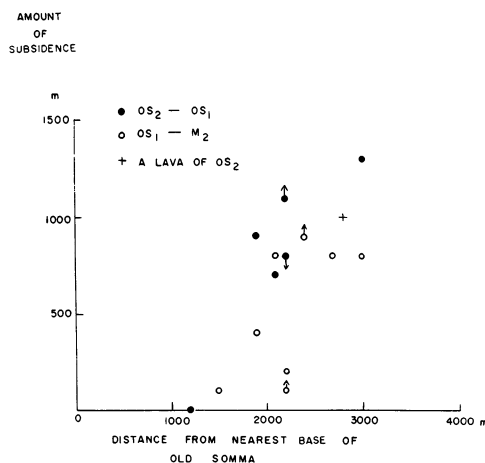


**Fig. 3-11.** Diagram showing the amount of subsidence at the drill site given in Fig. 3-9. OS₂-OS₁, OS₁-M₂, and a lava of OS₂ denote the reference horizons by which the amount of subsidence was estimated (Kuno et al. 1970).

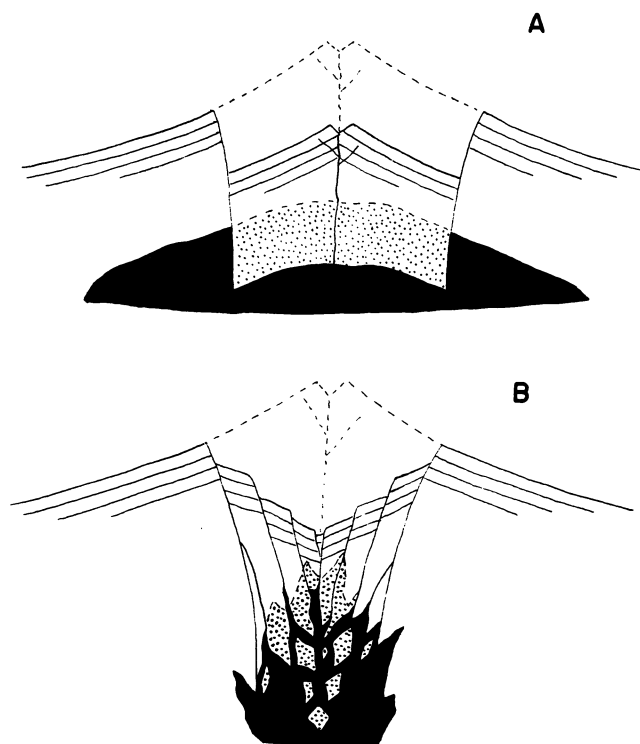
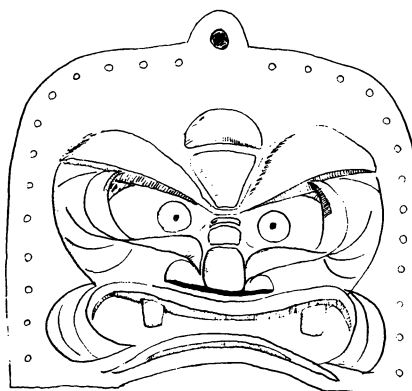


**Fig. 3-12.** Modes of subsidence in relation to the size and shape of magma reservoir (black area). The dotted area represents the extent of the magma reservoir before the subsidence (Kuno et al. 1970).



## 4. The Quaternary Volcanoes of the Izu Peninsula

### 4.1 General statement

The Quaternary volcanoes in the Izu peninsula are aligned in two parallel lines running north to south as shown in Figure 4-1. The eastern row passes along the eastern shore of the peninsula and the volcanoes are, from north to south, Hakone, Yugawara, Taga, Usami and Amagi. The western row is made up of Ida, Daruma, and Tanaba volcanoes from north to south, interrupted in the central part of the peninsula but extends to Jaishi and Nanzaki volcanoes near the southern tip. Thus these two rows of Quaternary volcanoes determine the topographic framework of the Izu peninsula, especially its northern half. The broad valley running from south to north in the central part was the scene of the major human activity in the old days while the eastern and the western coasts were bounded by precipices and difficult to access. In the southern part of the peninsula, the basement rocks of Yugashima and Shirahama groups form a relatively low undulating topography. A small volcano, Tenshi, is situated between Usami and Amagi volcanoes but is a little offset to the west of the main axis.

	Acidic		Basic		Unknown	Total	
	N	Vol. Km ³	N	Vol. Km ³	N	N	Vol. Km ³
Lava Flow only			16	0.04		16	0.04
Lava Flow + Pyrocl.Cone			24	1.94		24	1.94
Lava Dome	3	0.04	1	0.005		4	0.045
Pyrocl.Cone or Pyrocl.Fall			21	0.12		21	0.12
Crater only					9	9	
P.Fa.→PFI →Lava Flow	1	0.26				1	0.26
Small Stratovolc.			1	0.05		1	0.05
Total	4	0.30	63	2.155	9	76	2.455

**Fig. 4-1.** Index map showing the distribution of the Quaternary volcanoes in the Izu peninsula. The area of the Higashi-Izu monogenetic volcanoes is shown where individual vents are indicated by solid circles.

All the Quaternary volcanoes belonging to the western row are deeply dissected with a tendency that the northern ones retain more of the original conical shape as compared with the southern ones. The same is true for the eastern row. Amagi volcano situated at the south end of the row is deeply dissected with a large (5 km x 5 km) erosion caldera opening toward southeast. Tenshi and Usami volcanoes are also deeply dissected and the K-Ar ages of the lavas of Usami volcano range from 900,000 to 600,000 years (Kaneoka et al. 1970). The general geology and stratigraphic sequence of the northern four volcanoes, i.e. Usami, Taga, Yugawara and Hakone volcanoes are established by the late Prof. Kuno (Kuno, 1950 b, 1951, 1952), who found that age becomes progressively younger toward north. Thus the general picture of the Quaternary volcanism in the Izu peninsula is the northward shift of the activity but this is broken by the latest volcanic eruptions which broke out around Amagi volcano. In Figure 4-1 this is shown by a group of small volcanoes called Higashi-Izu monogenetic volcano group (Aramaki and Hamuro, 1977). These small volcanoes occur in a large area but their mode of eruption is characteristically similar. All of them were formed by a single episode of eruptive cycle lasting for a very short time geologically speaking while all the other Quaternary volcanoes (possibly excepting Nanzaki volcano) were made up by repeated eruptions of lavas and pyroclastics, probably lasting up to 500,000 years. The time span of the whole Higashi-Izu monogenetic volcano group was probably less than 50,000 years (Aramaki and Hamuro, 1977). Moreover, this group is made up of about 88% (by volume) of basalt and 12% of dacite with no andesites of the intermediate composition whereas other volcanoes are composed of much andesites, smaller amounts of basalts and still smaller amounts of dacites. Similar monogenetic volcanoes are present underwater immediately off the eastern coast over the sea floor between Oshima island and the Izu peninsula. A single dredge haul from the area produced a fresh tholeiitic basalt.

## **4.2 Yugawara volcano**

The Yugawara volcano is a medium-sized stratovolcano made up of mafic andesite lava flows and pyroclastics of rather uniform composition. The central vent was situated around the town of Yugawara which is now a bustling hot-spring resort area. The central portion of the volcano has been completely eroded to show thick pile of Pliocene basalts (Tensho-zan basalt) and Miocene Yugashima group. Only the western slope of the volcano remains forming a continuous ridge along the crest of which the Izu Skyline toll road runs in the north-south direction.

### **4.3 Taga volcano**

Taga is larger than Yugawara volcano to the north and Usami volcano to the south. This is a complex group of stratovolcanoes whose eruptive vents shifted from time to time with the general central vent near and/or east of the present town of Taga on the east coast. Like Yugawara volcano, the eastern half of the volcanic structure has been completely destroyed and the presumed vent areas now correspond with such active hot-spring resorts like Atami, Taga and Ajiro (Ajiro). The earliest activity began probably in shallow water to produce thick deposit of hydro-brecciated volcanoclastic andesite. The later main stage of cone-building is represented by mafic andesites and basalts with minor felsic andesite. To the west of the Izu Skyline drive and westward-dipping slopes of Taga volcano are cut and displaced by the north-south trending, left-lateral Tanna fault, the main fault of the Kita-Izu fault system (Fig. 5-12).

### **4.4 Usami volcano**

Immediately south of Taga volcano lies the profoundly dissected stratovolcano Usami. Its eastern half is eroded away and its northern part is buried by Taga volcano. Only the remaining western and southern slopes indicate that this was a medium-sized stratovolcano made up of olivine-augite-hypersthene andesite lava flows and pyroclastics. A sequential paleomagnetic study revealed that the lower part of the cone was built during the last major reversal of the earth's magnetic field about 700,000 years ago (Kono, 1968).

### **4.5 Amagi volcano**

South of Usami lies a large stratovolcano Amagi made up mainly of pyroxene andesites (Kurasawa, 1959). Amagi once was as large as Hakone but probably not as high though it now forms the highest peak (1,405 m) in the Izu peninsula. The present-day volcanic edifice of Amagi rises high because of the high altitude of the basement composed mainly of Yugashima group reaching above the height of 1,000 m. The net thickness of the Amagi lavas does not exceed 500 m. The top of the main cone has been breached to form an erosion caldera opening toward southeast. The lavas are thicker and more felsic than those of the four volcanoes (and Hakone also) to the north. They are pyroxene andesites and some hornblende andesites the latter being relatively rare in the Izu peninsula.



#### 4.6 Volcanoes in the western row

Three volcanoes in the northwestern part of the peninsula are Ida, Daruma and Tanaba volcanoes, all of them are stratovolcanoes overlapping one another. Ida, the smallest, consists of much basaltic lavas and pyroclastics with some andesites while Daruma and Tanaba are solely made up of pyroxene andesites (Kurasawa and Michino, 1976). The slopes are well preserved on the eastern side of these volcanoes but the western side is deeply eroded with top craters opening wide toward west.

Jaishi volcano in the southwestern part of the peninsula is a remnant of a small andesitic stratovolcano resting upon the Miocene submarine basement (Shirahama group). Nanzaki volcano near the southern tip of the peninsula is very unique, though very small in size, in that it erupted scoria and lava flow of olivine-augite basalt (basanitoid) with about 7% of normative nepheline.

#### 4.7 Higashi-Izu Monogenetic Volcano Group

The last 50,000 years have seen very low or dormant volcanic activity in the Izu peninsula except in the area around Amagi volcano. Most of the stratovolcanoes had passed into the stage of extinction and in the process of extensive denudation. This is in contrast with the highly active Fuji volcano which was then vigorously depositing basaltic ash and scoria over the eastern slopes as far as the vicinity of Tokyo. Hakone volcano was at that time in the stage of building several andesite lava domes inside the younger caldera. There are 76 vents thus far identified in the area of Higashi-Izu monogenetic volcano group distributed over an area of several hundred square kilometers (Table 4-1). The general geology is shown in Figures 4-2 and 4-3. Of these, 63 erupted basaltic material, 4 dacitic and 9 erupted practically no juvenile materials but formed only circular depressions (Table 4-1). Figure 4-4 shows a histogram of the volume of the ejecta according to the  $\text{SiO}_2$  content. A bimodal character with a hiatus in the range  $\text{SiO}_2 = 60 \sim 65\%$  is remarkable. Most of the dacitic activity was concentrated in the last 3,000 years while the major basaltic activity probably started more than 40,000 years ago. Almost all of the vents were active for a single cycle of eruption to produce small-scale, simple-structured volcanic edifices such as scoria and ash cones, lava flows and lava domes.

One of the largest scoria cones is Omuro-yama, about 8 km south of a popular hot spring resort of Ito (Fig. 4-2). It is a beautiful symmetric cone rising 581 m above the sea level. The diameter of the base of the cone is about 1,000 m and the net height is 280 m, with a slope dipping about  $30^\circ$ . The top crater is 250 m across and 75 m deep. The side of the cone is buried by a small shield volcano made up of basaltic lava flows which issued mainly from a



# LEGEND

# 凡例 (降下火砕堆積物は、すべて取り除いてある)

	ALLUVIUM	河床礫・湖水堆積物および崖堆積物
	LAVA DOME	矢筈山・孔ノ山・岩ノ山・台ノ山(溶岩円頂丘)
	IYU-ZAN	伊雄山
	ANANO-KUBO	孔ノ窪
	AKAKUBO	赤窪
	OMURO-YAMA	大室山
	KOMURO-YAMA	小室山
	UCHINO	内野
	JOBOSHI	城星
	KADONO	門野
	IKEDA-HIGASHI	池田東
	KAWANA-MINAMI	川奈南
	SANOHARA-KITA	三野原北
	HARAI	払
	CHIKUBO	地久保
	AMAGI VOLCANO	天城火山噴出物
	IKEITA ADNESITES	池北安山岩類
	TOTARI ANDESITES	十足安山岩類
	USAMI VOLCANO	宇佐美火山噴出物
	SHIOFUKI-ZAKI BASALTS	汐吹崎玄武岩類
	SHIRO-YAMA DACITE	城山石英安山岩類
	AWARADA ANDESITES	阿原田安山岩類
	SHIRAHAMA GROUP	白浜層群
	YUGASHIMA GROUP	湯ヶ島層群
	CRATER	火口
	VENT OF LAVA FLOW	溶岩流出口
	PYROCLASTIC CONE	火砕丘
	FLOW DIRECTION	溶岩流出方向

## LAVA FLOWS

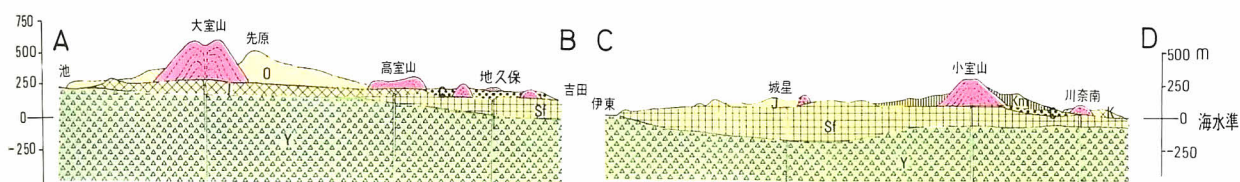






**Fig. 4-3.** Aerial view of the part of the eastern coast of the Izu peninsula occupied by the Higashi-Izu monogenetic volcano group. Looking toward south; Sagami Bay on the left. In the upper center, the grass-covered scoria cone of Omuro-yama is an outstanding topographic feature of the area. Lava flows jutting into the Sagami Bay (left). Small circular lake is Ippeki-ko, a maar-like crater. Amagi volcano in the far right. (Photo; Izu Natural History Park, Shaboten-kōen)



Omuro - yama scoria viewed from south. Topographic high at the eastern (right) foot is the vent of the lava flow.

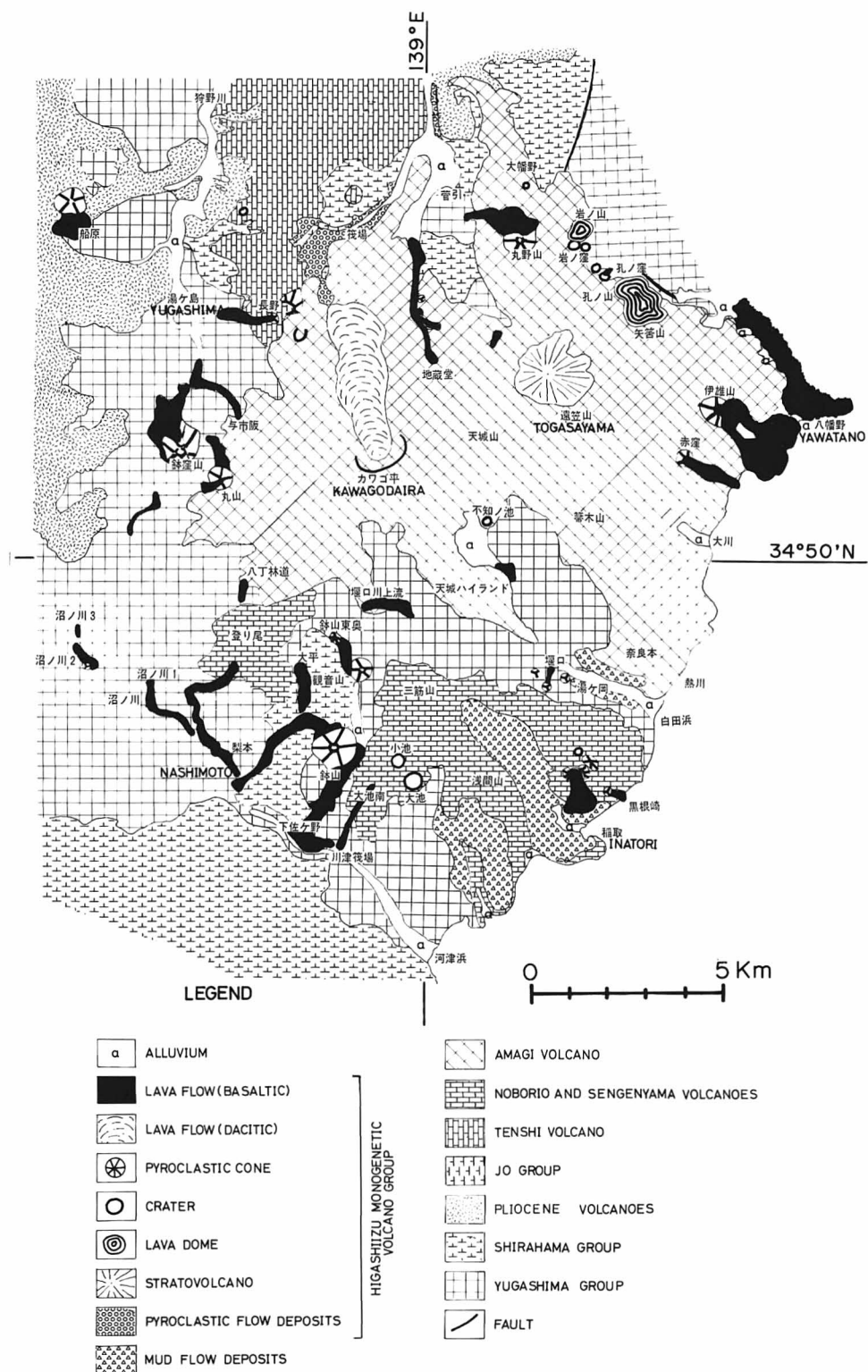
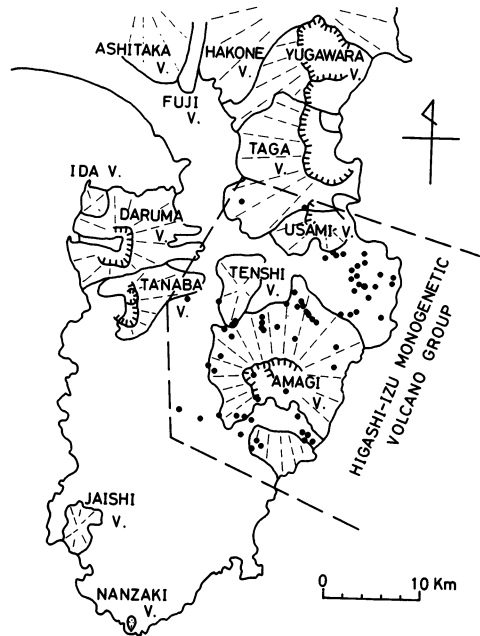


Fig. 4-4. Geologic map of Amagi volcano area corresponding to the southwestern part of the Higashi-Izu monogenetic volcano group (Aramaki and Hamuro, 1977).



**Table 4-1.** Frequency and volume of ejecta erupted from the vents of the Higashi-Izu monogenetic volcano group as classified according to the character of vents and composition of magma (Aramaki and Hamuro, 1977).

vent near the northeastern foot of the cone of Omuro-yama. The whole picture of the pyroclastic cone and the basaltic shield is very much similar to Paricutin volcano in central Mexico, which was formed by a 9-year eruptive episode during 1945 – 1952. In Paricutin and very probably in Omuro-yama, the main vent ejected basaltic scoria and ash together with bombs by repeated explosions of the Strombolian type. The ejecta thus formed a pyroclastic cone (cinder cone) and the liquid lava quietly issued from the base of the cone to spread laterally forming a flat lava shield. Komuro-yama, (Fig. 4-2) about 4 km southeast of Ito city, Maruno-yama, Hachikubo-yama, and Maru-yama (Fig. 4-3) all in the western part of the area are other outstanding pyroclastic cones with lava flows very much similar to Omuro-yama.

Another group of smaller-scale volcanic bodies is found under water just off the coast of the Higashi-Izu monogenetic volcano group. The size and position of these submarine volcanoes are shown in Figure 4-5 as well as the subaerial Higashi-Izu monogenetic group. Most of the submarine volcanoes display symmetrical conical outlines with smooth surface suggesting their recent origin. Their much gentler dips of the slopes indicate the internal structure different from the subaerial equivalents. From Figure 4-5, it may be seen that the vents either on land or under water tend to align in the direction northwest-southeast i.e. parallel to the direction of the maximum compression of the local crust (See p. 56 – 57).

The dacitic magma produced steep-sided lava domes (Yahazu-yama, Iwano-Yama etc. in Fig. 4-2) and one thick lava flow (Fig. 4-3, Kawago-daira lava flow). The latter was erupted about 3,000 years ago ( $^{14}\text{C}$  dating, Hamuro, 1978). The vent was formed on the northern crest-line of the erosion caldera of Amagi volcano at an altitude of about 1,000 m. Abundant pumice and ash were first ejected and fell over a wide area forming a layer which serves as a good key bed for the tephrochronology (Hamuro, 1978). Next erupted more voluminous pumice that rushed down the northern slopes as a pyroclastic flow (hot avalanche). It buried a thick forest of cedar which was charred and has been preserved as huge carbonized logs. The pyroclastic flow deposits probably extended more than 12 km down the stream along whose course the destructive effect must have been very great. The last phase of the eruption was the outflow of viscous dacitic lava that formed a continuous lava bed about 4.4 km long, 1 km wide and more than 20 m thick. Topmost part of the lava flow is glassy and in some parts it is compact (obsidian) and in other parts it is so highly vesiculated into pumiceous blocks that they are now being quarried as thermally insulating materials.

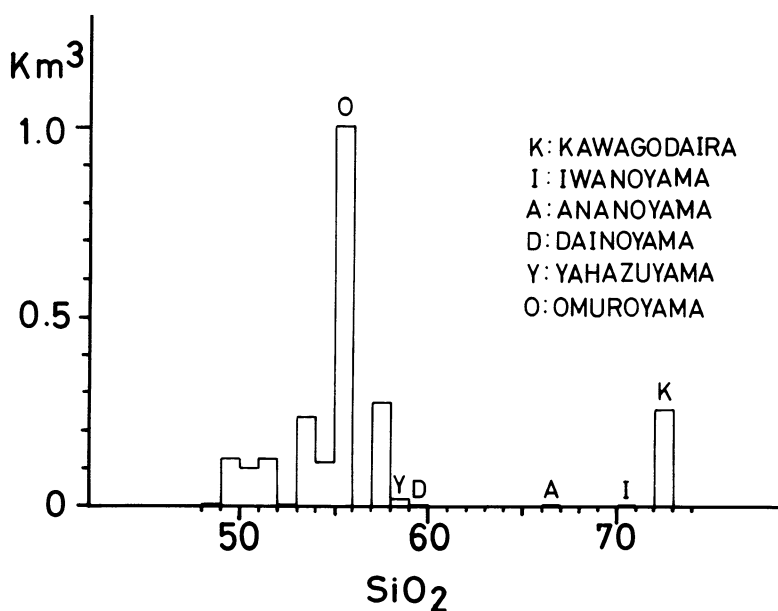


**Fig. 4-5.** Bar diagram showing volume relation between the  $\text{SiO}_2$  content of the erupted materials of the Higashi-Izu monogenetic volcano group (Aramaki and Hamuro, 1977).

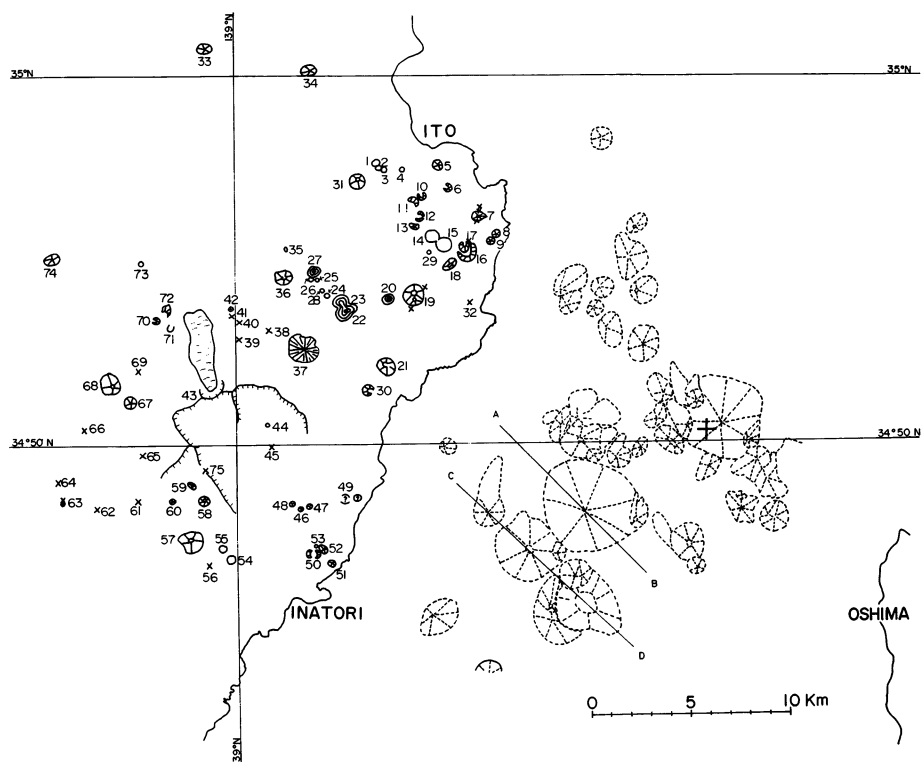


**Fig. 4-6.** Map showing the distribution of the vents and volcanic structures in the Higashi-Izu monogenetic volcano group (Aramaki and Hamuro, 1977). Submarine volcanic structures interpreted from the topographic map by the Hydrographic Department are also shown in dashed lines.

- |                      |                           |                           |
|----------------------|---------------------------|---------------------------|
| 1 Hachiga-kubo 1     | 26 Iwanokubo-nishi        | 51 Inatori-2              |
| 2 Hachiga-kubo 2     | 27 Iwano-yama             | 52 Inatori-3              |
| 3 Hachiga-kubo 3     | 28 Fujimikubo             | 53 Inotori-4              |
| 4 Hachiga-kubo 4     | 29 Arayama                | 54 Oike                   |
| 5 Uchino             | 30 Akakubo                | 55 Koike                  |
| 6 Joboshi            | 31 Hachiga-kubo 5         | 56 Oike-minami            |
| 7 Omuro-yama         | 32 Harai                  | 57 Hachi-yama             |
| 8 Kawana-minami      | 33 Takatsuka-yama         | 58 Hachi-yama-higashi-oku |
| 9 Sannohara-kita     | 34 Sukumo-yama            | 59 Kannon-yama-higashi    |
| 10 Akasaka-minami    | 35 Ohatano                | 60 Odaira                 |
| 11 Kadono            | 36 Maruno-yama            | 61 Noborio-minami         |
| 12 Ikeda-higashi     | 37 Togasa-yama            | 62 Numano-kawa-1          |
| 13 Ogi               | 38 Sugehiki               | 63 Numano-kawa-2          |
| 14 Ippekiko          | 39 Jizodo-1               | 64 Numano-kawa-3          |
| 15 Higashi Oike      | 40 Jizodo-2               | 65 Haccho-rindo           |
| 16 Chikubo, outer    | 41 Jizodo-3               | 66 Hontani-gawa-shiryu    |
| 17 Chikubo, inner    | 42 Jizodo-4               | 67 Maru-yama              |
| 18 Takamuro-yama     | 43 Kawago-daira           | 68 Hachikubo-yama         |
| 19 Omuro-yama        | 44 Shiranutano-ike        | 69 Yoichi-zaka            |
| 20 Daino-yama        | 45 Amagi Highland-higashi | 70 Nagano                 |
| 21 Iyu-zan           | 46 Sekiguchi-1            | 71 Hokibara-higashi       |
| 22 Yahazu-yama       | 47 Sekiguchi-2            | 72 Nagano-higashi         |
| 23 Anano-yama        | 48 Sekiguchi-3            | 73 Kitano-hara-higashi    |
| 24 Anano-kubo        | 49 Yugaoka                | 74 Funabara               |
| 25 Iwanokubo-higashi | 50 Inatori-1              | 75 Sekiguchi-gawa-joryu   |



Starting from the summer of 1975, unusual crustal upheaval and swarms of microearthquakes were detected over the area occupied by the Higashi-Izu monogenetic volcano group and the adjacent submarine counterparts. Local upheaval reached more than 15 cm within a period of three years in the area southwest of Ito city (Fig. 4-6). Microearthquake swarms culminated to a  $M = 5.4$  earthquake of Aug. 18, 1976 on the southern slope of Amagi volcano, which caused some property damage. By the end of 1977, the microearthquakes have subsided considerably but this is very much reminiscent of an event in 1930. The 1930 earthquake swarms and local uplift were centered around the area off the coast of the city of Ito and lasted about 2 months. As shown in Figure 4-6, the general distribution of the earthquake foci of 1975 – 1977 event matches with that of the vents of the Higashi-Izu monogenetic volcano group and the submarine volcanoes off the coast. The subterranean movement of the magma as a cause of the 1930 Ito earthquakes and upheaval was a popular hypothesis among the scientists at that time (Nasu, 1932, Kuno, 1954 etc.). The same possibility applies to the 1975 – 1978 event occurring over much wider areas than in 1930, but there are no positive evidence so far to support the hypothesis.

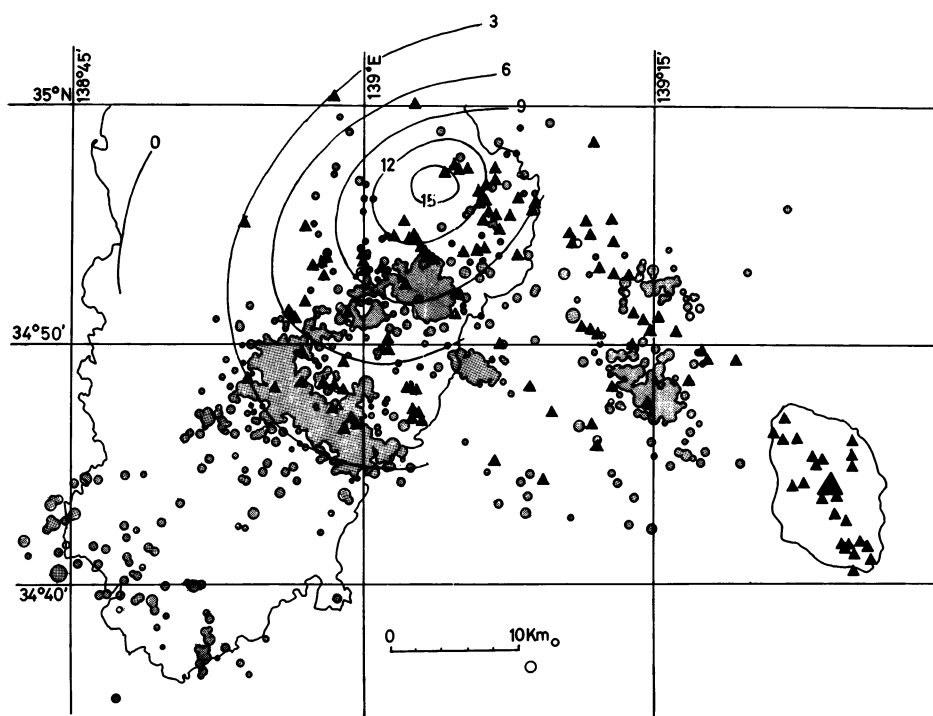


**Fig. 4-7.** Map showing the distribution of epicenters of small earthquakes (magnitude larger than 0.5) during the period from Nov. 20, 1975 to Dec. 31, 1976 (after Tsumura et al., 1977). Solid triangles indicate locations of vents of the Higashi-Izu monogenetic volcano group (see Fig. 4-5).

## 5. Izu-Oshima Volcano

### 5.1 Introduction

Izu-Oshima is known as an island of an active basaltic stratovolcano in Sagami Bay. The island is located some 100 km SSW of Tokyo between  $34^{\circ}40.5'$  –  $34^{\circ}48'$  north latitude and  $139^{\circ}21'$  –  $139^{\circ}27'$  east longitude. On a fine day, its profile of a flattened triangle is seen from the Sagami Bay shore. The island is easily accessible both by airplanes and boats. Airplanes leave Tokyo domestic airport (Haneda) daily in the morning and take about 40 minutes to the Oshima airport on the northwestern coast of the island. Boats are scheduled daily from several harbors of Honshu, including Tokyo, Atami and Ito, and take a few to several hours. The boats arrive at either northern (Okata) or western (Motomachi) harbor, depending on the wind direction. In the island, scheduled bus transportation is available as well as rent-a-cars.

Izu-Oshima, which means a big (O) island (shima) of the Izu province, is the biggest island of the Izu archipelago or Seven Izu island, all of them being volcanic islands, either basaltic or rhyolitic in composition. These volcanic islands are the northern most insular volcanoes of Izu-Mariana island arc, which continues to the north into East Japan volcanic belt via Hakone and Fuji volcanoes.

Izu-Oshima island has been occupied by ancestral Japanese since at least 9,000 years ago (Isshiki et al., 1976) and the volcano has frequently been active since a few tens of thousand years ago when it emerged above the sea level. The overall explosion index (one hundred times volume ratio of fragmental/total products of the volcano) is about 60. This is rather low (or less explosive) compared with normal values (90 or more) of other Japanese volcanoes which are mostly andesitic. The latest eruption with lava outflow occurred in 1950 – 1951 and in 1953 – 1954, which triggered extensive studies of the volcano. The results are summarized in the following pages.

### 5.2 Topography

The island is parallelogram-shaped and has an area of about 92 km². Most valleys are shallow and dry, regardless of precipitation of about 3,000 mm per year. The island consists mostly of the products of Izu Oshima volcano. Sea cliffs are higher along eastern and northern coast where remnants of underlying old dissected volcanoes are exposed. Oshima volcano has a collapsed summit caldera, 3 km x 4 km wide. It is surrounded by walls up to 110 m high, except in the NE and SW parts where the original wall is buried beneath the post-caldera lava flows and scoria falls. The caldera is of Kilauean type and formed some 1,300 years ago after violent steam explosions from the summit crater (Fig. 5-1).

On the southern floor of the caldera, there is an active central cone, Mihara-yama (literally means divine hole mountain) with a crater 700 – 800 m in diameter, standing some 100 m from the floor. Mihara-yama as we see today was formed by a large-scale fire fountaining at the 1777 – 1778 eruption (the great An'ei eruption) which is the last major eruption that showered appreciable scoria and ash over outer slopes of the caldera. All the later eruptions, including those of 1950's, were far smaller and less explosive than this eruption and affected mainly inside the caldera or even the crater of Mihara-yama.

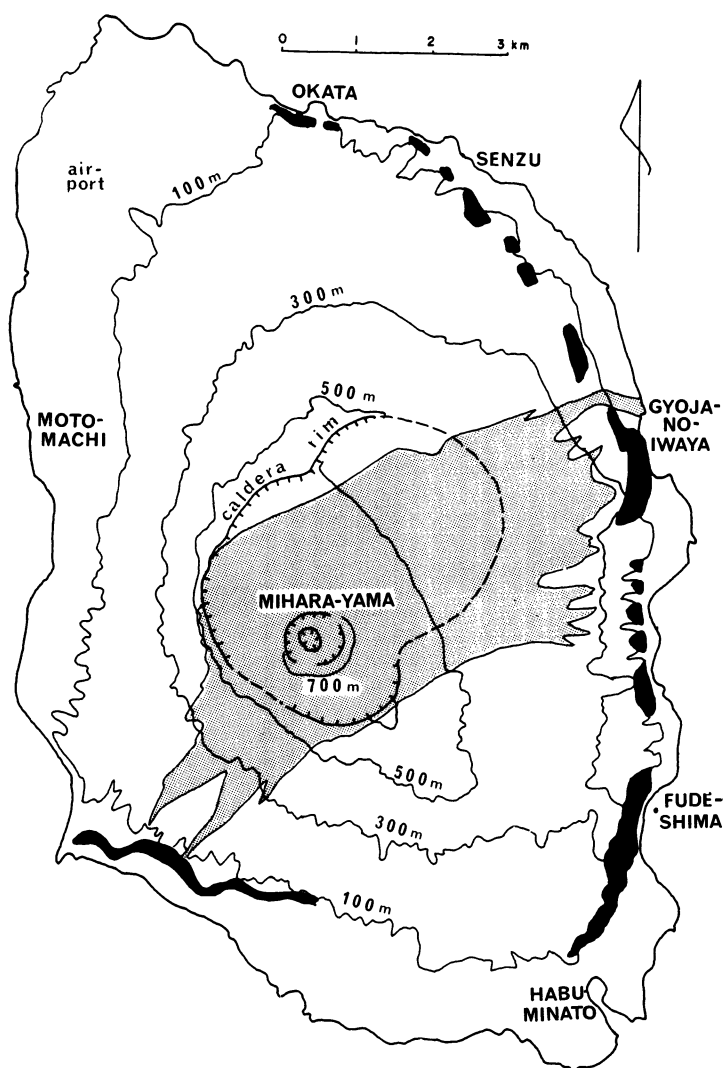


**Fig. 5-1.** Map of Oshima island. Contour interval 200 m. Shaded area: desert like area with less vegetation (after air-photos taken in 1947). Solid: inner old coastal cliff (cf. Fig. 5-2).

The highest point, 758 m above sea level, is marked by a small scoria cone formed on the south rim of Mihara-yama at the time of 1950 – 1951 eruption. Half of the scoria cone has collapsed into the crater pit renewed right at the former location of a pit. A still smaller scoria cone, formed at the 1953 – 1954 eruption toward the north of the 1950 – 1951 cone, has also collapsed by half into the same pit and shows up a nice cross section of it.

Dominant wind direction in the island has been WSW and NE. A belt of down wind desert develops through Mihara-yama because of the more or less continuous volcanic smoke from the crater. That part of the coast, where the belt attains at SW and ENE directions of Mihara-yama, is exceptionally sandy due to the sand supplied from the desert. The rest of the coast is generally rocky and provides places for beach fishing.

The slope of Oshima volcano is dotted with more than 20 flank volcanoes on the north and southeast. They are mostly scoria cones with or without lava flows and a few phreatomagmatic explosion craters.

### 5.3 Geology

The island of Oshima consists of highly dissected remnants of three old volcanoes and the products of Oshima volcano, which cover the old ones and occupy most of the subaerial portion (ca. 23 km³) of the island. Stratigraphic sequence is tabulated in Table 5-1. Schematic east-west cross section of the island is shown in Figure 5-2.

#### Older volcanoes

Following is an excerpt from Isshiki (1964) with minor revisions.

The immediate basement of Oshima volcano is made up of three highly dissected volcanoes exposed on the northwestern, eastern and southeastern coasts where cliffs up to 300 m in height face the sea. They are named Okata, Gyoja-no-iwaya and Fude-shima volcanoes, respectively. Okata volcano consists of alternate layers of lavas and pyroclastic rocks of pyroxene-olivine basalt and olivine basalt with a subordinate amount of dribble agglutinates and lavas of pyroxene andesite. These layers are cut by several olivine basalt dikes which are now exposed on the sea-cliff west of Okata harbor. They are also cut by many faults with small displacements possibly related directly with the volcanic activity. Fude-shima volcano also consists of lavas and pyroclastic rocks of pyroxene-olivine basalt and olivine basalt cut by explosion breccias and numerous dikes of the same petro-

**Table 5-1.** Stratigraphy of Izu-Oshima island (modified from Nakamura, 1964)

	Volcanic products	Years B. P.	Volcanic edifices	
Exposed in the island	Younger Oshima Group (lavas and pyroclastics, 3.6 km ³ )	10 ³		Mihara-yama (central cone )
			↑ ? ↓	← Formation of summit caldera
	Older Oshima Group (lavas and pyroclastics, 40 km ³ )	10 ⁴	Flank volcanoes (more than forty)	
	_____ ? _____ _____ ? _____		?	The Main cone (the somma)
	Senzu Group (4 km ³ )	10 ⁵	Mud-flows and explosion breccias with minor amount of lavas.	
	_____ ? _____			
*	Lavas and pyroclastics of base- ment volcanoes	10 ⁶	Remnants of three dissected volcanoes (Okata, Fudeshima and Gyoja-no-iwaya Volcanoes)	
	_____ ? _____			
	Yugashima Group	10 ⁷	A complex of altered andesite and basalt with submarine clastic sedimentaries intruded by quartz-diorites.	
	_____ ? _____			

* Found as accidental fragments in the Senzu Group.

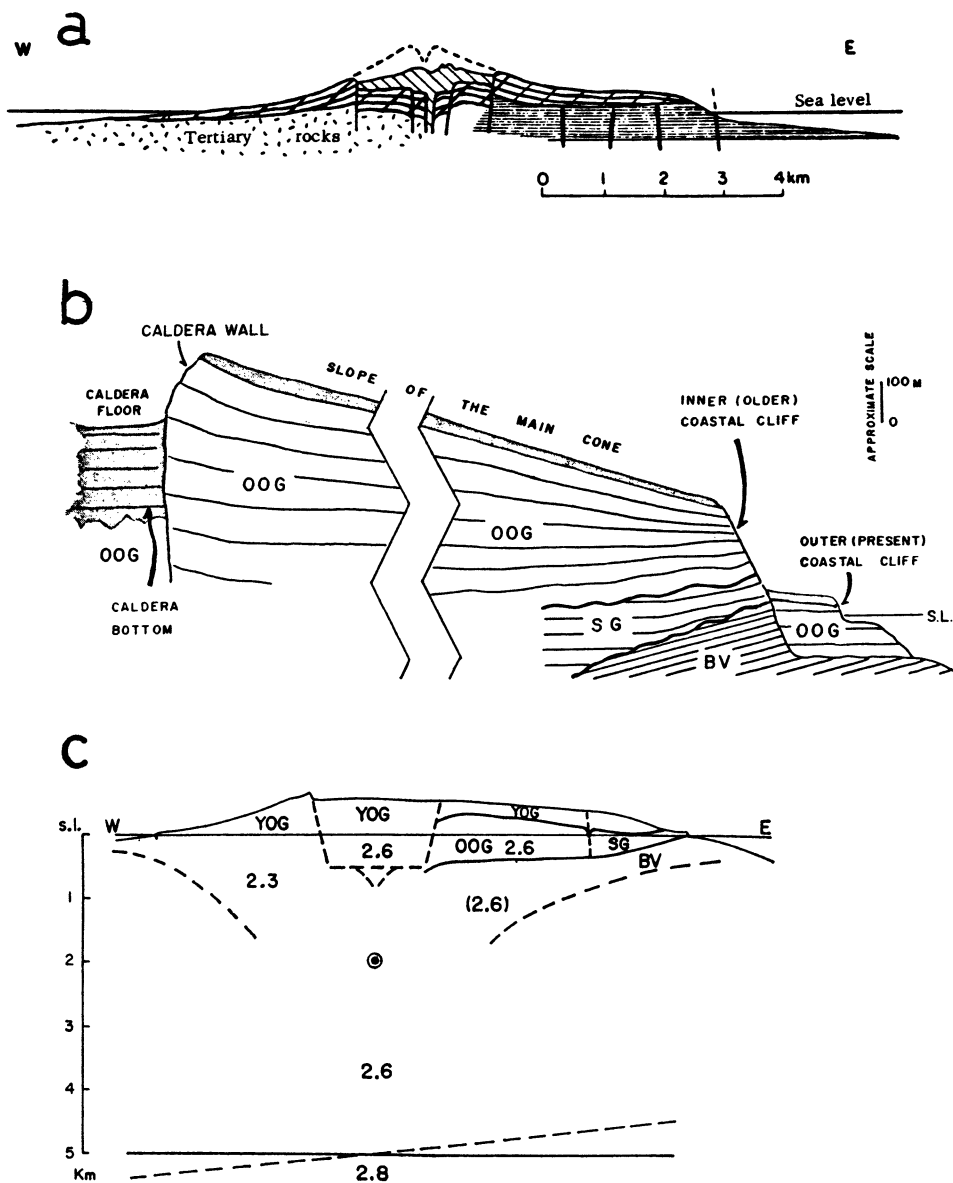


**Fig. 5-2.** Cross sections of Oshima island.

- a. Geologic cross section (Kuno, 1959 b).  
Thin oblique ruling: central cone lavas. Somma lavas constitute major parts of the island. Horizontal dense ruling: Fudeshima basalt group.
- b. Schematic cross section of the western half of the island (Nakamura, 1964).  
Half-tone area: Younger Oshima group. OOG: Older Oshima group. SG: Senzu group. BV: Erosion remnants of basement volcanoes.
- c. Section showing a density (g/cc) structure of the island (Yokoyama, 1969). Double circle: dipole responsible for the geomagnetic anomalies. Abbreviations are the same in b.

graphic character as that of the lavas. A surface geological survey and a drilling made near the southeastern coast revealed that the volcano was more than 950 m in thickness near the center. These two volcanoes must have been typical stratovolcanoes, when they are restored. Gyoja-no-iwaya volcano is represented only by three thick pyroxene basalt lavas and interbedded scoria layers. It could also be a part of a stratovolcano, although it is difficult to infer its original form and center of eruptions.

These volcanoes were formed in some period from late Pliocene to Pleistocene age. They are probably underlain by the Yugashima group (Table 5-1), a complex of altered andesite, basalt and dacite of early Miocene age widely exposed in the Izu Peninsula (cf. ch. 2). No exposure of the Yugashima group is found in the island, however. Fragments probably of the rocks of this group and the related plutonic masses are found in the coarse-grained volcanoclastic rocks (Senzu group) of Oshima volcano.

### **Oshima volcano**

Oshima volcano is a stratovolcano consisting of lava flows and volcanoclastic rocks of olivine basalt, pyroxene-olivine basalt and subordinate amount of pyroxene andesite with or without olivine phenocrysts.

Rocks of Oshima volcano are divided into lower and upper units. The lower unit (Senzu group, Table 5-1 and Fig. 5-2), exposed mainly on the north-eastern coastal cliffs, is composed largely of volcanoclastic rocks of mudflow and explosion breccia origin and partly of lava flows. The lower unit probably marks the stage of emergence of the volcano as an island above the sea level, when sea water still found its way to the vent area causing phreatomagmatic explosions.

The upper unit of rocks of the Oshima volcano is a normal subaerial basaltic product, that is, alternating lava flows and scoria and ash falls with minor amount of volcanoclastic flows and secondary deposits. The unit as a whole records continuous growth history of Oshima as a subaerial stratovolcano.

The upper unit is further subdivided into pre-caldera and co- and post-caldera deposits. The pre-caldera deposits are the Older Oshima group whose exposures are confined to coastal cliffs and deeper road cuts. The co- and post-caldera deposits are the Younger Oshima group, which crops out at scattered road cuttings and valley walls all over the island.



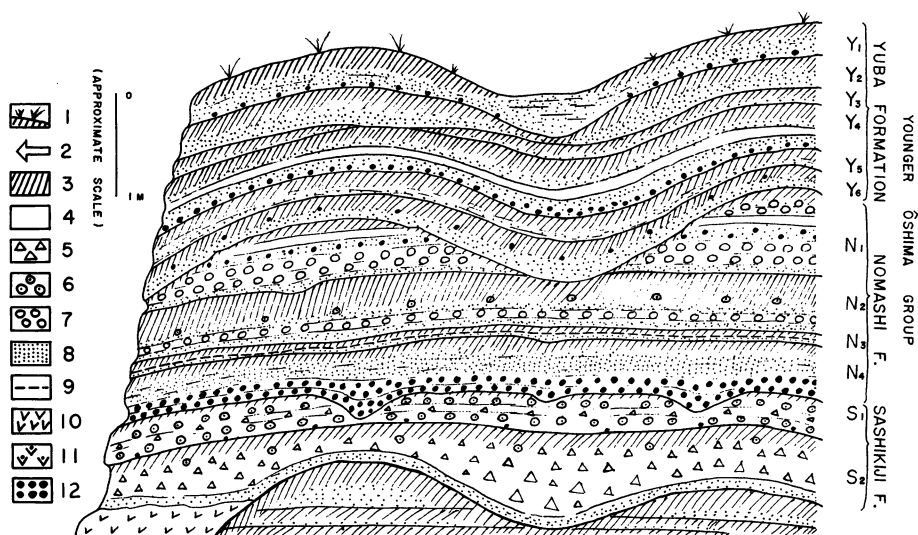


**Fig. 5-3.** An idealized sketch of a road-side exposure on the mid-slope of Oshima volcano (Nakamura, 1964).

1, present ground surface. 2, excavated horizon of pottery remains. 3, weathered ash or soil. 4, fine volcanic ash. 5, tuff breccia. 6, accretionary lapilli tuff. 7, rounded lithic lapilli. 8, coarse volcanic ash. 9, rhyolite ash in the N₃. 10, lava-flow. 11, agglutinated dribble. 12, scoria-fall.

### Stratigraphy of the Younger Oshima group

Figure 5-3 is an idealized exposure of the Younger Oshima group on the mid-slope of the Oshima volcano. The deposits of the group comprise scoria and ash falls, lava and volcanoclastic flows, and wind and water laid secondary deposits. By the presence of buried soils of similar degree of maturity (or immaturity), the Younger Oshima group is subdivided into twelve horizons. Each individual horizon has a soil layer in its top and is labelled as Y₁ to Y₆, N₁ to N₄ and S₁ and S₂ in descending order. The present soil occupies the uppermost part of the Y₁ horizon.

The stratigraphic classification is traceable all over the island as shown in Figure 5-4 and revealed a continuous recent history of larger and explosive activity of Oshima volcano. As seen in Figure 5-4, air-fall deposits of all horizons increase their thickness to the SW and ENE of Mihara-yama as one moves around the volcano. These are down wind directions from the crater of Mihara-yama, of predominant wind. Each horizon marks a large continuous eruptive episode separated by the period of relative quiescence as represented

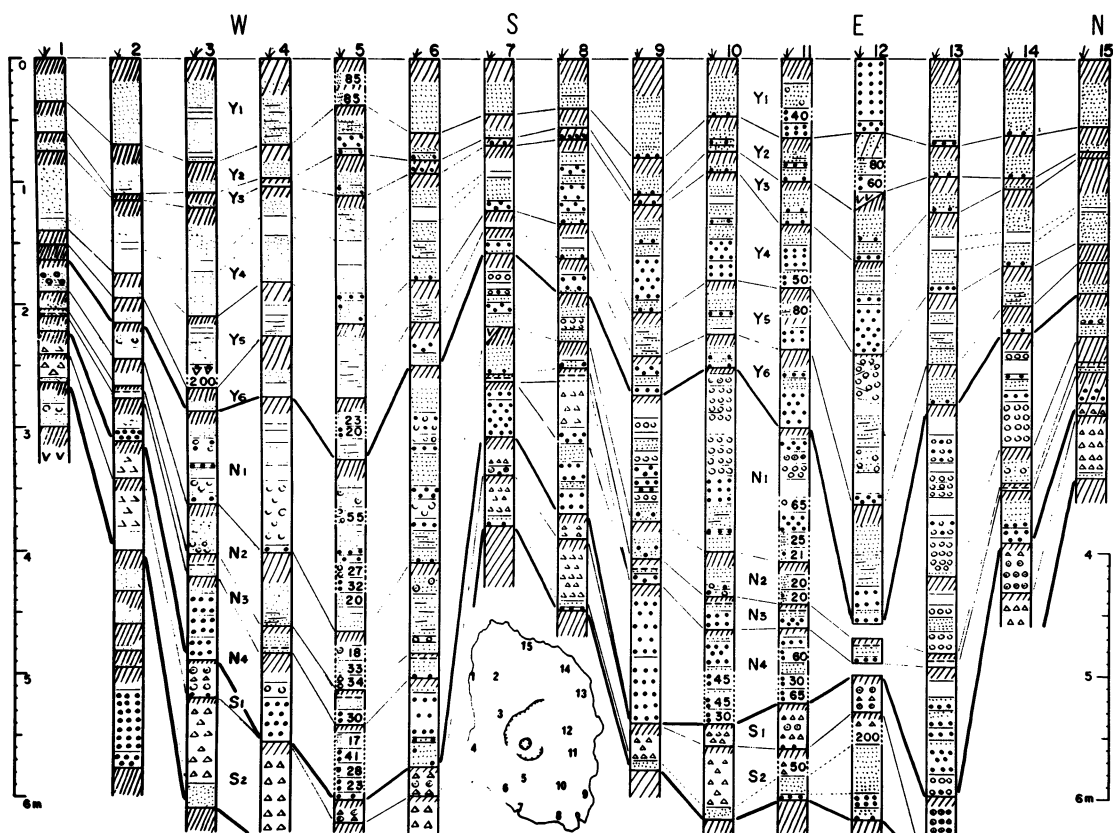


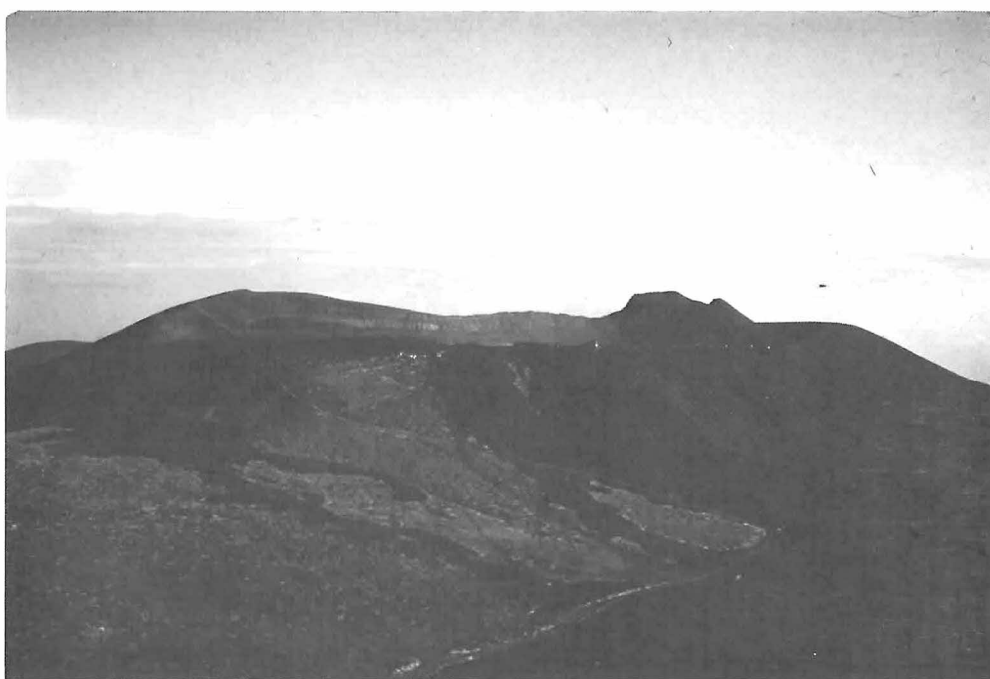
Fig. 5-4. Anti-clockwise arrangement (left to right) of columnar sections of the Younger Oshima group at 15 localities. Symbols are the same in Figure 5-3. Numerals in some columns are the thickness of the layer in cms. (Nakamura, 1964).

by soil formation. Calendar dates were inferred for each episode by means of examination of historical documents (Table 5-2), archeological pottery remains from various localities in the island and by  $^{14}\text{C}$  dates of wood fragments in volcanoclastic flows. Results are summarized in Table 5-3. Thus, the Younger Oshima group was found to represent volcanic products during these 1,300 years or so. And Oshima volcano shows a remarkable periodicity in its larger eruptions during this period.

**Table 5-2.** Volcanic activity recorded in literatures (Isshiki, 1964).

- 684 Nov. 26. Detonations were heard from an easterly direction in Kyoto, about 350 km west of Oshima. It is said to be caused by increase of the land area on the north-western coast of the island. However it is not certain whether this record is really of this volcano or not.
- 1112 Nov. 11 to the end of this month. Detonations were also heard from an easterly direction and earthquakes frequently occurred in Kyoto. It is reported that a volcanic eruption took place in the sea off the coast of the Izu Peninsula. Some scientists regarded the eruption to have occurred in Oshima, but old literature tells no exact location.
- 1338 October or thereabouts. Heavy ash falls. In these days, the volcano appears to have been continuously active, accompanied with glowing columns above the crater and detonations like thunder.
- 1415 May 12. An eruption followed by thunderous detonations took place. Sea-water became hot.
- 1416 Aug. 24. An eruption followed by thunderous detonations took place.
- 1421 May 5. An eruption followed by thunderous detonations took place. Sea-water boiled and many fishes were killed.
- 1442 August to the next year. Eruptions occurred.
- 1552 Oct. 7 to November. An eruption broke out on Oct. 7 from Mihara crater. On Oct. 15, a lava newly flowed out formed an island at Kozu whose exact location has not been clarified. Columns of glowing smoke rose high in the air and hung over the island. Many earthquakes and air vibrations followed.
- 1600 or 1601 A minor eruption.
- 1612 or 1613 Ditto.
- 1623 Ditto.
- 1634 Ditto.
- 1637 to 1638 Ditto.
- 1684 to 1690 A violent eruption took place from a newly formed crater (the Mihara crater at present ?) on Mar. 31, 1684 and continued till the middle of April. A lava flowed down toward the east-northeast and reached the sea. Repeated severe earthquakes destroyed furnitures. From summer to autumn, detonations were sometimes heard and ash accumulated to a depth of several tens of centimeters near villages on the coasts. After that, the activity became calm but continued for seven years.
- 1695 April 12. An eruption occurred.

1777 to 1792. The most violent activity ever recorded in the history of this volcano started on Aug. 31, 1777. It was followed by detonations, earthquakes and fall of ash, scoriae and Pele's hair 3 to 10 cm long. This type of activity continued, with some intervening periods of quiescence, at least till the end of February, 1778. On April 27, 1778, lava was discharged from a side crater or craters on the northern foot of Mihara-yama and flowed down toward the north-northeast along a valley for a distance of 6 km. After that, the activity became calm and only black smoke which was occasionally given off from the Mihara crater was seen. In October, the activity renewed and on Nov. 6, lava from a crater on the southern foot of Mihara-yama overflowed the southwestern caldera wall and streamed down the slope for 3 km. On Nov. 14 or 15, another stream of lava was issued with loud detonations and thick smoke, crept down toward the northeast and reached the sea 5 km away from the crater. On and after Dec. 14, the activity became severer and on Dec. 18, an eruption occurred near the terminal of the first lava flow. From 1783 to 1786, ash fell frequently, accumulating to a depth of 1 m or more. Many houses were destroyed. The activity came to an end in the fall of 1792.



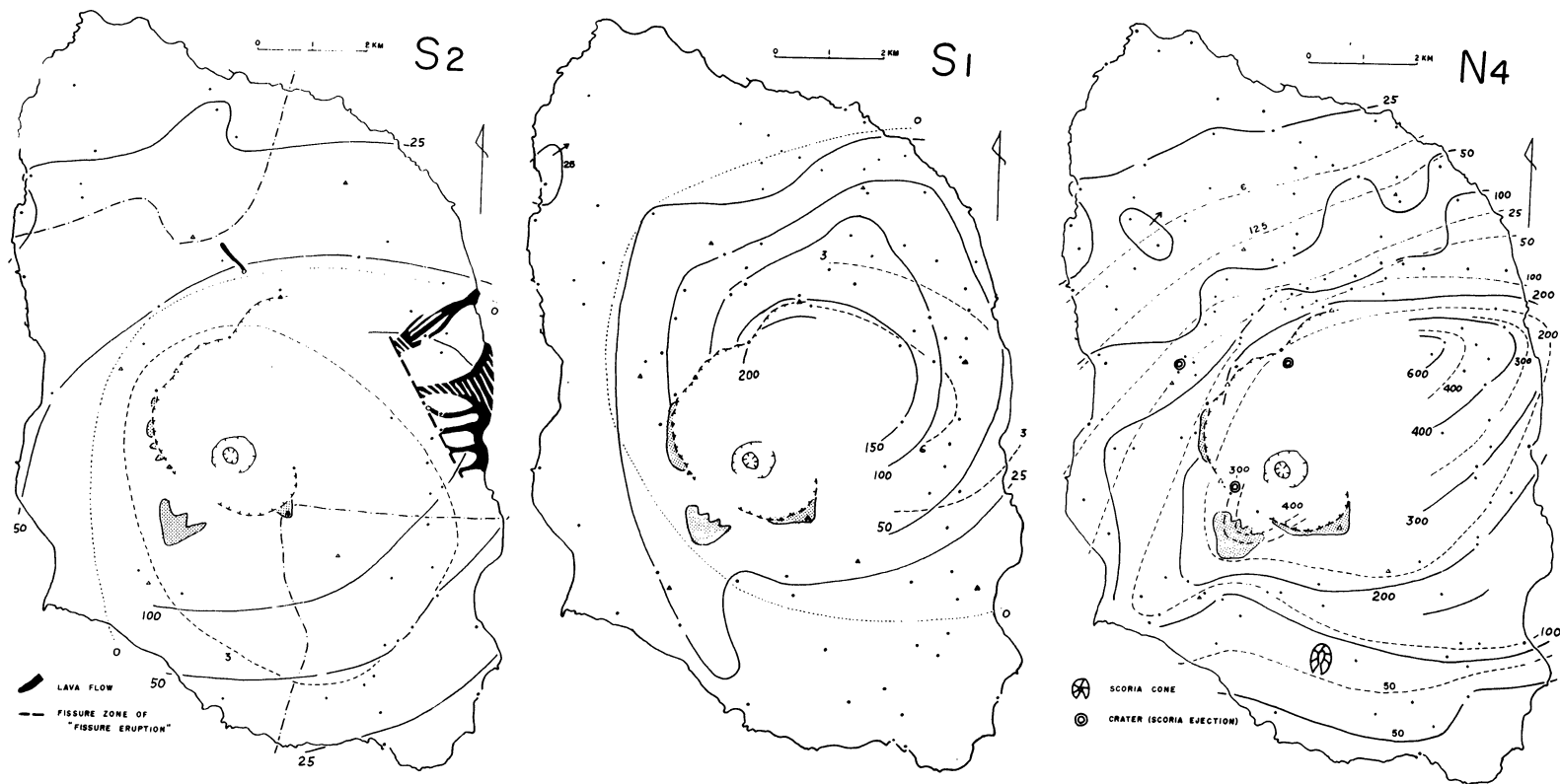
Mihara-yama, the only active post-caldera cone of Oshima volcano, viewed from NW about 700 m above the sea level over the caldera rim.

The 1950- 1951 pyroxene basalt flows run down the slope of Mihara-yama after filling up the crater and spread over the caldera floor (lower right). The skyline of Mihara-yama is the far side of its crater rim which is higher by about 50 m than this side. On the crater wall is seen mantle-bedded, densely welded agglutinate resulted from the huge fire-fountain during 1777-1778 activity. Lava flows of 1778, erupted from the foot of Mihara-yama occupy the lower left of the photo. A sinuous paved footway from the caldera rim to the crater rim is seen in the center. Taken by K. Nakamura on March 1, 1974.

**Table 5-3.** Chronology of the Younger Oshima group (Nakamura, 1964).

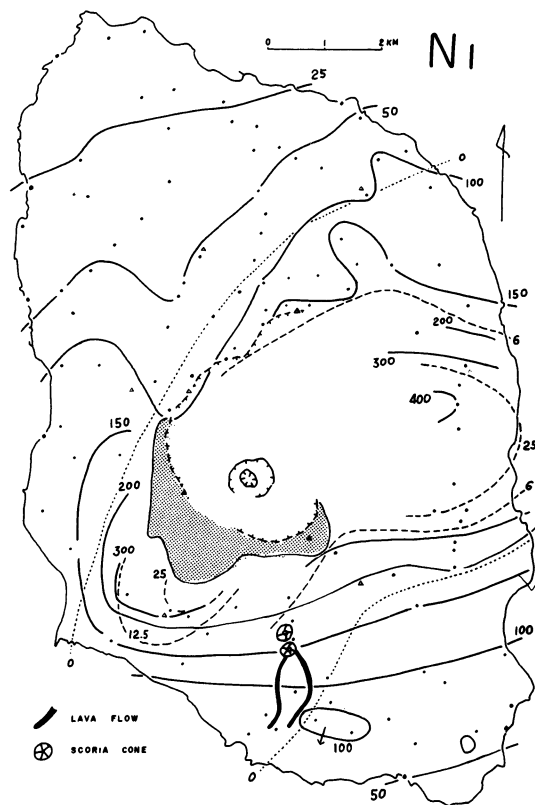
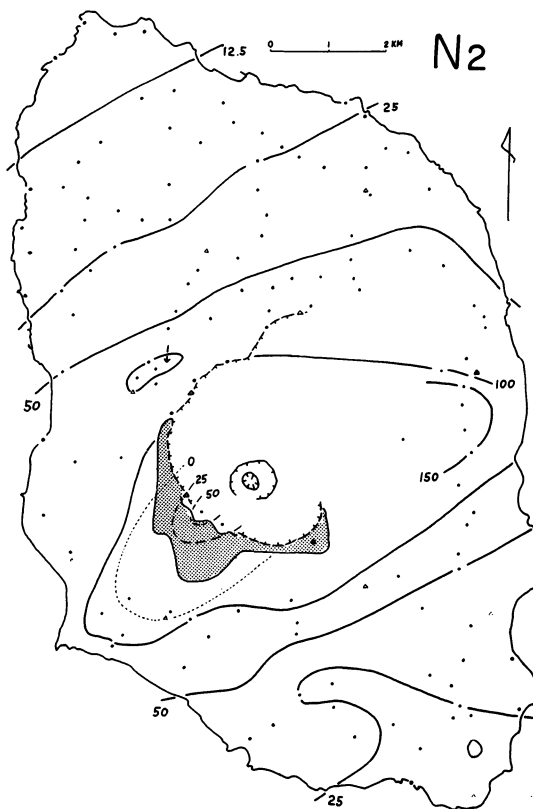
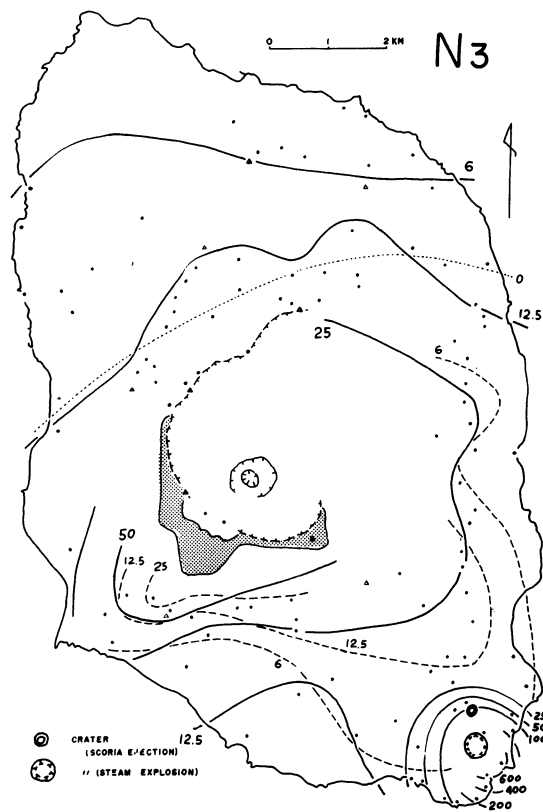
Stratigraphic succession	Most probable beginning-dates of eruption, deduced from the three different sources (A.D.)	Interval (year)	Dates of eruption as inferred by		
			historical documents	pottery remains	¹⁴ C measurement
The Younger Oshima Group	Y ₁	187 +	—1777 —	-----	
	Y ₂	93	—1684 —	-----	
	Y ₃	134	—1552 —	-----	
	Y ₄	130	—1421 —	-----	
	Y ₅	85	—1338 ? —	1300 ± 50	
	Y ₆	135	-----	-----	
	N ₁	100	1112 ? ?	-----	
	N ₂	140	-----	-----	
	N ₃	100	886 or 838	750 ± 100	(Gak. 351a)
	N ₄	110	-----	550 ± 100	( „ 351b )
	S ₁	100	-----	300 ± 100	( „ 353 )
	S ₂	150	684 ? ?	200 ± 200	{ 620 ± 90 600 ± 100 450 ± 160
	500 ± 200				
The older Oshima Group					

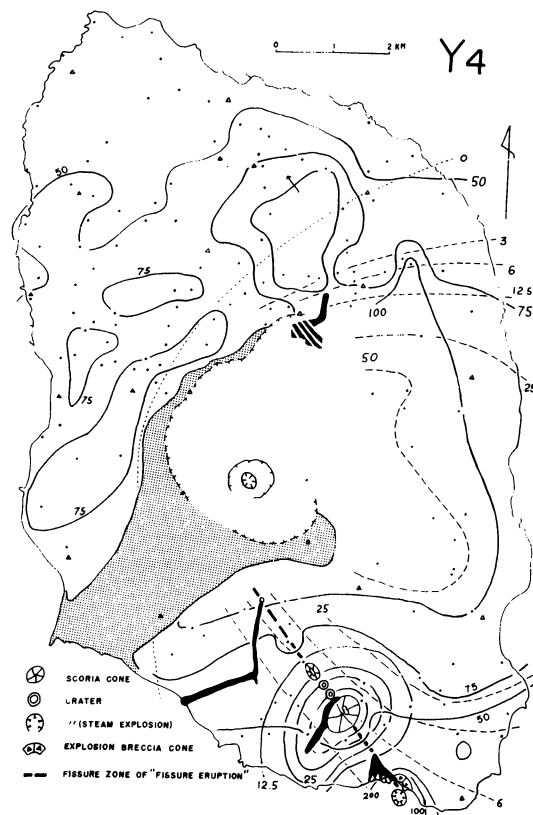
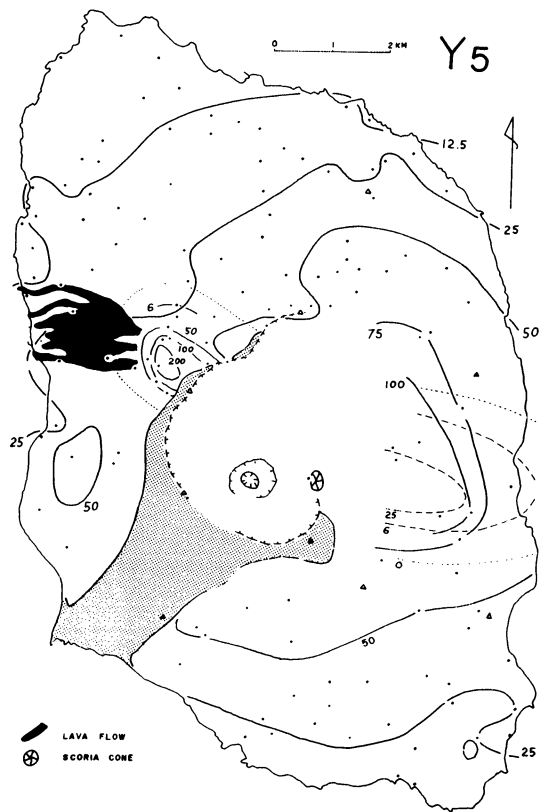
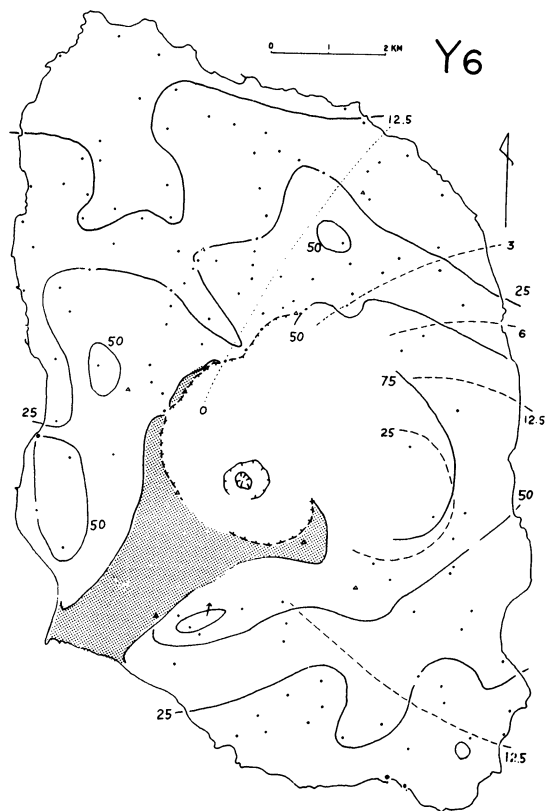
Air-fall deposits of the Younger Oshima group are naturally thicker and coarser near the summit crater. Lava flows from summit and flank craters are identified in seven different horizons. Products of flank craters, such as lava flows, scoria falls and explosion breccias are found in six different horizons. They are mapped as twelve successive maps in Figure 5-5. In this figure, basal scoria falls are mapped by broken lines together with the total thickness of falls of the each horizon. The twelve maps of Figure 5-5 is compiled into a single map, Figure 5-6. As seen from Figures 5-5 and 5-6, main eruptive centers during the period represented by the Younger Oshima group have been located at the summit where the present Mihara-yama is located, except at the time of the S₁. Lava flows from the summit crater are observed at the time of the Y₄ and later. Apparently, those of the Y₅ and earlier horizons were consumed for the burial of the depression of the caldera. During this period, lava flows observed on the slope of the main cone are all from flank craters.

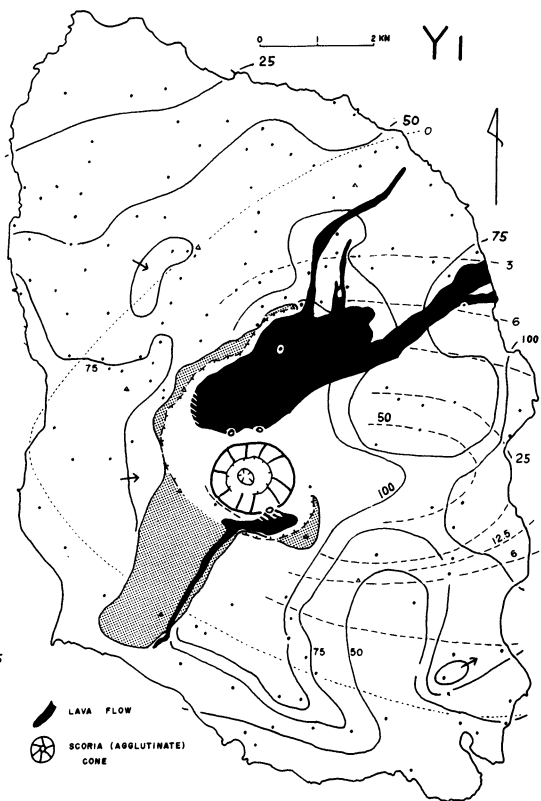
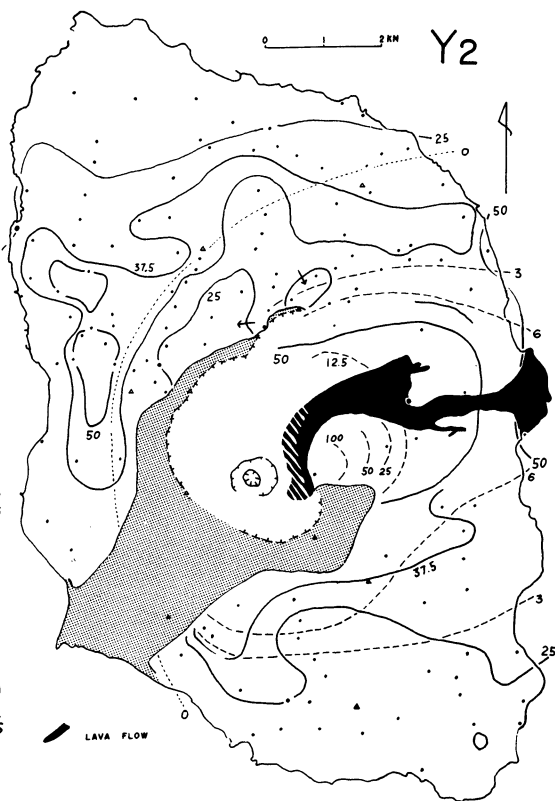
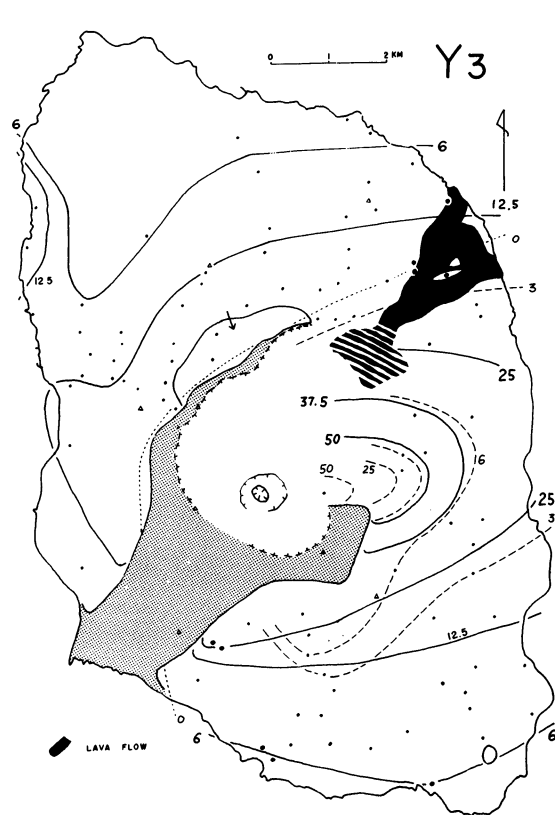


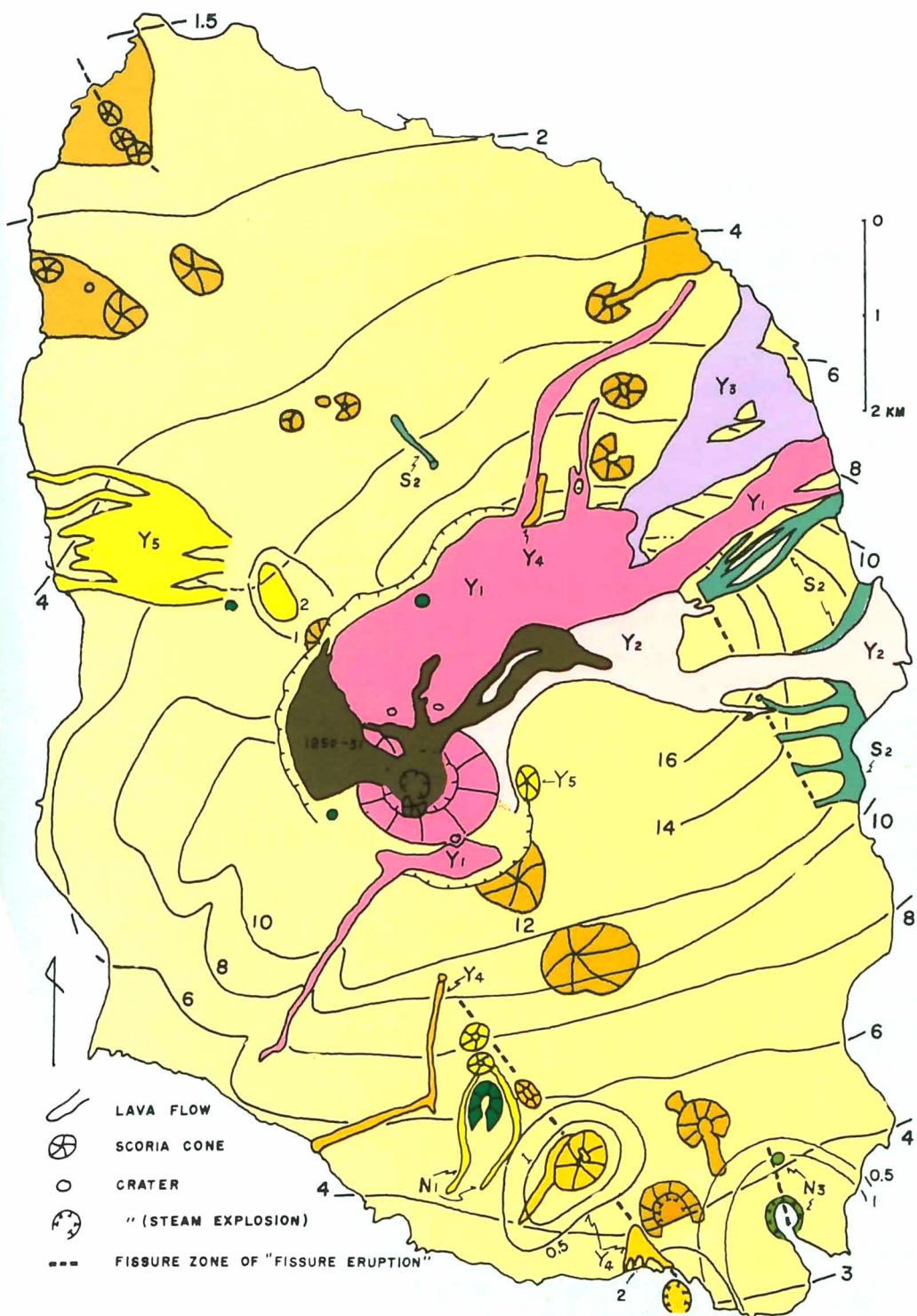
**Fig. 5-5.** Geologic maps of twelve horizons ( $Y_1 - Y_6$ ,  $N_1 - N_4$ ,  $S_1$  and  $S_2$ , in descending order) of the Younger Oshima group (Nakamura, 1964). Arrangement is from older to younger. Stippled area: area where the deposits have entirely removed away by later erosion. Numerals by isopach lines are in cms. Thick lines (A) denote those from the central craters, thin lines (B) for those from flank craters, broken lines (C) for basal scoria falls. A + B represent the total thickness of fall deposits. C is included in A. The crater rim and pit of the present Mihara-yama are shown in each map, irrespective of their actual presence or absence at that time. Dash-dot line for the  $S_2$  shows an approximate boundary for the distribution of the volcanoclastic flows, secondary derivative of phreatic explosion breccia from the central crater.











Summit caldera of Oshima volcano is gourd-shaped, 3 km x 4 km, and has an area of about 10 km². The location of the buried portion of the wall is inferred from the distribution of post-caldera lavas which once ponded in the caldera depression and overflowed the rim onto the slope of the main cone (Fig. 5-6).

The timing of the formation of the present caldera wall, or the last enlargement of the caldera is assigned to the  $S_1$  and the  $S_2$  horizons based both on the mode of eruptions represented by the  $S_1$  and the  $S_2$  and on the depositional-structural relations observed on the caldera rim (Nakamura, 1964). Pyroclastic fall deposits of the  $N_4$  and later ages conformably cover the relief of the caldera walls indicating that the relief was formed prior to their deposition. On the other hand, volcanoclastic flows in the  $S_2$  are distributed outside and all along the caldera rim, suggesting that they are pre-caldera deposits. From these observations, it may be concluded that the possible candidates for the time of caldera formation, provided it is associated with the volcanic eruption, are the period of the  $S_1$  and a part of the  $S_2$  later than the volcanoclastic flow, that is ash-falls with accretionary lapilli.

The eruptions represented by the  $S_2$  and the  $S_1$  are characterized by phreatic explosions from the summit craters, located at the centers of SW and NE portion of the caldera, respectively, the southwestern one being at the present location of Mihara-yama (Fig. 5-5). These eruptions remind us of the sequence of events in 1924 occurred at Kilauea volcano, Hawaii (Jaggard, 1947). In fact, close similarity is found between the eruptions of the  $S_2$  and Kilauea in January to May, 1924 and it suggests the way how the caldera of Oshima was formed. Both eruptions started as a flank fissure eruptions. Long continued lava lake in Halemaumau disappeared due to the draining of the magma by the flank outflow. Then phreatic explosions followed at the both craters as indicated by explosion breccias and accretionary lapilli tuff. Collapse of the crater wall enlarged Halemaumau to the present size, ca. 1 km in diameter, which is more than three times of the earlier one.

The collapse is explained as the result of the strong vibration associated with the phreatic explosions which occurred at the deep bottom of the crater pit. The explosions were caused by the inflow of the ground water immediately after the draining of magma. Because of the similarity of the sequence of events between the two volcanoes, we expect that also at Oshima collapse and drastic enlargement of the caldera occurred at the time of the  $S_2$  explosion. The  $S_1$  also includes the product of phreatic explosions from the summit crater and the center of the explosion coincides with the northeast center of the caldera floor (Fig. 5-5).

We infer based on the above consideration that the present caldera of Oshima was formed successively at the time of the  $S_2$  and the  $S_1$  by engulfment of the SW and NE summit portions, respectively, associated with phreatic explosions.

Volumetric relation is not inconsistent with the above inference. The lava flows of the  $S_2$  are in excess of  $0.02 \text{ km}^3$  in volume. No lava flow is observed in the subaerial  $S_1$ . The explosion products of the  $S_2$  and the  $S_1$  are  $0.09 \text{ km}^3$  and  $0.08 \text{ km}^3$  in volume, respectively, and are far smaller than the volume of restored depression,  $3.1 \text{ km}^3$ , calculated by topographic and drill data.

### Common sequence in great eruptions

Twelve horizons in the Younger Oshima group represent twelve major eruptions during and after the summit caldera formation. The distribution of the eruptive products are mapped separately in Figure 5-5 and collectively in Figure 5-6. A common sequence is recognized in the twelve eruptive episodes. The sequence in a complete form is as follows in ascending order:

Scoria fall  $\rightarrow$  lava flow  $\rightarrow$  ash fall with or without accretionary lapilli  $\rightarrow$  secondary deposits  $\rightarrow$  soil.

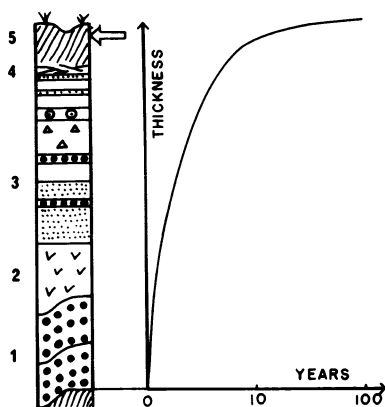


**Fig. 5-7.** Schematic drawing of sequence of phases in a single horizon and time vs depositional thickness of the deposit. 1, basal scoria falls. 2, lava flows. 3, alternation of ash falls. 4, secondary deposits. 5, soil (Nakamura, 1964).

Basal scoria falls, as shown by broken lines in Figure 5-5, are present in all twelve horizons and the distribution is much narrower than the overlying ash falls. Ash falls cover most of the island and elongate in ENE and SW directions in their distribution. Difference between the ash falls and the basal scorias in their distribution implies that the period of ash falls endured longer and that the eruption clouds were generally lower in ash falls. Lava flows are intercalated between the two kinds of falls of seven horizons,  $Y_1 - Y_5$ ,  $N_1$  and  $S_2$ . Lava flows of  $Y_5$ ,  $N_1$  and  $S_2$  are from flank craters, whereas those of  $Y_1 - Y_4$  are from summit craters. Lava flows from the summit craters after the caldera formation may have ponded inside the caldera, therefore concealed beneath later ejecta, until the  $Y_4$  time.

Historical records about 1777 – 1792 and 1684 – 1690 eruptions document that the lava outflow occurred for a few to several months, within a year or so after the commencement of the eruption. Ash falls, on the other hand, continued intermittently for up to ten years.



To summarize the above statement, there is a common sequence of phases in a major eruption and the time needed for deposition of later phases may have taken longer, as schematically shown in Figure 5-7. This may be explained in the following way: The first phase is the high velocity ejection of magma rich in volatile material, in the form of scoria, then it passes into the second phase of lava outflow after most volatile-rich portion of the magma was ejected. The third phase of ash-fall may represent the process of gradual lowering of magma head, associated with occasional scoria ejection along with weak blasting off of the talus debris in the crater. This sequence of events in a single large eruption may be regarded as a fluid magma version of an often observed sequence of similar events in the case of a viscous magma (Aramaki and Yamasaki, 1963), and may represent a process of pressure release by means of transfer of stored material under the gravity field.

### Periodicity of the great eruptions

During the period of the Younger Oshima group, twelve great eruptions occurred periodically in every one hundred and a few tens of years. The last one occurred in 1777 – 1792, about 200 years ago. The situation is illustrated in Figure 5-8, which shows cumulative volume of air-fall deposits on the subaerial slope of Oshima volcano.

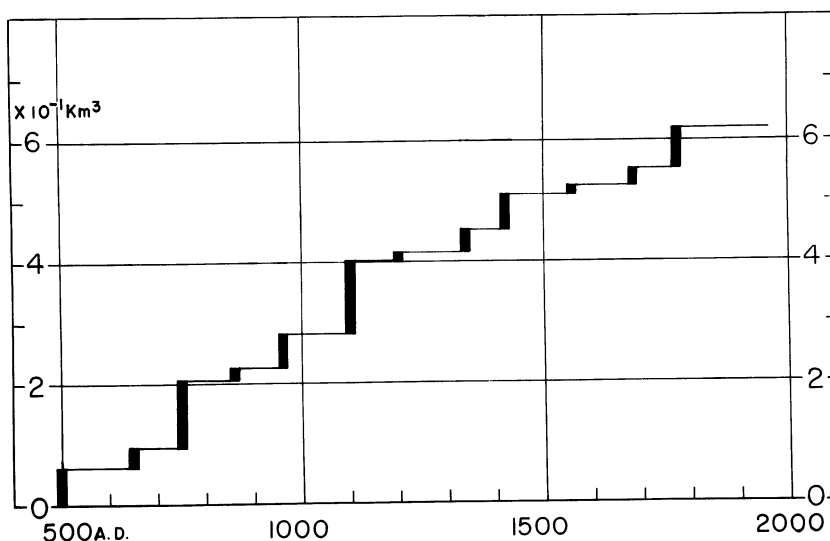


**Fig. 5-8.** Cumulative volume of fall deposits from the central (summit) craters on the slope of the main cone (Oshima volcano). Horizontal portions indicate the periods of practical nondeposition and weathering (Nakamura, 1964).



**Fig. 5-9.** Air-fall sequence of the Older Oshima group exposed on large road cuttings near the southwest coast. For details, see text (Nakamura, 1972).

Recent stratigraphic studies of the Older Oshima group by Isshiki and Matsumura (1976) and K. Tazawa (unpublished data) indicate that the similar periodicity of great eruptions in every one to two hundred years existed also during the last 9,000 years or more. Tazawa (unpublished data) was successful in correlating the horizons of about 9,000 years ago and number of others over the large parts of the island, including the spectacular exposure as shown in Figure 5-9. In Figure 5-9, the horizon of apparent unconformity is dated as about 10,000 years ago, according to Tazawa.

The exposure of Figure 5-9 consists mostly of alternation of air-fall basaltic deposits and soil or subaerially weathered ash, indicating broadly periodic explosive eruptions of the volcano. The number of the soil horizon is over 100, the time period covered by the whole deposits being something like 20,000

years. This part of the slope of the volcano form a radial ridge. This explains the reason why there is no lava flow intercalated. The road is cut on the middle of old steep sea cliff and the result is this high exposure. The wavy structure is interpreted as merely representing the mantle bedding of air-falls but not the result of later deformation. Nearly horizontal layering of occasional secondary deposits interbedded in the pyroclastic falls demonstrates that no significant deformation took place since their deposition. That the dips of the strata are less than about  $35^\circ$  or angle of repose supports this explanation. When the horizon of the apparent unconformity in the nearer exposure is traced to the far exposure in Figure 5-9, the same horizon occurs within no more than regularly accumulating layers. This may mean that a portion of the surficial deposits in the near exposure was removed by a landslide or erosion of any kind at about 10,000 years ago.

### Recent activity

After the last great eruption, the An'ei eruption, Oshima volcano was active intermittently in a far less explosive manner, producing no appreciable air-fall deposit outside the caldera (Table 5-4). In this century, the volcano was active at low levels with two large eruptions in 1912 – 1914 and 1950 – 1951. The low level activities include emission of volcanic gases, occurrence of minor explosions with or without ash falls anything up to  $10^5 \text{ m}^3$  in volume, volcanic tremors and swarm earthquakes.

During the 1912 – 1914 and 1950 – 1951 eruptions, volcanic material of the order of  $10^7 \text{ m}^3$  was erupted, including lava flows. At the 1950 – 1951 eruption, lava filled up the crater of Mihara-yama and overflowed the rim, spreading onto the caldera floor. After 1951, a pit appeared in the crater floor at the same place where it existed before 1950 and gradually became deeper until mid-1960's. Later in the mid-1970's, the crater bottom was elevated by newly supplied lava. The maximum height of the bottom after mid-1960's was observed in 1974, a few days after the Izu-hanto-oki earthquake ( $M = 6.9$ ) occurred at the southern tip of Izu peninsula.

Height of the crater bottom of Mihara-yama fluctuated in excess of 400 m in this century, culminating at the time of 1912 – 1914 and 1950 – 1951 eruptions (Fig. 5-10). The height may well be an indicator of the activity level of the volcano in a long term (Tsuya et al., 1956). Also during the same period, reflected glow above the crater of Mihara-yama has been observed frequently (Tanaka, 1974), indicating exposure of lava head at the bottom of the crater. Strombolian eruptions of small scale and lava lakes have actually been witnessed there on a few occasions. These observations led Nakamura (1971) to regard the bottom as an approximate free head of magma column in the volcano and, on this basis, to interpret the fluctuation of the height as the result of volumetric strains associated with great earthquakes in 1923 and 1953 along the Sagami trough. Kanamori (1972) also suggested a physical correlation

**Table 5-4** Post-An'ei Activity (1777 – 1792, Y₁) of Oshima volcano. (Data source next page)

Date	Duration (day)	Preceded years of repose	Volume of erupted solid material ( $\times 10^6$ m ³ )		
			scoria fall	lava-flow	total
1803, Nov. 14	10 >	11	Eruption, ash fell in Tokyo		
1822, 1824,	?	9±	Ash fell.		
1837 ~	?	13±	Eruption, cloud with sulphur odour.		
1846	?	9±	Eruption, for twenty years.		
1870	4	36±	Small eruption.		
1876, Dec. 27 ~ 1877, Feb. 5	40	6	2	1+	3+
1910, Dec.	10	33	0.07	—	0.1
1912, Feb. 23 ~ June 10 July 27 ~ 29 Sept. 16 ~ Oct. 30 1913, Jan. 14 ~ 25 1914, May 15 ~ 26	96 } 3 } 44 } 166 12 } 11 }	2	0.05 } 0.5 } 2 }	6 } 2.6 } 9 } 15 }	30 } 33 }
1915, Oct. 10 ~	15 ~	1	—	—	0.1 – ?
1919, May 18 ~ July 5 Dec. 20 ~ 23	49 } 4 } 53	6	—	—	0.1 – ?
1922, Dec. 8 ~ 1923, Jan. 30	54	3	0.4	6	6.4
1933, Oct. 14	10 – ?	10	—	+	} 0.1 – ?
1934, Apr. 15	10 – ?	1	—	+	
1935, Apr. 26	10 – ?	1	—	+	
1938, Aug. 10 ~ 11	1	3	—	0.2	0.2
1939, Sept. 1 ~ 3 Sept. 16	4	1	—	0.2	0.2
1940, Aug. 18 ~ 19,	2	1	—	0.2	0.3
1950, July 16 ~ Sept. 23 1951, Feb. 4 ~ March 31 Apr. 1 ~ June 28	69 } 56 } 194 69 }	10	3.6	23	27
1953, Oct. 5 ~ 12 Nov. 9 ~ 13 Dec. 1 ~ 18 Dec. 29 ~ Jan. 15 1954, Jan. 27 ~ Feb. 8	8 } 5 } 18 } 64 20 } 13 }	3	0.05	0.22	0.29
1955, Dec. ~ 1956, Jan.	60	1.8	+	—	+
1957, Sep. 28 ~ Dec.	100	1.7	+	—	+
1958, Jun 13 ~ '59, May 25 1959, May 25	inter- mittent	0.5	+	—	+
1959, Dec. 12 ~ 1960	„	0.5	+	—	+
1964, Dec. 29 ~ 1965, Jan. 7	10	4.5	0.1	—	0.1
1974, Feb. 28 ~ March 1	0.1	8	0.003	0.5 ?	0.5 ?
1974, May 9 ~ June	45	0.2	0.005	0.3 ?	0.3 ?

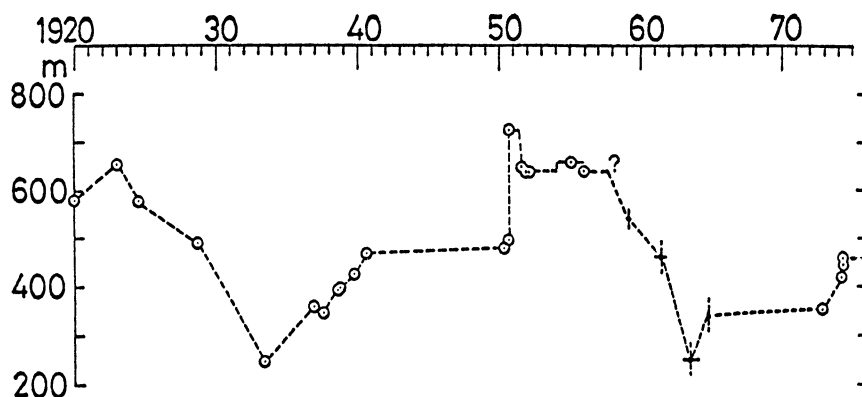


**Fig. 5-10.** Change in bottom height of the crater of Mihara-yama, compiled by Yamashina et al., in press.

between recent large eruptions of Oshima volcano and great earthquakes along the Sagami trough, mainly on the basis of temporal coincidence of the two phenomena. The bottom height may follow that of the magma head more closely during its rise than its fall, since the solidified crust of the magma head may persist at the highest position reached for some time before collapsing.

### Flank volcanoes and tectonic stress

Flank volcanoes were active before, during and after the summit caldera formation until fifteenth century. The last flank eruption occurred from a fissure on the south slope at the time of the  $Y_4$ . The volume of the product from the whole flank volcanoes occupies only a few percent of that of Oshima volcano.

Distribution of flank volcanoes are confined into two parallel zones, trending  $N35^\circ W$ , with Mihara-yama in the middle of the larger zone (Fig. 5-11). Several dikes and fissures of flank fissure eruptions occur also in the zone and trend in similar directions.

The fissure of the  $Y_4$  extends into the sea, causing phreatic explosions with explosion breccias covering the lava flows and scoria cone just formed on the subaerial extension of the same fissure. On the face of sea cliff, the feeder dike is exposed which continues on the face to lava flows to the east and a scoria cone to the west. Explosion breccias, supplied from the seaward extension of the fissure, cover the lava flow and the scoria cone and are oxidized by the heat of them, demonstrating that the breccias settled while the lava and the scoria were still hot.

**Table 5-4** (p.55)

Data source: Isshiki, 1964; Nakamura 1964 and unpublished data; Kimura and Toyoda, 1975 Bull. Volcanol. Soc. Japan. vol. 20, p. 65 – 78.

Another notable fissure is on the southeastern tip of the island. The phreatomagmatic eruption from a part of the fissure produced a circular explosion crater through a terrace-like flat lava plain, at the time of the  $N_3$  (Fig. 5-5). Around the crater, there are distributed explosion breccias, the volume of which is similar to that of the depression of the crater ( $10^7 \text{ m}^3$ ).

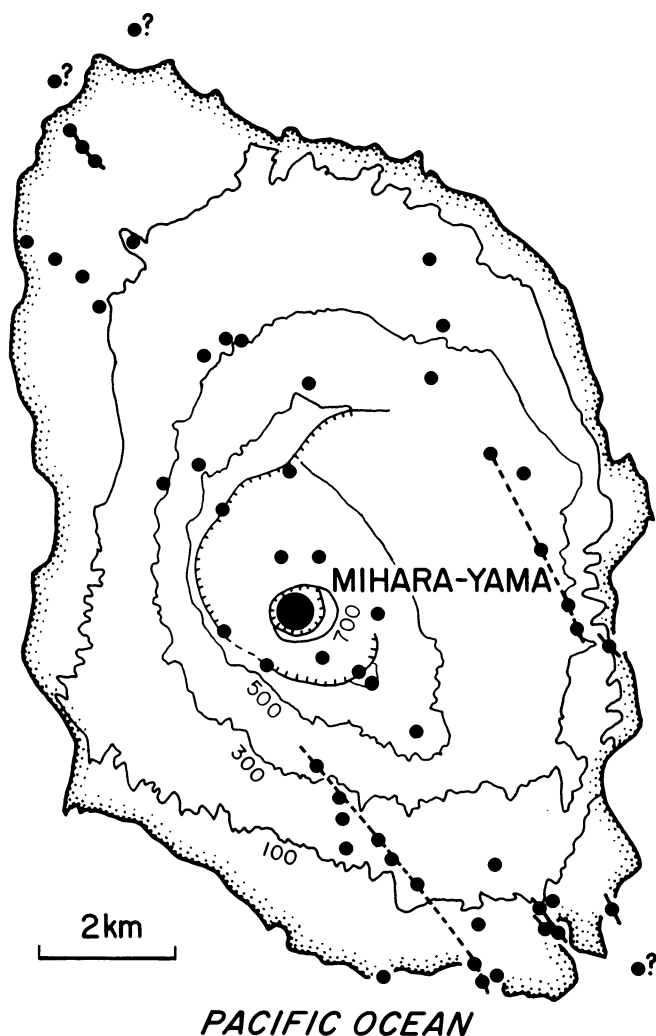


**Fig. 5-11.** Distribution of flank craters (ball) and dikes (ball with bar) of Oshima volcano (Nakamura, 1964, partly revised). Dashed lines are fissures of fissure eruptions.



Part of the crater wall was destroyed by the tsunami caused by 1703 earthquake ( $M = 8.2$ ). The connection with the sea was artificially enlarged later and the crater is now an ideal harbor of refuge for fishing boats.

The trend of the zone of flank volcanoes of Oshima are common with those of Fuji and Hakone volcanoes (Fig. 5-12 and Fig. 3-6). Flank eruptions are

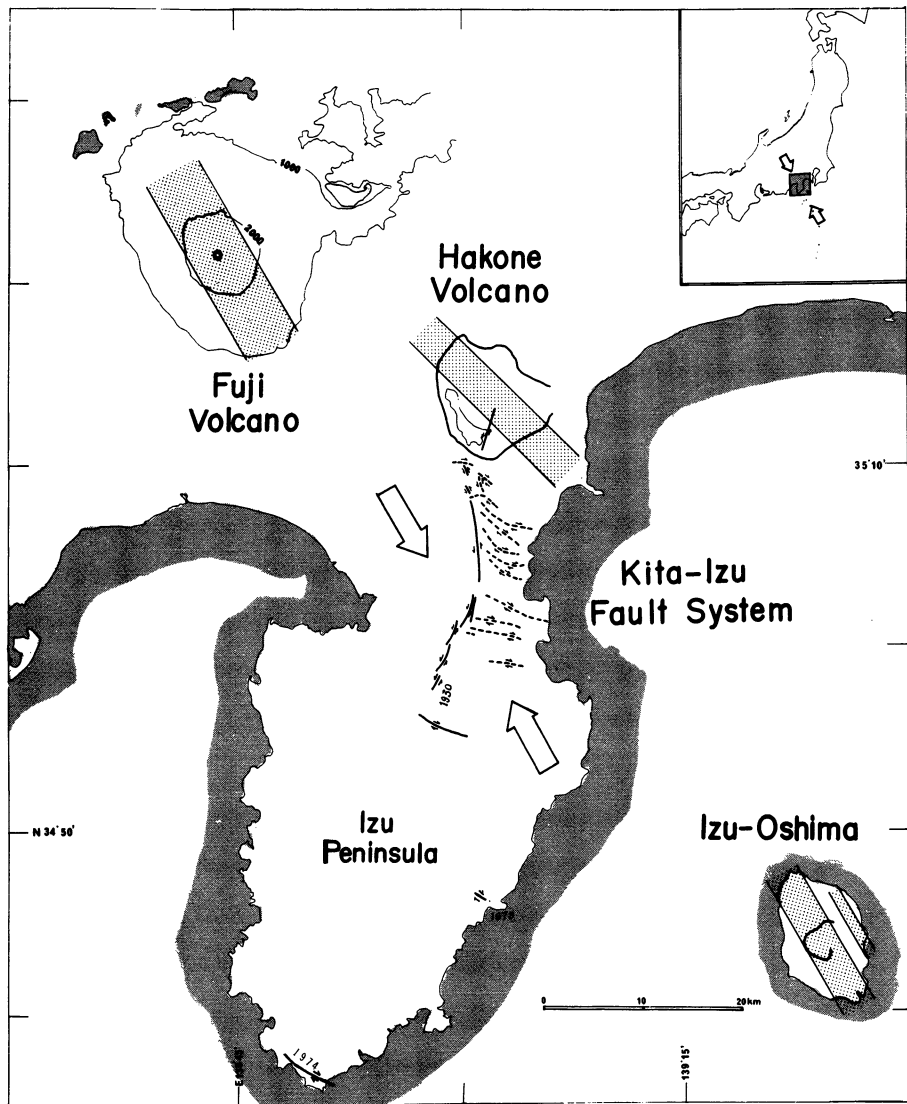


**Fig. 5-12.** Zones of concentration of flank and post caldera volcanoes of Fuji, Hakone and Izu-Oshima volcanoes (stippled area) and surface trace of the Kita-Izu fault system (Nakamura, 1969). Arrows indicate the direction of the maximum compressive stress for the conjugate fault system. 1974 and 1978 dextral fault trace is added.

understood as surface expressions of radial dike formation, therefore the trend indicates that of the radial dike concentration (Fig. 5-13). Because radial dikes concentrate into the direction of the maximum horizontal compression (MHC)

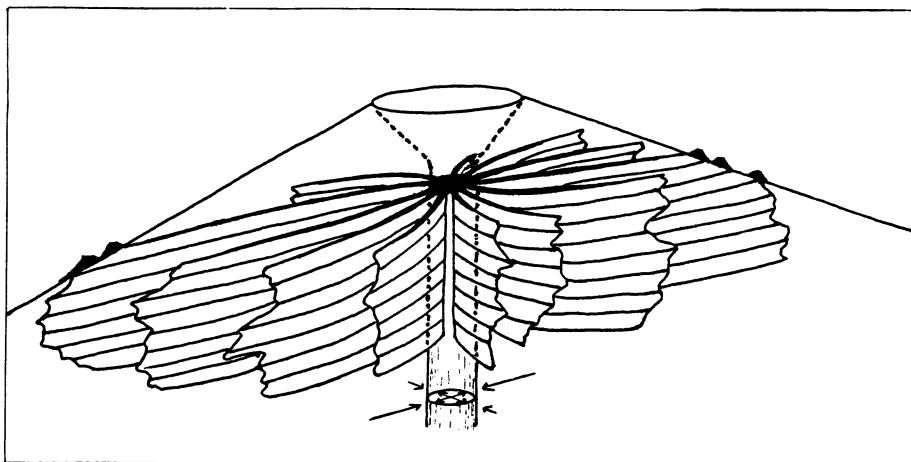
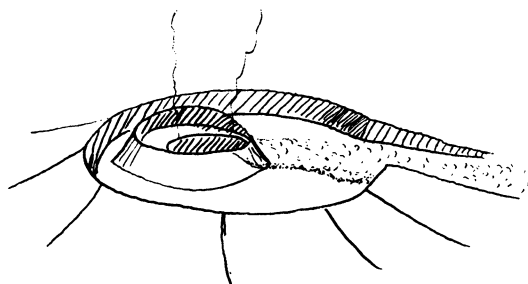


**Fig. 5-13.** Diagram showing the radial dikes and flank volcanoes of a polygenetic volcano (stratovolcano and shield volcano of Hawaiian type) under a differential horizontal stress. The zone of flank volcanoes corresponds to the trend of radial dike concentration; hence to the trend of maximum compression of the horizontal component of the ambient stress (Nakamura, 1977).

in the crust, then the nearly NW directions of the distribution of flank and post caldera cones observed for these volcanoes may represent the direction of MHC probably of regional tectonic origin. This explanation is consistent with the directions of the maximum pressure axis obtained from the conjugate active fault, the Kita-Izu fault system last moved at the time of 1930 earthquake ( $M = 7.0$ ), and from a number of focal mechanism solutions including the 1978 earthquake ( $M = 7.0$ ) occurred between Oshima and Izu peninsula. This direction of MHC is generally parallel to that of relative motion between Japan and the Philippine sea plate.



## 6. Petrology

### 6.1 Chemical and mineralogical characteristics

The volcanic rocks occurring in the regions of Hakone, Izu, and Oshima volcanoes range from olivine basalt (the least silicic being  $\text{SiO}_2 = 45.7\%$ ) to dacite very close in composition to soda-rhyolite ( $\text{SiO}_2 = 76.1\%$ ). The overall spectrum is similar for the Quaternary suites as well as for the Miocene and Pliocene suites. Of these the most abundant are the pyroxene andesites while very small amounts of allivite, eucrite, gabbro, quartz-diorite, etc. occur as plutonic cognate inclusions. Quartz gabbro, diorite porphyrite, quartz-diorite porphyrite, etc. are the relatively coarse-grained intrusives while many intrusives are as fine-grained as to be called basalt, andesite and dacite.

The volcanic rocks in this region form a distinct group which is one of the most silicic (i.e. richest in excess  $\text{SiO}_2$ ), least alkalic, and most anorthositic in its normative feldspar composition in the world (Tsuya, 1937, Kuno, 1950 a).

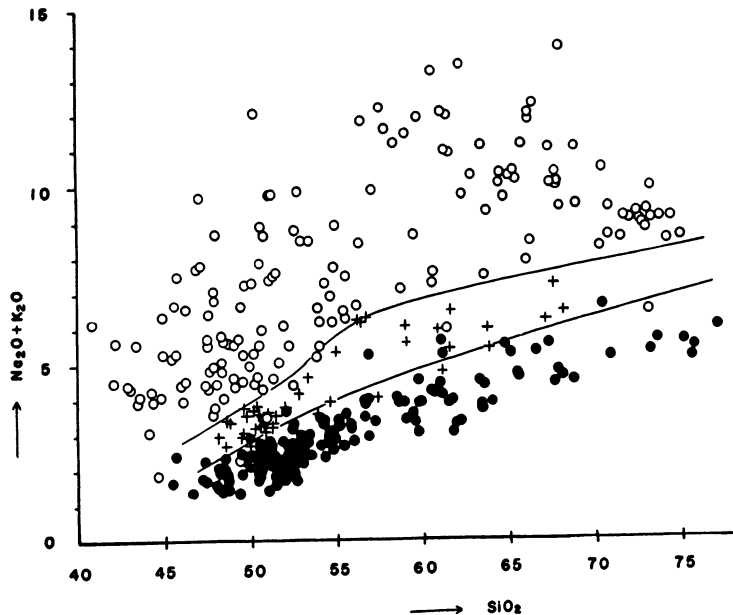


**Fig. 6-1** Total alkalis- $\text{SiO}_2$  relation in Miocene to Recent volcanic rocks of tholeiite series (pigeonitic rock series, solid circles), high-alumina basalt series (cross), and alkali rock series (open circles) from the Izu Islands, central Honshy, Japan Sea coast of southwestern Japan, Korea, and Manchuria. The two lines mark the general boundaries between the fields of the tholeiite series, high-alumina basalt series, and alkali rock series. These lines are reproduced in some of the succeeding figures. After Kuno (1966).

**Table 6-1.** Average compositions and norms of aphyric rocks of the pigeonitic and hypersthene rock series from the Izu-Hakone region as grouped according to the solidification index (SI) (Kuno, 1968, tables 1 and 2).

SI =  $100 \times \text{MgO} / (\text{MgO} + \text{FeO} + \text{Fe}_2\text{O}_3 + \text{Na}_2\text{O} + \text{K}_2\text{O})$ . 1 : basalt, 2 : basalt-andesite, 3 : andesite, 4 : dacite, A : high-alumina basalt of Sukumo-yama, Higashi-Izu monogenetic volcano group, 5 : basalt-andesite, 6 : andesite, 7 : andesite-dacite, 8 : dacite.

pigeonitic rock series					hypersthene rock series				
	1	2	3	4	A	5	6	7	8
SI range	39-30	29-20	19-10	9-0	38	39-30	29-20	19-10	9-0
No. of analyses	5	53	4	8	1	8	13	9	10
SiO ₂	50.03	53.09	58.98	71.37	48.90	53.81	55.55	66.55	75.93
Al ₂ O ₃	15.71	15.44	14.96	13.59	17.58	17.79	17.24	15.35	13.47
Fe ₂ O ₃	2.92	4.02	3.29	1.89	2.47	2.44	3.68	2.21	0.77
FeO	8.83	9.01	7.59	2.94	8.00	6.60	5.96	3.19	0.91
MgO	7.35	4.66	2.74	0.66	7.79	5.87	4.42	1.74	0.41
CaO	11.95	9.68	7.30	3.44	10.82	8.79	8.40	5.11	1.90
Na ₂ O	1.47	2.12	3.03	3.84	2.32	2.76	2.92	3.66	3.92
K ₂ O	0.24	0.45	0.69	1.42	0.27	0.62	0.68	1.17	2.31
TiO ₂	0.84	1.17	1.06	0.48	0.97	0.95	0.83	0.68	0.18
P ₂ O ₅	0.09	0.12	0.15	0.19	0.09	0.19	0.13	0.19	0.12
MnO	0.27	0.23	0.19	0.18	0.16	0.19	0.18	0.15	0.10
Cr ₂ O ₃	—	—	—	—	0.04	—	—	—	—
Total	100.31	99.99	99.98	100.00	99.82	100.01	99.99	100.00	100.02
Calculated average SI	36	23	16	6	38	32	25	15	5

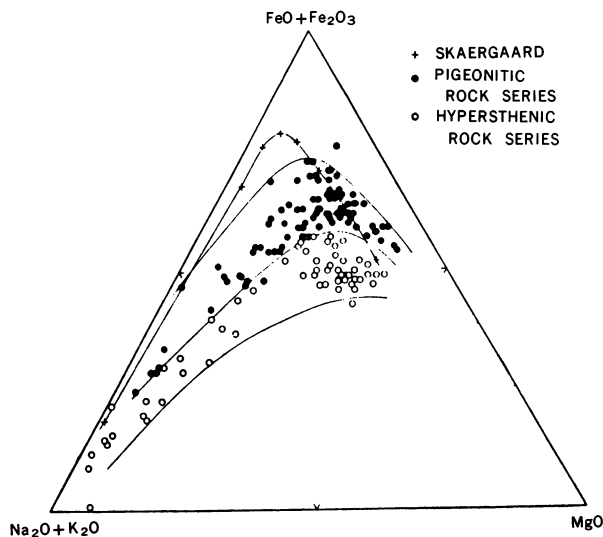
  

Norm									
	1	2	3	4	A	5	6	7	8
Q	3.36	9.80	17.09	34.24	—	6.02	10.55	26.75	39.49
Or	1.45	2.67	4.06	8.36	1.61	3.67	4.01	6.90	13.64
Ab	12.42	17.93	25.64	32.45	19.60	23.33	24.69	30.93	33.14
An	35.54	31.29	25.20	15.66	36.75	34.29	31.93	22.03	8.68
Wo	9.70	6.67	4.22	0.13	7.04	3.42	3.76	0.93	—
En	18.30	11.60	6.83	1.65	18.46	14.62	11.00	4.34	1.02
Fs	12.91	11.72	9.83	3.38	10.85	8.89	6.86	3.20	0.95
Fo	—	—	—	—	0.60	—	—	—	—
Fa	—	—	—	—	0.37	—	—	—	—
Mt	4.24	5.84	4.77	2.74	3.60	3.54	5.35	3.20	1.11
Il	1.59	2.21	2.02	0.91	1.84	1.81	1.58	1.29	0.32
Ap	0.20	0.91	0.37	0.45	—	0.44	0.30	0.44	0.30
C	—	—	—	—	—	—	—	—	1.35
Cm	—	—	—	—	0.07	—	—	—	—

These chemical characteristics are expressed in their mineralogy: it is common to find silica minerals such as cristobalite and tridymite in the groundmass of even the most mafic basalts in the region; it is not rare a basalt to carry (micro-) phenocrysts of anorthite with composition close to  $An_{100}$ ; dacites with  $SiO_2$  higher than 70% still carry phenocrysts of andesine; no biotite nor K-feldspar phenocrysts are found throughout the region, etc.

## 6.2 Zonal variations

However, upon close look of the aerial distribution of the rock series in the region, it is apparent that a zonal arrangement is present running roughly in N-S direction. The above-stated characteristic features are the most pronounced in the extreme east, along the “volcanic front” (Sugimura, 1960) connecting the sites of volcanoes which are situated at the eastern, trench side edge of the volcanic zone. The volcanic rocks of the Izu-Hakone region are probably the best representative of the island-arc type volcanism in Japan. The nomenclature and definition of terms such as calc-alkali rock series and tholeiitic series would not pass today without some confusion and/or debate, yet this is one of the regions where such petrological models have been and will be tested most effectively. According to Kuno, the chemical and mineralogical features of the volcanic rocks of the Izu-Hakone region (and other parts of the Japanese islands) may best be characterized in bivariate classification (Kuno, 1950 a, 1959 a, 1965, 1966, 1968, etc.). One is a set of variables which monotonously



**Fig. 6-2** M-F-A diagram for aphyric rocks of the pigeonitic and hypersthentic rock series of Izu-Hakone region compared with the trend of the successive liquids of Skaergaard. Kuno (1965).

change more or less perpendicularly to the axis of the arc; if only basalts are taken, the degree of silica saturation will decrease gradually away from the volcanic front (Pacific Ocean-side) toward west and the alkali content will increase in the same direction. The rocks in the easternmost row belongs to the tholeiitic series and the westernmost the alkali (olivine) basalt series. In the intermediate zone, Kuno (1960) found that most of the aphyric basalts are remarkably richer in  $\text{Al}_2\text{O}_3$  (mostly above 17 wt %) than the corresponding basalts of the both sides and he named the rock suite of the zone "high-alumina basalt series". The basalts of Fuji and Higashi-Izu monogenetic volcanoes are the representatives (Table 6-1, column A). The high-alumina basalt are intermediate in the degree of silica saturation and alkali content between the tholeiitic and alkali basalts. Figure 6-1 shows plottings of  $\text{Na}_2\text{O} + \text{K}_2\text{O}$  against  $\text{SiO}_2$  of aphyric rocks in the region ranging from basalt to dacite which are interpreted by Kuno to have chemically differentiated mainly through fractional crystallization. The gradual shiftover of the three series is apparent and the general relation is unchanged when porphyritic rocks are included in the plotting.

### 6.3 Difference in the groundmass pyroxenes

The second variable noticed by Kuno (1950 a) is best expressed in the groundmass mineralogy. Taking for example lavas of Hakone volcano which can be considered to constitute a single comagmatic suite, some lavas carry hypersthene and augite in the groundmass while some carry pigeonite (with or without augite). The stability (liquidus-solidus-solvus) relations between the orthopyroxene, calcium-poor clinopyroxene (pigeonite), and calcium-rich clinopyroxene (augite) solid solutions clearly indicate that crystallization of pigeonite ( $\pm$  augite) takes place at higher temperature than the crystallization of hypersthene + augite, provided other conditions remain the same. Kuno (1950 a) named the series of volcanic rocks carrying only clinopyroxene in the groundmass the "pigeonitic rock series" and those carrying orthopyroxene the "hypersthene rock series", with the implication that these two series of rocks are derived through some different processes. Kuno successfully demonstrated that these twofold classification holds widely throughout the Japanese islands, irrespective of the zones of tholeiitic, high-alumina and alkali basalt series. Moreover, he could show the two series represent distinct chemical trends as shown in Figure 6-2. The enrichment of total iron in the middle stage of differentiation in the pigeonitic rock series relative to hypersthene rock series is clearly demonstrated. Kuno's interpretation is that in the course of differentiation of basaltic magma in the reservoir by fractional crystallization, the liquidus temperature remains relatively high when the magma stays relatively dry (low in  $\text{H}_2\text{O}$  concentration) so that pigeonite crystallizes as the groundmass mineral. In this case the oxidation state of iron in the magma is kept relatively low so that early precipitation of magnetite is suppressed thus resulting in

concentration of iron in the middle stage. In case the magma contained more  $H_2O$ , the lower liquidus temperature results in crystallization of orthopyroxene in the groundmass stage, and the high oxidation state enhances magnetite crystallization and reduces the degree of iron concentration in the liquid magma. In the latter case variation trend of the bulk of the hypersthene rock series coincides with the so-called calc-alkalic rock series.

In Table 6-1, average compositions of the pigeonitic and hypersthene rocks are given for the Izu-Hakone region. In Figure 6-3, the combinations of the two sets of variables explained above are shown for each volcano of the region (Kurasawa and Michino, 1976). Volcanoes composed only of lavas of the pigeonitic rocks of the tholeiite series are Taga, one of the Higashi-Izu monogenetic volcanoes, Oshima, Miyake-jima and the volcanoes south of Miyake-jima. Hypersthene rocks, i.e. low-temperature suites seem to be mostly restricted on land, or at most to the area where the crust is substantially thick.

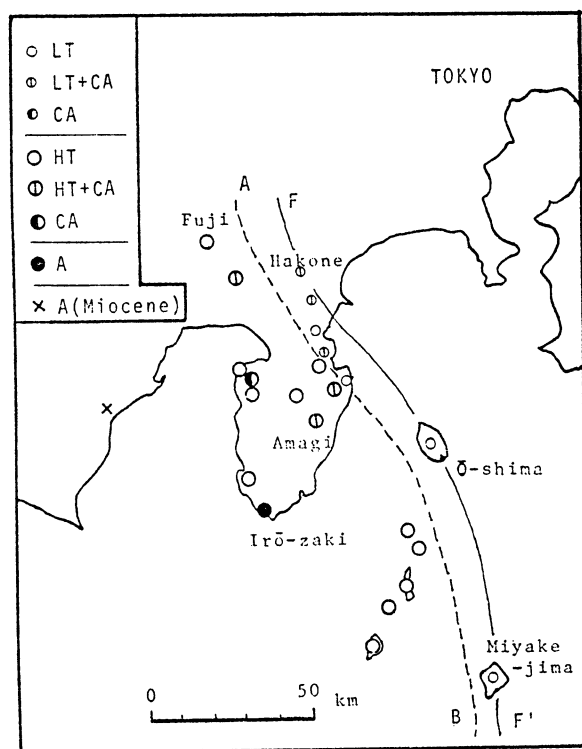


**Fig. 6-3** Distribution of volcanoes in Izu Peninsula and Izu Seven Islands, central Japan.

LT : low-alkali tholeiite series  
HT : high-alkali tholeiite series  
A : Alkali rock series  
CA : calc-alkali rock series

Line A-B is the boundary line between the zone of low-alkali tholeiite and high-alkali tholeiite series. Line F-F' represents the volcanic front, that is, the outer limit for the distribution of Quaternary volcanoes. After Kurasawa and Michino (1976).



## 7. Hot Springs

### 7.1 Hot springs and hydrothermal system of Hakone

#### Historical aspect

Hot springs of Hakone like others of Japan have long been used for the special cure of medical treatment as well as bathing of relaxation since the first discovery of Yumoto Hot Springs in 738 by the Priest Shaku-Teijobo. Later on, many new sites of hot springs were successively found out. In the period of Edo era, about 200 years ago, Hakone was known for the seven sites of hot springs, which were mostly located along the deep valley Haya-kawa. Besides for general health consideration, hot springs are believed to be very helpful in the case of certain physical and medical diseases excepting those caused by bankrupt and broken heart. In Hakone, for example, Ubako Hot Springs are known for the treatment of eye disease. Steam bath of Miyanoshita Hot Springs was once used specifically for the treatment of hemorrhoids combined with the treatment of moxibustion in the Edo era (Figure 7-1).

There is an old saying about the occurrence of hot springs in this district. “We can’t expect hot springs where we can see Mt. Fuji.” Kuno proposed a new saying that hot springs are expected where the Yugashima group, the basement rocks of the Izu and Hakone district, is exposed. We will demonstrate that both of the sayings are valid in the light of our scientific work on the hydrothermal system.



Fig. 7-1. Treatment of moxibustion for hemorrhoids after the treatment of steam bath at Miyanoshita, Hakone (Toto Bunso and Roka, 1811).

## Thermal structure

There are more than 300 deep wells for thermal waters. Their average depth is about 500 m, several reach a depth of 1,000 m. More than 60 temperature loggings were made in deep drilled wells, from which an isothermal map at the sea level was drawn as given in Figure 7-2 (Oki and Hirano, 1970). It is interesting that temperature is the highest in the middle part of the caldera, decreasing outward with a concentric pattern showing a correlation with the structure of the caldera. The interval between the isothermal lines of the western side are narrower than that of the eastern side. The isothermal lines are expanding toward the east, suggesting a flow mechanism of thermal water from west to east.

## Hydrology of thermal waters

The hydrology of the Hakone system is essentially controlled by the water level of Ashinoko (lake) in the west and by that of the Haya-kawa valley in the east. The water table inferred from the water levels observed in deep wells is gently inclined to the east. An interesting fact is that with increasing depth in drilling operations, the water level of perched water appeared in the drilled hole declines and finally stops when the hole reaches the major reservoir. A comparison of the water levels of deep wells suggests again the presence of subsurface flow from west to east. Temperature in the body of the Old Somma is relatively low, which means that the body of the composite cone is just like a sponge partly filled with cold groundwater.

## Zonal distribution of thermal waters

Zonal mapping of thermal waters is mostly based on the relative abundance of major anions such as  $\text{Cl}$ ,  $\text{SO}_4$ , and  $\text{HCO}_3$ . Four zones are recognized, as shown in Figure 7-3.

Zone I, characterized by acid-sulfate waters associated with solfataric fields, is found at the highest part of central cones Kami-yama and Koma-gatake. Zone II, characterized by bicarbonate-sulfate waters with moderate temperature and pH, is widely distributed in the western half of the caldera. The distribution and mode of the occurrence of zone II waters strongly suggest that the major part of  $\text{HCO}_3$  is supplied by the decomposition of fossil plants, which are commonly intercalated in the volcanic deposit.

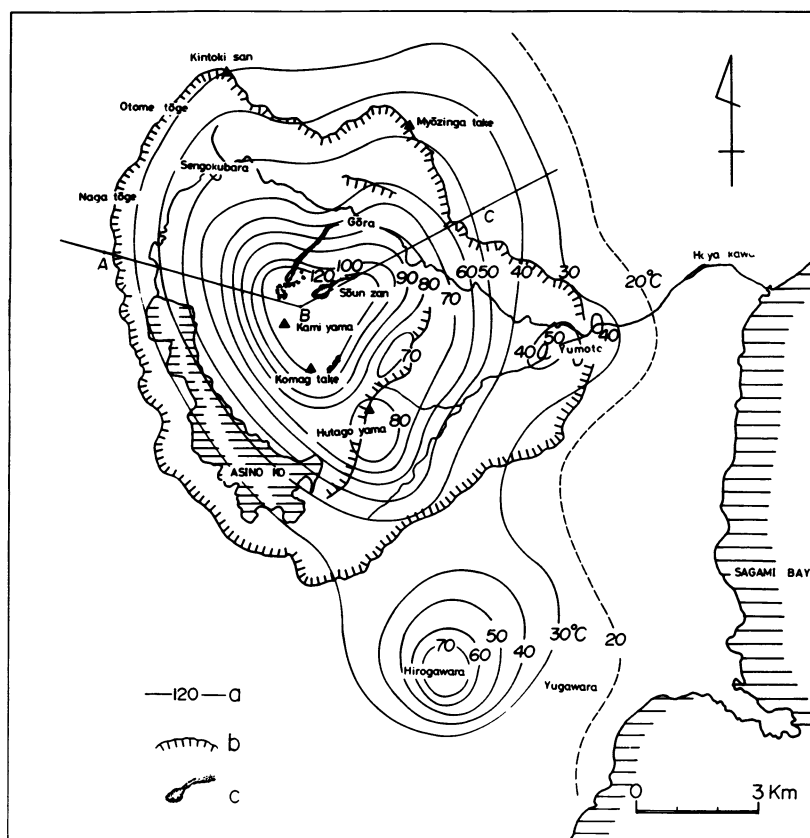


**Fig. 7-2a.** Thermal structure of Hakone volcano at the sea level (Oki and Hirano, 1970).  
a : isotherm, b : caldera rim, c : solfatara

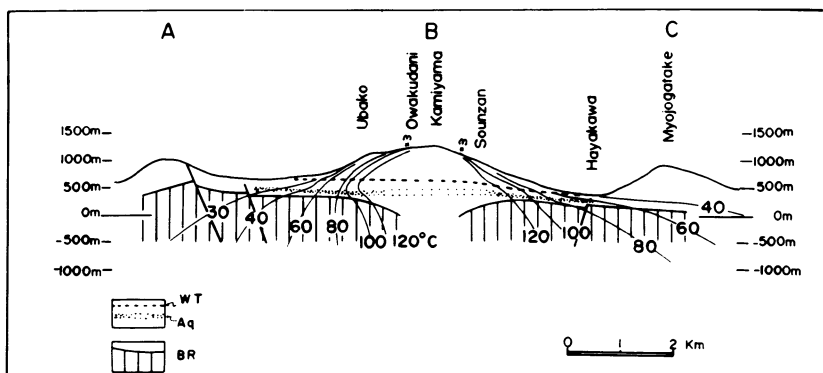


**Fig. 7-2b.** East-west cross section of Hakone illustrating geologic structure and isothermal profile (Oki and Hirano, 1970).

WT : water table, Aq : aquifer, BR : basement rocks

Zone III, characterized by sodium chloride waters with high temperature, occurs as subsurface streams starting from a depth of 300 m beneath an active solfatara, Soun-jigoku, trends to the east, and finally appears as hot springs on steep slopes of Haya-kawa valley.

Zone IV, some times referred to mixed type waters, is widely distributed in the eastern side of the caldera, which is deeply dissected by the two drainages of Haya-kawa and Sukumo-gawa.

Zone IVa is mixed type waters restricted to the basal part of the central cones.

Zone IVb is waters restricted to the basement rocks of the Hakone volcano.

Table 7-1 shows the chemical composition of each type of thermal waters. Water of zone I is low in pH and Cl, but high in  $\text{SO}_4$ , Ca, Mg and Al. Water of zone II is also low in Cl, but high in  $\text{SO}_4$ ,  $\text{HCO}_3$ , Ca, and Mg. Water of zone III is quite high in Cl, Na, and  $\text{SiO}_2$ , but low in  $\text{SO}_4$  and  $\text{HCO}_3$ . Water of zone IV contains appreciable amounts of the major anions.

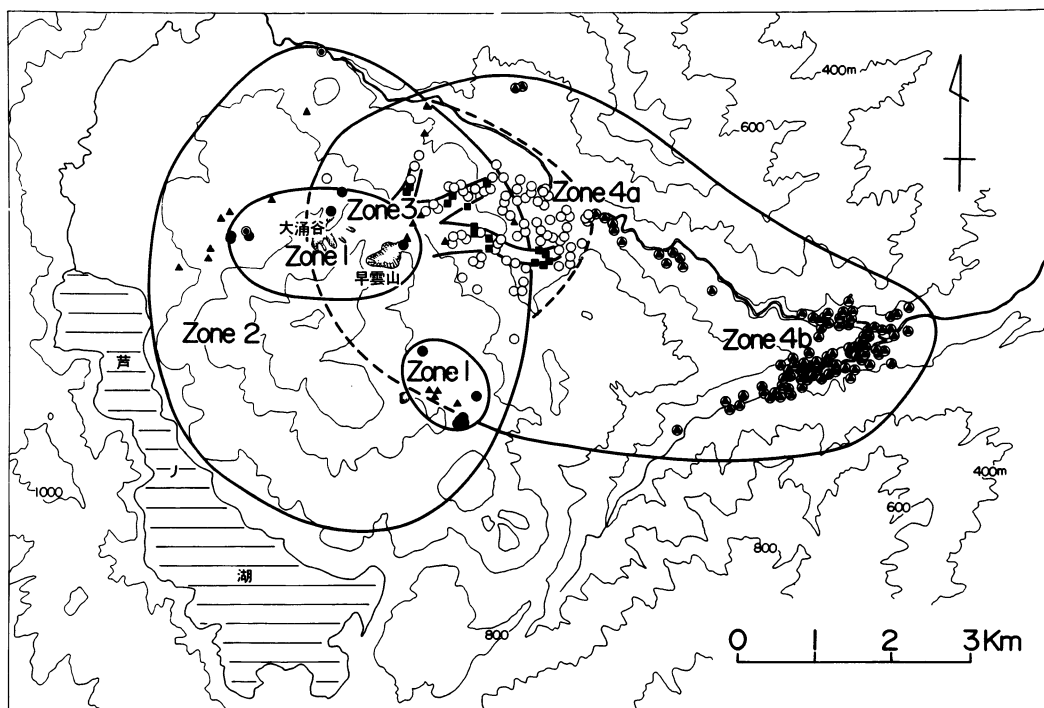


**Fig. 7-3.** Zonal mapping of thermal waters (Oki and Hirano 1970) .

- Zone I : acid sulfate waters
- Zone II : bicarbonate-sulfate waters
- Zone III : sodium chloride waters
- Zone IV : mixed type waters

Table 7-1. Chemical composition of Hakone thermal waters (Oki and Hirano 1974).

ZONE	I	II	III	IV	
NO.	1	2	3	4	5
Type	A.S.	S.B.	NaCl	M.	(M)
Temp.C	49.7	57.5	91.5	65.5	56.0
pH	2.9	8.1	7.7	8.4	8.0
H ⁺	1.18				
Li	0.0	0.068	2.43	.27	.042
Na	42.7	88.5	1490.	441.	348.
K	8.90	12.1	154.	39.8	3.40
Ca	87.4	140.	114.	106.	53.9
Mg	24.3	84.9	0.0	16.8	0.0
Fe ⁺⁺	.099	.56	.105	.257	0.00
Al	22.6	.22	.12	.05	.03
Mn	n.d.	.00	.007	.44	.00
Cl	7.15	19.8	2568.	617.	549.
HSO ₄ ⁻	52.4				
SO ₄ ⁻⁻	526.	381.	81.5	226.	85.1
HCO ₃ ⁻	0.	590.	29.7	287.	36.7
CO ₃ ⁻⁻		1.72		2.11	0.26
BO ₂		.34	3.58	2.34	0.70
HSiO ₃ ⁻		5.87	4.09	13.9	1.74
H ₂ SiO ₃	301.	238.	411.	282.	67.2
HBO ₂		5.79	122.	16.1	20.6
CO ₂		14.2	2.19	2.75	
Total	1074.	1583.	4983.	2053.	1166.
Li/Na		.00077	.0016	.0006	.00012
K/Na	.21	.14	.10	.09	.01
B/Cl				.006	.01
ΣCO ₂ /Cl		22.5	.009	.35	.016
SO ₄ /Cl	80.8	19.2	.032	.366	.155
Depth of well	Hot Spring	525m	506m	351m	650m

Analyzed by T.Hirano and Y.Tajima

A.S. acid sulfate water,

S.B. sulfate-bicarbonate water,

NaCl sodium-chloride water of central cones area

M. mixed type (sodium chloride-sulfate-bicarbonate water)

(M.) mixed type (from basement rocks, sodium chloride-

## Compositional trend of thermal waters

Like the ties of parents and children, there are some compositional trends in the chemical properties of thermal waters. Figure 7-4 is a triangular diagram of the three major anions showing the compositional trends of the Hakone thermal waters. Zone I waters, acid sulfate type are in the  $\text{SO}_4$  corner and zone III waters, sodium chloride type are in the  $\text{Cl}$  corner. Zone II waters, bicarbonate-sulfate type are deep groundwater infiltrated through the caldera floor and central cones, extending along the  $\text{CO}_2 - \text{SO}_4$  side. Zone IV waters are distributed in the area suggesting the mixing of zone II and zone III waters. The convex trend of zone IV waters toward the total  $\text{CO}_2$  apex may indicate the formation of bicarbonate during mixing and flowing of thermal waters.

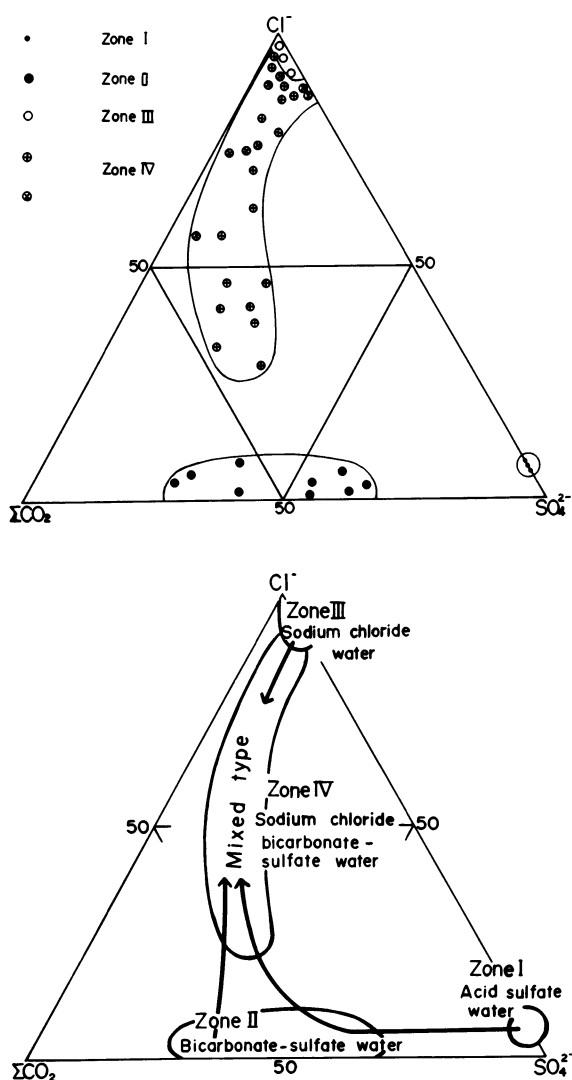
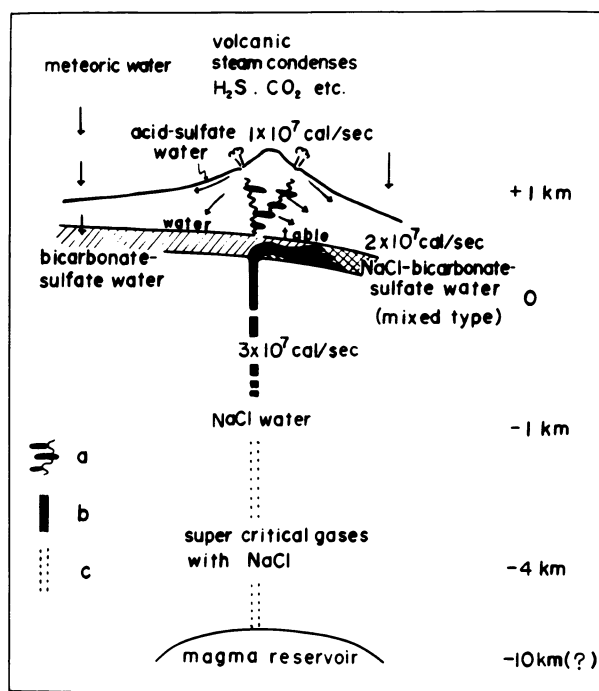


Fig. 7-4. Cl-total  $\text{CO}_2$ - $\text{SO}_4$  diagram (7-4a) and compositional trends of Hakone thermal waters (7-4b) (Oki and Hirano, 1970).

## Genetic model of Hakone hydrothermal system

Figure 7-5 is a genetic model of the Hakone hydrothermal system (Oki and Hirano, 1970). Asymmetric patterns of the isothermal structure and zonal distribution of thermal waters as well as the eastward inclination of water table all suggest the following mechanism for the genesis of the Hakone hydrothermal system.

Groundwater which infiltrates through the western side of the caldera is flowing eastward, passing through the basal part of the central cones, and then contacts high temperature volcanic steam coming up through the volcanic conduit. At a depth of a few kilometers below the central cone Kamiyama, temperature and vapor pressure are high enough to dissolve a considerable amount of sodium chloride and silica in steam. By mixing of low temperature groundwater with high temperature dense steam, high temperature streams of sodium chloride water are formed that run through the permeable zone and mix with groundwater percolating down from the surface, and then finally appear as hot springs on the steep slopes of the Haya-kawa valley.



**Fig. 7-5.** Genetic model of Hakone hydrothermal system (Oki and Hirano 1970).  
a : repeated processes of vaporization and condensation of volcanic steam resulting in concentration of volatile components such as  $H_2S$  and  $CO_2$ .  
b : sodium chloride water (zone III)  
c : super critical gases (steam) with NaCl

At the top of the major reservoir being penetrated by the steam vent, the thermal water boils. The confining pressure on the thermal water decreases as it approaches the surface. This means that most salts dissolved in the gas phase are left behind in the liquid phase. Condensation of secondary steam derived from depth may take place repeatedly within local layers of thermal waters in the body of central cone above the major reservoir.

With repeated processes of vaporization and condensation of thermal water, volatile components such as hydrogen sulfide and carbon dioxide are enriched in the gas phase, which finally appears as volcanic gases in solfatara. We should like to propose a term “volcanic cone effect” for this process. The physical and chemical properties of the high temperature steam will be given in a later section.

### Seismic activity of Hakone

Local seismic activity sometimes takes place in the Hakone caldera. Since the earthquake swarms of 1959 to 1960, seismic observations have been made by Minakami, and more recently by Hiraga of the Hot Spring Research Institute. Minakami (1960) reported that the Hakone earthquakes occur mostly in a narrow area bounded by the isothermal line of 100°C at the sea level. Depths of the foci are generally shallower than 4 km, mostly 1 to 2 km below the surface (Fig. 7-6). The generation of the Hakone earthquakes may correlate with boiling of thermal water at various depths in the central part of the caldera.

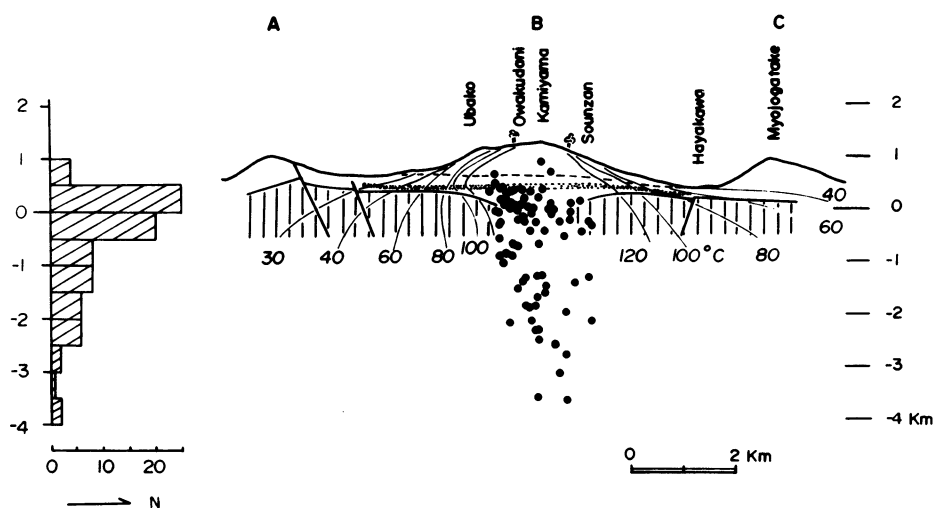


**Fig. 7-6** Distribution of micro-earthquakes and the depth frequency relation plotted on east-west cross section (Minakami 1960, Minakami et al. 1969, Hiraga 1972, and Oki and Hirano 1974).



## Sodium chloride waters

White (1957) emphasized the importance of sodium chloride in the origin of volcanic thermal waters based on the experiment of  $H_2O - NaCl$  system that the superheated dense steam at above  $374^\circ C$  and 221 bars (critical temperature and pressure) can dissolve considerable amount of sodium chloride in the gas phase. The existence of sodium chloride water can predict the existence of a high temperature hydrothermal system good enough for the geothermal power generation.

As shown in chemical analyses, zone III waters are extremely rich in sodium chloride, but poor in  $SO_4$  and  $HCO_3$ . Figure 7-8 is a  $Cl - SO_4$  diagram of zone III waters. For convenience of description, subscripts a, b, and c are put to each branch of zone III (Fig. 7-7). Zone III waters of each branch are placed on each individual straight line on this diagram. By extrapolating the best fitting lines to  $SO_4$  equals zero, a possible content of sodium chloride in the original steam can be derived. It is seen from the diagram that the Cl content of original steam for zone IIIa is 6.010 g/kg, which is equivalent of 9.907 g/kg of sodium chloride. Similarly, that for zone III b is 3.406 g/kg, corresponding to 5.615 g/kg of sodium chloride. Thus, the sodium chloride content of volcanic steam responsible for zone III waters ranges from 0.6 to 1%.

We can estimate the temperature and pressure of the volcanic dense steam containing 0.6 to 1% of sodium chloride to be at around  $374$  to  $385^\circ C$  and 220 to 230 bars based on the experiment of  $NaCl - H_2O$  system (Fig. 7-9, Sourirajan and Kennedy, 1962). When temperature decreases down below  $374^\circ C$  (the critical temperature of water) sodium chloride is hardly dissolve in steam, but mostly remains in the liquid phase.

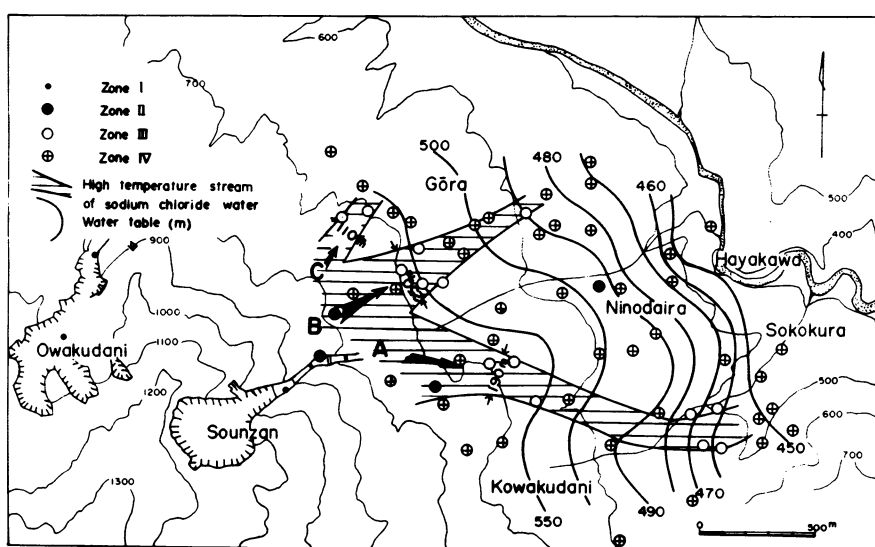


Fig. 7-7. Distribution of Zone III waters (Oki and Hirano, 1974).

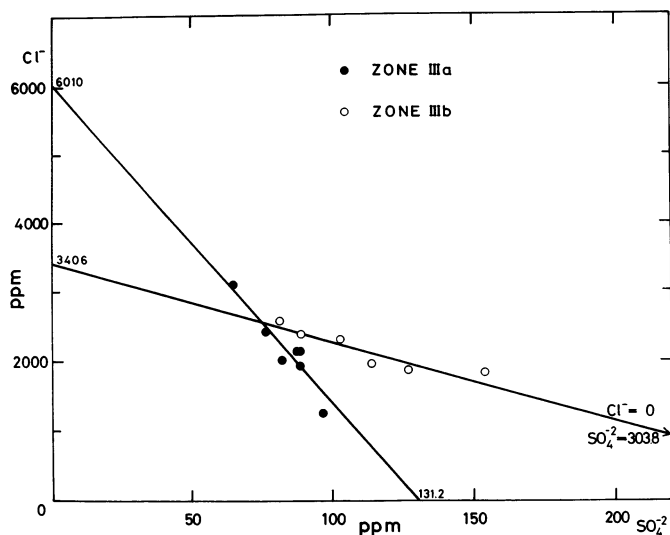


Fig. 7-8.  $\text{Cl-SO}_4$  diagram of Zone III waters (Oki and Hirano, 1974).

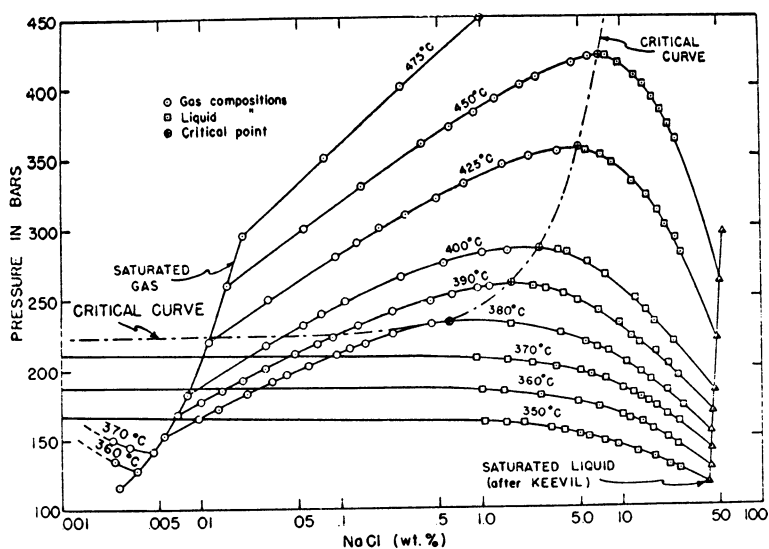


Fig. 7-9. Isotherms at 350 - 450°C showing composition of coexisting gases and liquids in  $\text{NaCl-H}_2\text{O}$  system (Sourirajan and Kennedy, 1962).

## Sodium chloride budget

The evaluation of sodium chloride discharge from the whole hydrothermal system permits the evaluation of energy discharge by the hydrothermal activity. Sodium chloride discharge by thermal waters directly related to the hydrothermal activity of Kamiyama is measured to be 0.22 kg/sec. The contribution of zone I and II waters to the discharge of sodium chloride is fairly small, about 0.01 kg/sec, and can be neglected. The most majority of sodium chloride is transferred by means of the zone III and IV waters, probably being supplied by high temperature dense steam coming up through the volcanic conduit.

The quotient of the total discharge of sodium chloride (0.22 kg/sec) by the sodium chloride content in the inferred original steam (0.6 to 1%) gives the steam discharge of 36.7 to 22 kg/sec through the conduit. Taking 600 kcal/kg for the heat content of steam as approximation, the thermal energy discharge amounts to  $2.2$  to  $1.3 \times 10^7$  cal/sec. Adding the energy discharge by thermal waters from the areas of the basement rocks (zone IVb) of  $0.48 \times 10^7$  cal/sec, the total thermal discharge of Hakone hydrothermal system is  $2.7$  to  $1.8 \times 10^7$  cal/sec.

Yuhara and his colleagues (1966) measured the thermal discharge from the solfataric fields of Kamiyama to be  $0.7 \times 10^7$  cal/sec, not including thermal waters from deep wells. We measured the energy discharge by thermal waters from deep wells to be  $1.98 \times 10^7$  cal/sec. The total energy discharge actually measured amounts to  $2.68 \times 10^7$  cal/sec, which is good agreement with the energy discharge obtained by the chloride chemistry.

## Isotope geochemistry

Matsuo et al. (1972, 1977), Matsubaya et al. (1973), and Sakai and Matsubaya (1977) studied the isotope geochemistry of the Hakone thermal waters. The results are given in Figures 7-11 and 7-12. The zonal distribution and the mixing model of the Hakone hydrothermal system is well supported by the isotope geochemistry. Thermal waters are linearly plotted from high temperature sodium chloride water (zone III) to the area of meteoric water through thermal waters of zones I, II, and IV. The steam condensates from a well of 100 m deep at Owakudani solfataric area are highly enriched in deuterium (D) and oxygen-18 ( $^{18}\text{O}$ ) (Fig. 7-11). Assuming the steam condensate of the highest isotopic ratio is direct fraction from the high temperature thermal brine at 240 to 280°C, Matsuo et al. (in preparation) estimated the isotopic composition of liquid phase in equilibrium with steam having the same isotopic ratio of the Owakudani steam condensate to be  $\delta \text{D} = 27.3\text{‰}$  and  $\delta ^{18}\text{O} = +1.4\text{‰}$ . The isotopic values of the thermal brine thus calculated are just fit on the liner

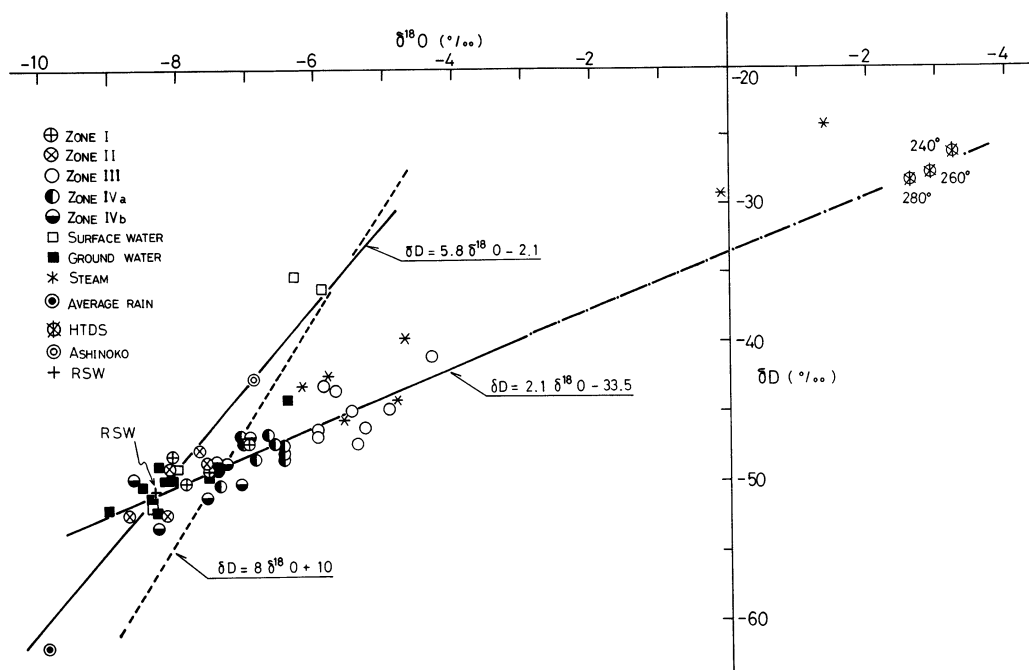


**Fig. 7-10.**  $\delta D$  vs  $\delta^{18}O$  plot for thermal waters of Hakone, compiled from Matsubaya et al. (1973) and Matsuo et al. (1972 and 1977). RSW means respective surface water (Matsuo et al., 1977, Matsuo et al. in preparation).

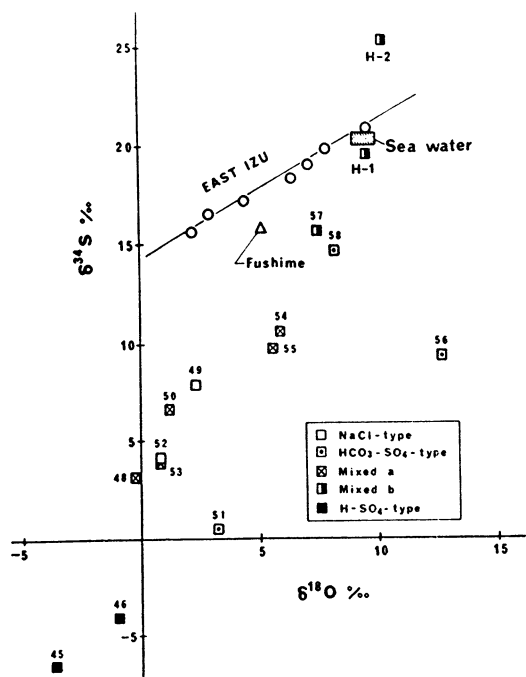


**Fig. 7-11.**  $\delta^{34}S$  vs  $\delta^{18}O$  plot for sulfates from the eastern Izu peninsula and Hakone (Sakai and Matsubaya, 1977).

extrapolation of the least square method for the Hakone thermal waters (Matsuo et al.).

As seen in Figure 7-11, the isotopic values of the lake Ashinoko water are considerably higher than those of the average rain and the local meteoric waters, due to the kinetic evaporation of rain water at the surface likewise the waters of the other caldera lakes (Sakai and Matsubaya 1977, Matsuo et al. in preparation). Matsuo et al. deny the possibility of the lake water as the major source for thermal waters, because of missing of thermal waters plots between the lake and the thermal waters actually analyzed. Sakai and Matsubaya suspect that the representative surface water defined by Matsuo et al. lies isotopically intermediate between the average rain and the lake water of Ashinoko resulted by mixing of the heavy lake water and the groundwaters. The hydrogeological feature of Hakone is essentially controlled by the water levels of the caldera lake in the west and of the major drainages of Haya-kawa and Sukumo-gawa. The geologic structure of the Hakone caldera obviously requires the percolation of the lake water into the major aquifer of thermal waters.

Figure 7-12 is the isotopic diagram of sulfur-34 and oxygen-18 for sulfates from the eastern Izu peninsula and Hakone thermal waters (Matsubaya et al., 1973 and Sakai and Matsubaya, 1977). Sakai and Matsubaya (1977) mentioned that the  $\delta^{34}\text{S}$  values of sulfate in acid water (zone I) are similar to those of the native sulfur in Owakudani fumarolic areas ( $-5.2$  and  $-8.2\%$ ) and suggest that the sulfates were formed by the surficial oxidation of volcanic sulfur and hydrogen sulfide. On the other hand, the  $\text{NaCl-HCO}_3\text{-SO}_4$  type waters have the heavier sulfates, the  $\delta^{34}\text{S}$  values rapidly increasing with the increasing distance from the central cones. The three heaviest sulfates are found in the waters from the basement Green Tuff formation and are considered to be similar in origin to the sulfates in Green Tuff-type thermal waters, which extract the sulfates such as gypsum, anhydrite from the altered Tertiary marine sediments. The  $\delta^{34}\text{S}$  and  $\delta^{18}\text{O}$  values of the sulfates from the  $\text{NaCl}$ -type and the subgroup zone IVa of the mixed type thermal waters are intermediate between the two types of sulfates mentioned above. The sulfates might essentially be formed by surface oxidation of volcanic sulfur at the fumarolic areas. The secondary sulfates may become isotopically heavier through the partial reduction by bacteria (Kusakabe 1976). As is shown in Figure 7-12, two isotopically heavy sulfates were found, one in groundwater and the other in a thermal water of  $\text{HCO}_3\text{-SO}_4$ -type. Note that both are from the western caldera and not directly related to the Tertiary basement rocks.

Sakai and Matsubaya (1974 and 1977) recognized that sulfates from thermal waters of the eastern coast of the Izu peninsula lie closely on a line extending from the oceanic sulfates towards the lower left in Figure 7-12. The isotopic ratios of the sulfates (open circles in Fig. 7-12) decrease steadily to the lower left as one moves southwards from the base of the Izu peninsula.

## 7.2 Hot springs of the Izu Peninsula

More than 40 geothermal areas are known in the Hakone and Izu district extending 80 km north-south by 30 km east-west (Fig. 7-12). All the geothermal areas are occupied by the hot spring resorts. Energy discharges from them are displayed by the areas of circles. The intense hydrothermal activity is seen along the east coast of the Izu peninsula. The total energy discharge from the areas amounts to  $11 \times 10^7$  cal/sec, of which Hakone has 27%, discharging  $3 \times 10^7$  cal/sec. Atami is the second largest followed by Ito. Geothermal areas in the west coast and the back bone of Izu are closely associated with epithermal gold-quartz veins. Hot springs of Toi and Rendaiji issue directly from tunnels of the mines. Notwithstanding of no Quaternary volcanoes in the southern Izu peninsula, hot springs of Kawazu, Mine, Rendaiji, and Shimo-kamo issue through fractures of the Neogene Tertiary rocks, possibly heated by the crypto-volcanic activity.

Hot waters discharged in the center of the intense geothermal area are mostly chloride type. Table 7-2 gives chemical composition of high temperature waters from the intense geothermal areas along the east coast, all which are chloride type. As seen in two triangular diagrams (Fig. 7-13 and 7-14), only the Hakone zone III waters are the sodium chloride type. Atami and Shimo-kamo waters are sodium-calcium chloride type. The high temperature waters of Yugawara belong to sulfate bearing sodium-calcium chloride type. Mine is sulfate bearing sodium chloride type. Atagawa water is bicarbonate and sulfate bearing sodium chloride type. The zone of high temperature water of chloride type is commonly surrounded by the zone of low temperature water of sulfate type sometimes with bicarbonate. Some warm waters in the coastal areas are extremely high in dissolved salts undoubtedly due to the percolation of sea water into the hot water system. Murozumi (1970) demonstrated chemically the mixing of sea water with hot water followed by lowering temperature in Atami and Ito as the result of overdischarging.

Mizutani and Hamasuna (1972) studied the geochemistry of the Shimo-kamo hot springs (Fig. 7-15). They pointed out that the thermal waters (orifice temperature  $100^\circ\text{C}$ ) discharged from drilled wells of 52 to 250 m deep are the mixture of local meteoric water and the deep geothermal brine. The relationship between deuterium and oxygen-18 concentrations in the Shimo-kamo waters indicates that sea water percolated through fractures in rocks turns to be the deep geothermal brine characterized by sodium and calcium chloride type through hydrothermal reactions with surrounding rocks at 221 to  $335^\circ\text{C}$ .

The compositional variation in major anions and cations may reflect the intensity of geothermal activity and variation of hydrothermal alterations as well as the structure of hydrothermal systems.

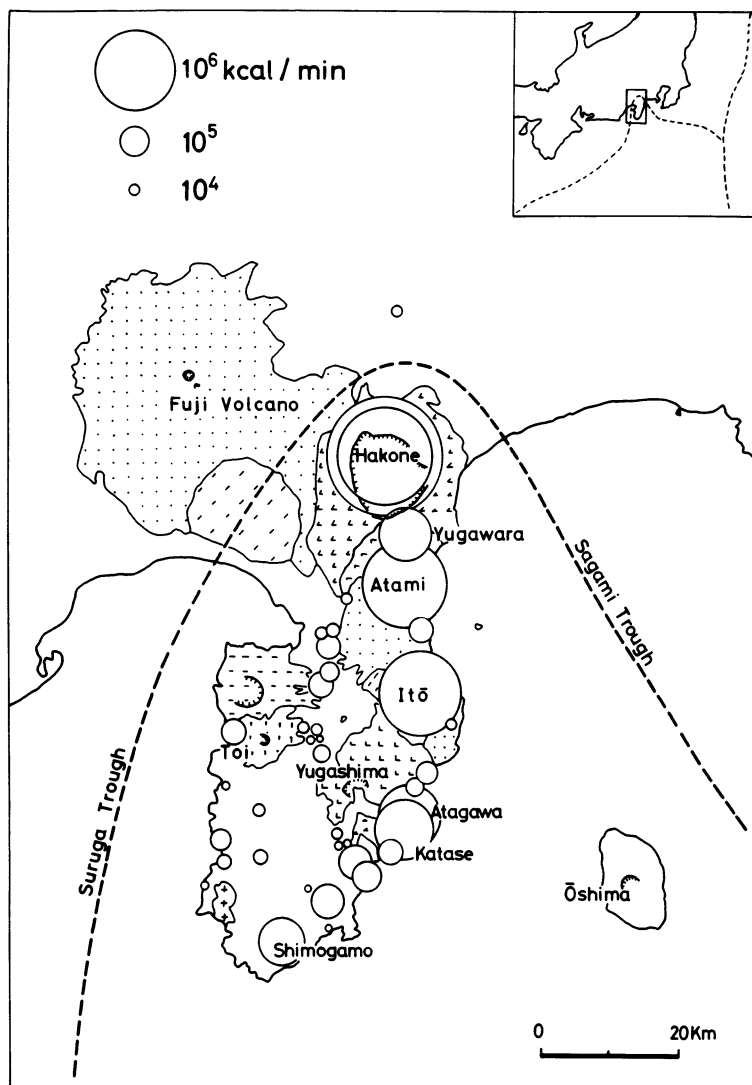


**Fig. 7-12.** Distribution of Quaternary volcanoes and geothermal discharge by thermal waters and steam. The outer circle of Hakone is thermal discharge by thermal waters and steam. The inner one is by thermal waters only (Oki and Hirano 1974).



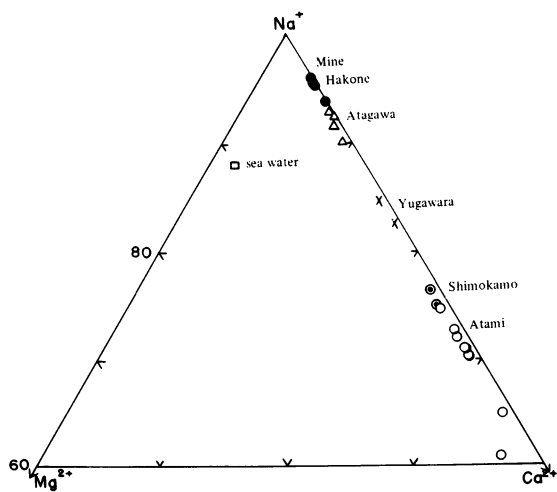


**Fig. 7-13.** Alkalis-Mg-Ca diagram of the Hakone and Izu thermal waters (Oki and Hirano 1972).

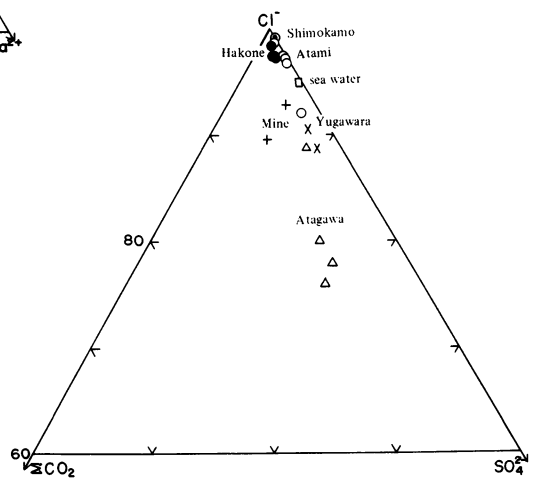
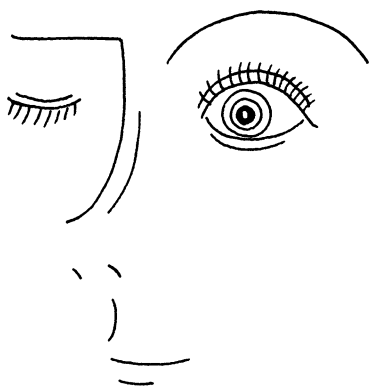


**Fig. 7-14.** Cl-total  $\text{CO}_2$ - $\text{SO}_4$  diagram of the Hakone and Izu thermal waters (Oki and Hirano 1972).



4.06.

Hot eye and cold eyelid.



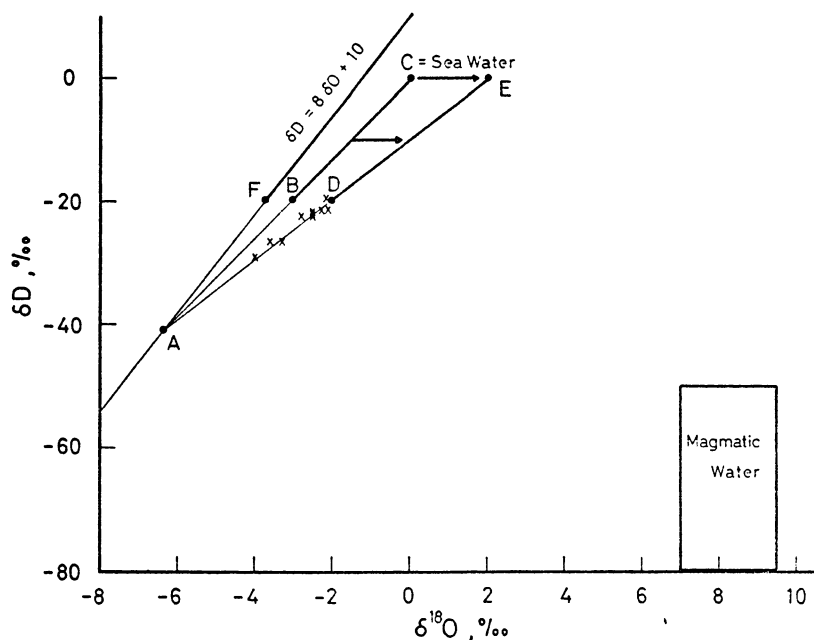


**Fig. 7-15.**  $\delta D$  vs  $\delta^{18}O$  plot showing possible mechanism for genesis of the Shimogamo geothermal brine (Mizutani and Hamasuna, 1972).

A : Local meteoric water, C : Sea water, D-E : predicted deep geothermal brine, x : Shimogamo geothermal brines discharged from drill-holes,  $\rightarrow$  :  $^{18}O$  shift. Magmatic water taken from Sheppard et al. (1969).

**Table 7-2** High temperature thermal waters of the Izu peninsula. (mg/kg)

	1	2	3	4	5
	Yugawara	Atami	Atagawa	Mine	Shimokamo
Temp °C	80.5	93.0	100.	100.	100.
pH	8.4	8.3	8. 8.5	8.6	
Li ⁺	.648				
Na ⁺	872.	2135.	820.	729.7	3815.9
K ⁺	50.8	166.0	103.4	37.50	242.2
Ca ²⁺	270.	2646.5	103.6	61.91	2184.1
Mg ²⁺	.388	9.6	1.851	.681	19.0
Fe ²⁺	.268	.8	1.80	.004	.9
Mn ²⁺	.104				
Al ³⁺	.34	.5	4.0	4.0	.3
Cl ⁻	1564.	7977.8	1032.	1058.	9820.
SO ₄ ²⁻	371.	363.4	582.8	161.9	261.3
HCO ₃ ⁻	55.6	9.2	122.8	77.64	8.3
CO ₃ ²⁻	.408	6.0	21.90	39.93	
BO ₂ ⁻	2.20	8.2			
HSiO ₂ ⁻	7.71			3.853	
H ₂ SiO ₃	130.	135.2	158.1	35.68	84.9
HBO ₂	15.0				5.6
CO ₂	.53				
Total	3342.	14058.5	2955.9	2219.8	16461.4

1. Yugawara-machi, Fudotaki (Hirano, Tajima, 1970)
2. Atami Hot Spring (Shizuoka prefecture, 1968)
3. Atagawa Hot Spring (Tables of mineral waters, Japan p. 407, 1954)
4. Mine Hot Spring (Tables of mineral waters, Japan p. 411, 1954)
5. Shimokamo Hot Spring (Tables of mineral waters, Japan p. 481, 1954)

### 7.3 Hot eye and cold eyelid

Figure 7-16a is an isothermal map of Hakone and the adjacent area at 400 m below the sea level and Figure 7-16b is a north-south cross sections of the isothermas (Oki and Hirano, 1974). It is seen that Hakone is an extremely large geothermal area about 12 km in diameter. The map suggests that important tectonic lines lie extending parallel with the maximum compressional stress axis of this area, through which a large amount of thermal water is discharged.

The map shows that several heat sources are aligned in general north-south directions which are parallel to the east row of Quaternary volcanoes (cf. section 4-1). Individual source areas broadly duplicate the location of volcanic centers of the east row.

Within the each source area, high temperature areas elongate in a NW-SE direction, which is best observed, in Figure 16 with the Atami area, (the one with a cross sectional line B-B'). This elongation, also observed at Hakone and Yugawara source areas, may indicate preferred development of open cracks in the NW-SE direction for the transfer of thermal water. The origin of the preferred orientation of open cracks may lie in the stress field of tectonic origin in this area, namely, the NW-SE direction is the one of the maximum compressional stress as will be discussed in section 5-3. That this direction is the maximum compressional stress is also seen in Figure 16 which describes left-lateral active fault running roughly north-south, just west of the Atami area.

The center of the geothermal activity is circled with many isotherms, reminding us of hot eyes which discharge thermal waters. The hot eyes are surrounded by low temperature zones which may well be compared to cold eyelids, that cover the hot eyes, where the temperature gradient is very small, sometimes less than 3 deg/ 100 m. It is also important that many of the hot eyes appear in the bottoms of the dissected calderas as described in the old saying. The cold eyelid actually lies on the caldera rim and high mountains, from which infiltration of groundwater is going on to compensate for the water discharge from the hot eyes. The combination of hot eyes and cold eyelids seems to be required for the development of the hydrothermal systems.

The young volcanoes like Fuji and Asama, composed of thick piles of volcanic materials, do not display hydrothermal activity on the surface, because the thick piles perform the role of the eyelid and prevent the activity of the hot eye. A large, deeply dissected calderas will be the best for the development of hydrothermal systems. When the geothermal activity is very strong, separating the vapor dominated hydrothermal system from the hot water system (White et al., 1971), the hot eye will appear in central cone like Hakone. If thermal waters are discharged faster than the water balance of the system permits their replacement, the hot eye will be closed by the invasion of the cold eyelid as the cold surface water replaces the hot thermal water.

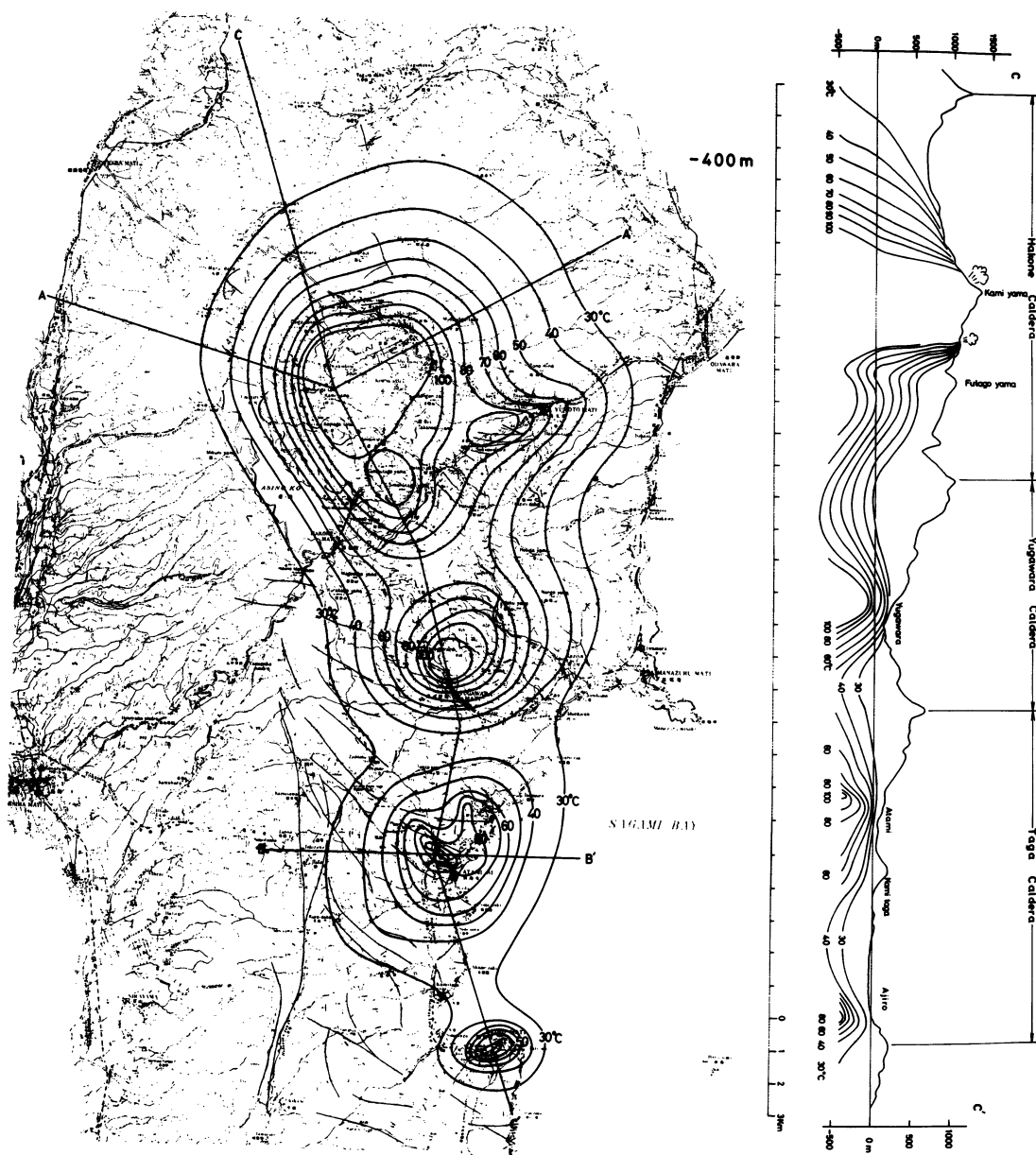


**Fig. 7-16.** Isothermal map of the Hakone and adjacent area at 400 m below the sea level (Oki and Hirano, 1974).  
 North-south cross section showing the isothermal structure of the Hakone and adjacent area (Oki and Hirano 1974).

## 7.4 Legal aspect of Hot springs

The Hot Spring Law enforced in 1948 defines that the hot springs and wells belong substantially to the individual owners of the land. The Prefectural Government gives certain regulation on the drilling and pumping for thermal waters based on the technical recommendation proposed by the Hot Spring Council of each Prefecture.

The registration of new drilled wells reflects the economic fluctuation of the country. Figure 7-18 illustrates the annual registrations of drilled wells in Hakone and Yugawara. The first rush of drilling appeared from 1931 to 1941 just after the construction of the Odakyu railway linking Tokyo to Hakone and the opening of the Tanna tunnel. During the World War II, no drilling had been made. The second rush of drilling occurred from 1950 to 1972 and more than 200 deep wells had been opened. In 1950 the air-lift pumping was allowed to discharge thermal waters and since then most of natural discharge of hot springs and artesian wells has decreased. By the enthusiastic development of deep wells together with setting of powerful pumping devices, the amount of thermal water discharge in Hakone totaled up to 75,000 l/min in 1970, which is three times larger than 23,000 l/min of 1950. Since 1965, considerable lowering of temperature, thermal water levels, and mineral dissolved has been yielded by over-discharge as a result of very traditional government control ignoring of the potentialities and limitation of the hydrothermal system (Fig. 7-17). The same type of the problem does exist in most places of the hot spring resorts located in the suburban areas. The government regulation based on scientific analyses should be established to overcome those exhausting problems.

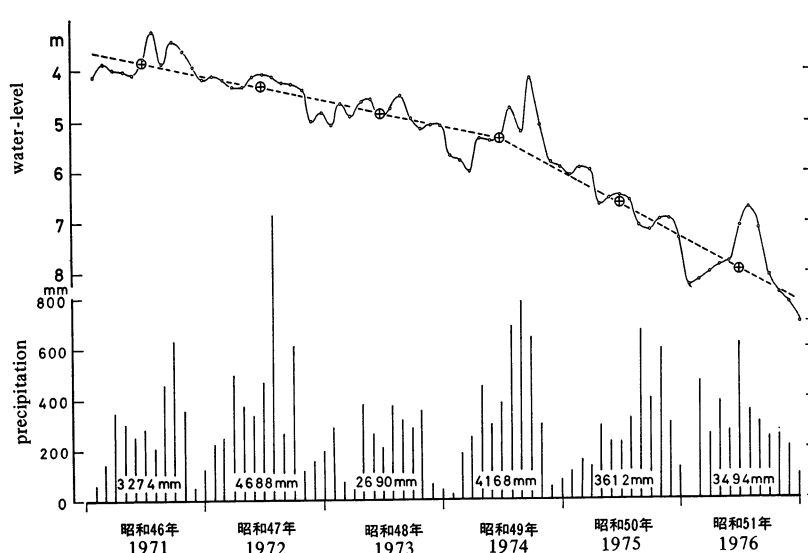


**Fig. 7-17.** Lowering of water-level at Yumoto (Zone IVb), Hakone due to over-discharge ignoring of potentialities and limitation of the hydrothermal system (Hirota and Odaka, 1977).

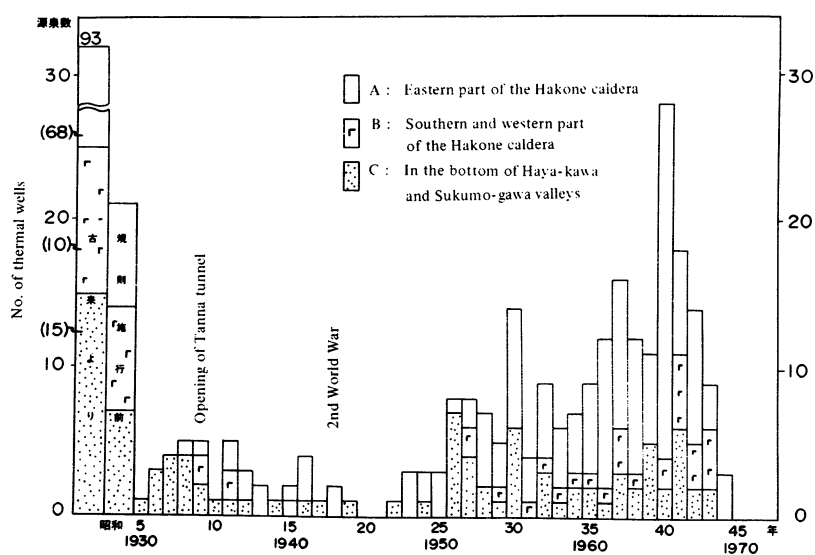


Fig. 7-18a

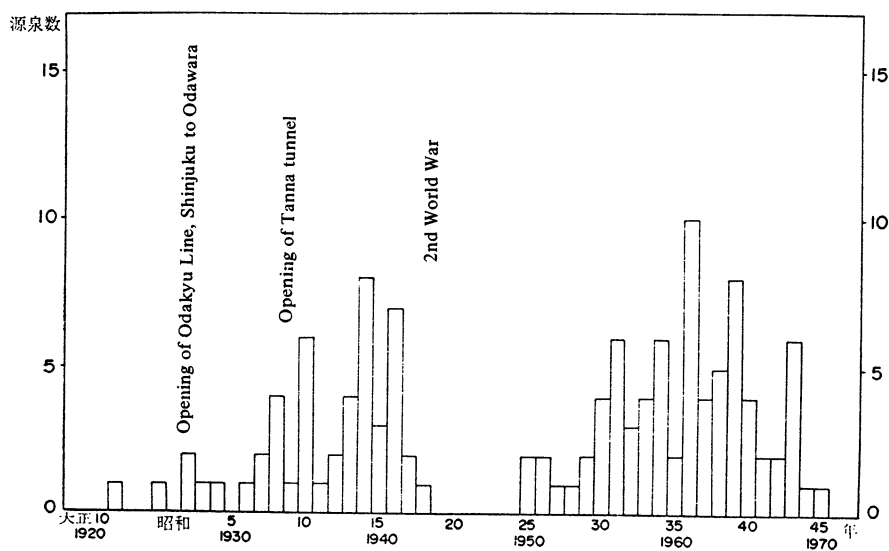


Fig. 7-18b

**Fig. 7-18.** Annual registrations of drilled wells at Hakone (7-18a) and Yugawara (7-18b). The sequence of registration of new drilled well reflects the economic fluctuation of Japan (Oki and Hirano, 1970).

## References

- Aramaki, S. and Yamasaki, M. (1963) Pyroclastic flows in Japan. Bull. Volcanologique, vol. 26, p. 89 – 99.
- Aramaki, S. and Hamuro, K. (1977) Geology of the Higashi-Izu monogenetic volcano group. Bull. Earthq. Res. Inst., vol. 52, p. 235 – 366. (in Japanese).
- Hiraga, S. (1972) Earthquake swarms of geothermal fields in Japan. Jour. Japan. Geoth. Ener. Associ., vol. 9, no. 1, (ser. no. 32), p. 30 – 39.
- Hamuro, K. (1978) Geology of the Omuroyama volcano group. Jour. Geol. Soc. Japan, vol. 84, in press, (in Japanese).
- Isshiki, N. (1964) O-shima Volcano. Guidebook for Excursion, 2. Geol. Surv. Japan. 24p.
- Isshiki, N. and Matsumura, K. (1976) Finding of the earliest Jo-mon site from O-shima Island, Izu Islands, and its significance as a time marker of the volcanic activity. The Quaternary Research, vol. 15, p. 1 – 7.
- Jaggard, T.A. (1947) Origin and development of craters. Geol. Soc. Mem. vol. 21, 508p.
- Kanamori, H. (1972) Relation between tectonic stress, great earthquakes and earthquake swarms. Tectonoph. vol. 14, p. 1 – 12.
- Kaneoka, I., Ozima, M. and Kuno, H. (1970) Paleomagnetism and K-Ar ages of successive lava flows (4) —K-Ar ages of the Usami Volcano, Izu Peninsula, Japan. Jour. Geomag. Geoelectr., vol. 22, p. 559 – 562.
- Kono, M. (1968) Paleomagnetism of Pleistocene Usami Volcano, Izu Peninsula, Japan—intensity of the earth's magnetic field in geological time II. Jour. Geomag. Geoelectr., vol. 20, p. 353 – 366.
- Kuno, H. (1950 a) Petrology of Hakone Volcano and adjacent areas, Japan. Bull. Geol. Soc. Amer., vol. 61, p. 957 – 1020.
- Kuno, H. (1950 b) Geology of Hakone Volcano and adjacent areas, Part 1. Jour. Fac. Sci., Univ. Tokyo, sec. 2, vol. 7, p. 257 – 279.-
- Kuno, H. (1951) Geology of Hakone volcano and adjacent areas Part II, Jour. Fac. Sci., Univ. Tokyo, sec. 2, vol. 7, p. 351 – 402.
- Kuno, H. (1952) Explanatory text of the geological map of Japan “Atami”. Geol. Surv. Japan, 141p. (in Japanese).
- Kuno, H. (1954) Geology and petrology of Omuro-yama volcano group, North Izu. Jour. Fac. Sci., Univ. Tokyo, sec. 2, vol. 9, p. 241 – 265.
- Kuno, H. (1959 a) Origin of Cenozoic petrographic provinces of Japan and surrounding areas. Bull. Volcanologique, ser. 2, vol. 20, p. 37 – 76.
- Kuno, H. (1959 b) Geology and petrology of O-shima volcano. Intern. Geology Review, vol. 1, p. 48 – 59.
- Kuno, H. (1960) High-alumina basalt. Jour. Petrol., vol. 1, p. 121 – 145.
- Kuno, H. and Minakami, T. and Iwasaki, I. (1962) O-shima, p. 208 – 218 in Catalogue of the active volcanoes and solfatara fields of Japan, Taiwan and Marianas. IAVCEI, Rome.
- Kuno, H. (1965) Some problems on calc-alkali rock series. Jour. Jap. Assoc. Petrol. Mineral. Econ. Geol., vol. 53, p. 131 – 142 (in Japanese).
- Kuno, H. (1966) Lateral variation of basalt magma type across continental margins and island arcs. Bull. Volcanologique, ser. 2, vol. 29, p. 195 – 222.
- Kuno, H. (1968) Origin of andesite and its bearing on the island arc structure. Bull. Volcanologique, ser. 2, vol. 32, p. 141 – 176.

- Kuno, H., Oki, Y., Ogino, K. and Hirota, S. (1970) Structure of Hakone caldera as revealed by drilling. *Bull. Volcanologique*, vol. 34, p. 713 – 725.
- Kurasawa, H. (1959) Petrological and chemical characteris of Amagi volcano group, Izu. *Earth Sci.*, no. 44, p. 1 – 18. (in Japanese).
- Kurasawa, H. and Michino, K. (1976) Petrology and chemistry of the volcanic rocks from the western and southern part of Izu Peninsula, central Japan. *Bull. Volcanol. Soc. Japan*, vol. 21, p. 11 – 29. (in Japanese).
- Kusakabe, M. (1976) Hydrogen, oxygen and sulphur isotope study of waters from the Hakone geothermal system, Japan (in preparation).
- Matsubaya, O., Sakai, H., Kusachi, I. and Satake, H. (1973) Hydrogen and oxygen isotopic ratios and major element chemistry of Japanese thermal water system. *Geochem. Jour.*, vol. 7, p. 123 – 151.
- Matsuo, S., Kusakabe, M., Niwao, M., Hirano, T. and Oki, Y. (1978) Water budget in the Hakone caldera in view of hydrogen and oxygen isotope ratios. (IAEA meeting in Wien, 1977, in press).
- Minakami, T. (1960) Fundamental research for predicting volcanic eruptions, Part I. *Bull. Earthq. Res. Inst.*, vol. 38, p. 497 – 544.
- Minakami, T., Hiraga, S., Miyazaki, T. and Uchibori, S. (1969) Fundamental reasarch for predicting volcanic eruptions, Part II. *Bull. Earthq. Res. Inst.*, vol. 47, p. 893 – 949.
- Mizutani, Y. and Hamasuna, T. (1972) Origin of the Shimogamo geothermal brine, Izu. *Bull. Volcanol. Soc. Japan*, vol. 17, p. 123 – 134. (in Japanese).
- Murozumi, M. (1970) Geochemistry of groundwaters in “Studies on Groundwaters in Japan”, Prof. G. Sakai, Memorial Volume, p. 175 – 203. (in Japanese).
- Nakamura, K. (1964) Volcanostratigraphic study of Oshima volcano, Izu. *Bull. Earthq. Res. Inst.*, vol. 42, p. 649 – 728.
- Nakamura, K. (1969) Arrangement of parasitic cones as a key to regional stress field. *Bull. Volcanol. Soc. Japan*, vol. 14, p. 8 – 20.
- Nakamura, K. (1971) Volcano as a possible indicator of crustal strain. *Bull. Volcanol. Soc. Japan*, vol. 16, p. 63 – 71.
- Nakamura, K. (1977) Volcanoes as possible indicators of tectonic stress orientation – principle and proposal. *Jour. Volcanol. Geotherm. Res.*, vol. 2, p. 1 – 16.
- Nasu, N. (1935) Recent seismic activities in the Izu Peninsula (Part 2), *Bull. Earthq. Res. Inst.*, vol. 13, p. 400 – 416.
- Oki, Y. and Hirano, T. (1970) Geothermal system of Hakone volcano. U.N. Symposium on the Development and Utilization of Geothermal Resources, Pisa. *Geothermics, Spec. Issue 2*, vol. 2, p. 1.
- Oki, Y. and Hirano, T. (1972) Geothermal activity and hot springs of Izu and Hakone district. Izu Peninsula, p. 133 – 154, Tokai Univ. Press, Tokyo. (in Japanese).
- Oki, Y. and Odaka, S. (1972) A revised structure of Hakone caldera as estimated by drillings. (Abstract) *Bull. Volc. Soci. Japan*, vol. 17, no. 2, p. 111. (in Japanese).
- Oki, Y., Hirano, T. and Suzuki, T. (1974) Hydrothermal metamorphism and vein minerals of the Yugawara geothermal area, Japan. *Proc. of Water-*

- Rock Interaction Symposium at Prague, Czechoslovakia, Geol. Surv. Prague. 209 – 222.
- Oki, Y., Fujita, M. and Hirota, T. (1974) Geothermal structure of Atami, Shizuoka Prefecture, Jinetsu vol. 11, no. 1 (ser. no. 40) p. 21 – 26. (in Japanese).
- Oki, Y. and Hakamata, K. (1975) Geologic history of caldera lake, Ashinoko. Kokudo to Kyoiku, ser. no. 30, vol. 5, no. 6, p. 2 – 9. (in Japanese).
- Sakai, H. and Matsubaya, O. (1974) Isotopic geochemistry of the thermal waters of Japan and its bearing on the Kuroko Ore solutions. Econ. Geol., vol. 69, no. 6, p. 974 – 991.
- Sakai, H. and Matsubaya, O. (1977) Stable isotopic studies of Japanese geothermal systems. Geothermics, vol. 5, p. 97 – 124.
- Sourirajan, S. and Kennedy, G.C. (1962) The system  $H_2O - NaCl$  at elevated temperatures and pressures. Amer. Jour. Sci., vol. 260, p. 115 – 141.
- Sugimura, A. (1960) Zonal arrangement of the some geophysical features in Japan and its environs. Jour. Fac. Sci., Univ. Tokyo, sec. 2, vol. 22, p. 133 – 153.
- Suzuki, M. (1970) Fission track dating and Uranium contents of obsidian (II). Quat. Res., vol. 9, no. 1, p. 1 – 6.
- Tanaka, Y. (1974) The mechanism of the “Gojinka” – one of the volcanic phenomena at Mt. Mihara – in Izu-Oshima Island. Quart. Jour. Seismol., vol. 39, p. 1 – 9.
- Tazawa, T. (1977) Geological Sketch-Book of the Izu-Oshima Volcano. p. 65. (in Japanese).
- Toto Bunso and Roka (1811) Seven Hot Springs of Hakone, translated by H. Sawada (1975), Hakone Town Office. p. 75.
- Tsuya, H. (1937) On the volcanism of the Huzi volcanic zone, with special reference to the geology and petrology of Izu and Southern Islands. Bull. Earthq. Res. Inst., vol. 15, p. 215 – 357.
- Tsuya, H., Okada, A. and Watanabe, T. (1956) Evolution of Mihara crater, volcano Oshima, Izu, in the course of its activities since 1874. Bull. Earthq. Res. Inst., vol. 34, p. 33 – 59.
- White, D.E. (1957) Thermal waters of volcanic origin. Bull. Geol. Soc. Amer., vol. 68, p. 1637 – 1658.
- White, D.E., L.J.P. Muffler and A.H. Truesdell (1971) Vapor dominated hydrothermal systems compared with hot-water systems. Econ. Geol., vol. 66, p. 75 – 97.
- Yamashina, K. and Nakamura, K. (in press) Mechanical correlation between earthquakes and volcanic activities of Izu-Oshima volcano, Japan. Jour. Volcanol. Geotherm. Res.
- Yokoyama, I. (1969) The subsurface structure of Oshima volcano, Izu. Jour. Physics Earth, vol. 17, p. 55 – 68.
- Yuhara, K., Kodai, K., Abe, K. Kotoda, K. and Hosono, Y. (1966) Hydrothermal system of Owakudani-Gora zone, Hakone volcano. Rep. Co-operative Res. Disaster Prevention, no. 8, p. 29 – 42.
- Volcanological Society of Japan (1971) Hakone Volcano, Hakone Town p. 185. (in Japanese).